



**US Army Corps
of Engineers**

Construction Engineering
Research Laboratory

USA-CERL INTERIM REPORT N-87/25

December 1987

Standard Methods to Assess Human
and Community Response to Impulse Noise

DTIC FILE COPY

AD-A188 838

Mitigation of the Building Vibration and Rattle Induced by Blast Noise: Development of a Test Facility and Systematic Investigative Procedures

by

Paul D. Schomer

Steven D. Hottman

Kenneth McK. Eldred

Occupants of buildings located in areas of high-level impulse noise usually report that the main annoyance factor is the rattle produced by house components upon vibration. This type of noise is associated with helicopter flybys and blast overpressure from artillery and other military training operations. Methods are needed for mitigating rattles both in existing structures and future construction.

This report describes work on an experimental test facility being developed to study the impulse problem systematically and empirically. This facility simulates blast noise on a repeatable basis and allows alternative solutions to be evaluated. Initial data are evaluated to identify ways of improving the facility and test methods used.

DTIC
ELECTE
FEB 12 1988
S H D

88 2 09 100

UNCLASSIFIED

SECURITY CLASSIFICATION OF THIS PAGE

REPORT DOCUMENTATION PAGE

Form Approved
OMB No 0704 0188
Exp Date Jun 30, 1986

1a REPORT SECURITY CLASSIFICATION Unclassified		1b RESTRICTIVE MARKINGS	
2a SECURITY CLASSIFICATION AUTHORITY		3 DISTRIBUTION / AVAILABILITY OF REPORT Approved for public release; distribution is unlimited.	
2b DECLASSIFICATION / DOWNGRADING SCHEDULE		5 MONITORING ORGANIZATION REPORT NUMBER(S)	
4 PERFORMING ORGANIZATION REPORT NUMBER(S) USA-CERL IR N-87/25		7a NAME OF MONITORING ORGANIZATION	
6a NAME OF PERFORMING ORGANIZATION U.S. Army Construction Engr Research Laboratory	6b OFFICE SYMBOL (if applicable)	7b ADDRESS (City, State, and ZIP Code)	
6c ADDRESS (City, State, and ZIP Code) P.O. Box 4005 Champaign IL 61820-1305		9 PROCUREMENT INSTRUMENT IDENTIFICATION NUMBER	
8a NAME OF FUNDING / SPONSORING ORGANIZATION OCE	8b OFFICE SYMBOL (if applicable) DAEN-ZCE	10 SOURCE OF FUNDING NUMBERS	
8c ADDRESS (City, State, and ZIP Code) The Pentagon Washington, DC 20310-2600		PROGRAM ELEMENT NO. 4A162720	PROJECT NO. A896
		TASK NO. A	WORK UNIT ACCESSION NO. 009
11 TITLE (Include Security Classification) Mitigation of the Building Vibration and Rattle Induced by Blast Noise: Development of a Test Facility and Systematic Investigative Procedures (Unclassified)			
12 PERSONAL AUTHOR(S) Schomer, Paul D.; Hottman, Steven D.; Eldred, Kenneth McK.			
13a TYPE OF REPORT Interim	13b TIME COVERED FROM _____ TO _____	14 DATE OF REPORT (Year, Month, Day) 1987, December	15 PAGE COUNT 80
16 SUPPLEMENTARY NOTATION Copies are available from the National Technical Information Service Springfield, VA 22161			
17 COSATI CODES		18 SUBJECT TERMS (Continue on reverse if necessary and identify by block number)	
FIELD	GROUP	SUB-GROUP	
24	02	impulse noise, test facilities buildings, vibration	
19 ABSTRACT (Continue on reverse if necessary and identify by block number)			
<p>Occupants of buildings located in areas of high-level impulse noise usually report that the main annoyance factor is the rattle produced by house components upon vibration. This type of noise is associated with helicopter flybys and blast overpressure from artillery and other military training operations. Methods are needed for mitigating rattles both in existing structures and future construction.</p> <p>This report describes work on an experimental test facility being developed to study the impulse problem systematically and empirically. This facility simulates blast noise on a repeatable basis and allows alternative solutions to be evaluated. Initial data are evaluated to identify ways of improving the facility and test methods used.</p>			
20 DISTRIBUTION / AVAILABILITY OF ABSTRACT <input type="checkbox"/> UNCLASSIFIED/UNLIMITED <input checked="" type="checkbox"/> SAME AS RPT <input type="checkbox"/> DTIC USERS		21 ABSTRACT SECURITY CLASSIFICATION Unclassified	
22a NAME OF RESPONSIBLE INDIVIDUAL Dana Finney		22b TELEPHONE (Include Area Code) (217) 352-6511 x389	22c OFFICE SYMBOL CECER-INT-E

DD FORM 1473, 84 MAR

83 APR edition may be used until exhausted
All other editions are obsolete

SECURITY CLASSIFICATION OF THIS PAGE

UNCLASSIFIED

FOREWORD

This work was performed for the Office of the Chief of Engineers (OCE) under Project 4A162720A896, "Environmental Quality Technology"; Task A, "Installation Management Strategy"; Work Unit 009, "Standard Methods to Assess Human and Community Response to Impulse Noise." The OCE Technical Monitor was LTC James Stratta, DAEN-ZCE.

The investigation was conducted by the Environmental Division (EN) of the U.S. Army Construction Engineering Research Laboratory (USA-CERL). Dana Finney, USA-CERL Information Management Office, was the technical editor. Kenneth McK. Eldred is with Ken Eldred Engineering, Concord, MA.

Dr. R. K. Jain is Chief, EN. COL Norman C. Hintz is Commander and Director of USA-CERL, and Dr. L. R. Shaffer is Technical Director.

Accession For	
NTIS GRA&I	<input checked="checked" type="checkbox"/>
DTIC TAB	<input type="checkbox"/>
Unannounced	<input type="checkbox"/>
Justification	
By	
Distribution/	
Availability Codes	
Dist	Avail and/or Special
A-1	

CONTENTS

	Page
DD FORM 1473	1
FOREWORD	3
LIST OF FIGURES AND TABLES	5
1 INTRODUCTION	9
Background	
Purpose	
Approach	
Mode of Technology Transfer	
2 EXPERIMENTAL FACILITY AND TEST DESIGN	11
Overview	
Test House	
Simulated Blast Acoustic Pressure Pulses	
Loudspeaker Steady-State Sound Field	
3 MEASURED RESPONSES OF TEST HOUSE COMPONENTS	15
Acoustic Modes Inside Test House Room	
Windows and Doors	
Walls, Floor, and Ceiling	
4 ACOUSTIC RESPONSE OF TEST HOUSE	23
Transmission Loss of the House	
Transmission Loss for Impulsive Noise	
Effect of Furnishings	
Effect of Attic Vents	
Effect of Opening Windows	
5 ADDITIONAL EXPERIMENTAL RESULTS	27
Intensity Measurement	
Background Noise	
Averaging Microphones	
6 CONCLUSIONS AND RECOMMENDATIONS	30
Overall Findings	
Effects of Experimental Manipulation	
Recommendations for Improving Test Methods and House	
METRIC CONVERSIONS	33
REFERENCES	77
APPENDIX: Chronological List of Experiments by Reel Number	78
DISTRIBUTION	

FIGURES

Number		Page
1	Test Facility Layout	34
2	Test House Exterior Elevations	35
3	Test House Foundation Detail	36
4	Test House Floor Framing on Floating Foundation	36
5	Test House Exterior Sheathing Showing Window and Door Openings and Roof Trusses	37
6	Test House Exterior With Foundation, Sheathing, and Roof Trusses	37
7	Test House Exterior With Clapboards and Shingles	38
8	Test House West Side	39
9	Test House Northeast Corner	39
10	Time History of Two Simulated Blast Acoustic Pressure Pulses	40
11	Difference Between Flat Peak Sound Pressure Level (PSPL) and Flat Sound Exposure Level (SEL) of Simulated Blast Pulses	41
12	SEL Spectrum of Simulated Blast Acoustic Pressure Pulse Compared With Average Values From 2-kg Charges at 2- and 5-mi Distances	42
13	Example of the Range of SEL Spectra for Simulation of Blast Acoustic Pressure Pulses With the Average Spectrum at 2 mi From a 2-kg Charge for Reference	43
14	Example Range of Control Over SEL Spectra for Simulated Blast Acoustic Pulses	44
15	Comparison of Measured Spectrum of Simulated Blast Acoustic Pressure Pulse With Measured Background Noise Immediately Following Pulse	45
16	Loudspeaker Spectra for Reference Exterior Position and a Location 5 ft East of the Northeast Corner of the Test House	46
17	Loudspeaker Comparison of Differences Between Spectra	47
18	Inside Room in Test House Unfolded to Indicate Principal Standard Transducer Locations	48
19	Relative Response to External Pink Noise Inside Test House at Five Positions	50
20	Picture Window Inner Pane	53

FIGURES (Cont'd)

Number		Page
21	Picture Window: Acceleration Transfer Function for a Pulse and Pink Noise and Intensity Transmission Loss	54
22	North Wall Sash Windows With Storm Windows Closed: Acceleration Transfer Function for a Pulse and Pink Noise and Intensity Transmission Loss Energy Average	55
23	Front Door With Storm Door Closed: Acceleration Transfer Function for a Pulse and Pink Noise and Intensity Transmission Loss	56
24	North Wall: Acceleration Transfer Function for a Pulse and Pink Noise and Intensity Transmission Loss for East Panel	57
25	South Wall: Acceleration Transfer Function for Pulse	58
26	Floor: Acceleration Transfer Function for Pink Noise	59
27	Ceiling: Acceleration Transfer Function for a Pulse and Pink Noise	60
28	Comparison of Pulse Acceleration Transfer Functions for North and South Walls and Ceiling	61
29	Room Constant Derived From "Volume Average" Sound Levels With ILG Reference Source	64
30	Transmission Loss Calculated From "Volume Average" Sound Level Measurements With Pink Noise	65
31	Comparison of Estimated Noise Reduction for Free Field Excitation of Test House With Estimated Values for Other Houses	66
32	Reduction of SEL for Simulated Blast Pulse and for Continuous Noise (SW Corner Microphone)	67
33	Reduction of SEL for Simulated Blast Pulse and for Continuous Noise (Standard Interior Reference Microphone)	68
34	Time Histories for an Impulsive Sound	69
35	Difference in 1/3-Octave Band Noise Reduction Between Inside and Outside Reference Microphones With and Without Furniture in the Room	70
36	Difference in 1/3-Octave Band Noise Reduction Between Inside and Outside Reference Microphones When the Attic Vents Are Sealed	71

FIGURES (Cont'd)

Number		Page
37	Noise Reduction Between Inside and Outside Reference Microphones Minus 5 dB for Three States of Window Closure	72
38	Comparison of Volume Average TL Curve From Figure 30 Compared With ITL Calculated for the North Wall	73
39	Comparison of Acoustic Intensity Radiated Into Room by Walls and Windows With Intensity Measured Outside Room and Flowing Into Wall	74
40	Comparison of 1/2-sec Average 1/3-Octave Band Levels in Test House at Interior Reference Microphone Position During and Subsequent to a Test Impulse Sound	75
41	Difference Between Energy Average of Five Microphones	76

TABLES

1	Low-Frequency Room Modes for Test House Interior	49
2	Estimated Test House Component Parameters and Dynamic Characteristics	51
3	Partial Summary of Formulas Used for Response Calculations	62

MITIGATION OF THE BUILDING VIBRATION AND RATTLE INDUCED BY BLAST NOISE: DEVELOPMENT OF A TEST FACILITY AND SYSTEMATIC INVESTIGATIVE PROCEDURES

1 INTRODUCTION

Background

The recent trend toward siting off-installation housing and other noise-sensitive land uses in areas exposed to high impulsive noise levels has produced a major concern among Army planners. Noise impact on off-installation land uses must be minimized in accordance with the Installation Compatible Use Zone (ICUZ) program, as described in Army Regulation (AR) 200-1.¹ The ICUZ program uses blast noise zone maps generated by the blast noise computer prediction program BNOISE, which was developed by the U.S. Army Construction Engineering Research Laboratory (USA-CERL).²

Impulsive noise presents unique problems compared with common, continuous noise sources such as fixed-wing aircraft, vehicles, trains, and factories. Long-term research by USA-CERL and other agencies has indicated that the main annoyance factor for impulsive blast noise is the rattle it produces when it excites building components.³ This rattle can be caused by vibrating windows, bric-a-brac, light fixtures, doors, and other structural elements.

Elimination of these rattles could eliminate some, if not all, of the annoyance for building occupants. Quantitatively, quieting the rattles could produce a 10-dB or greater benefit in noise reduction; in terms of the ICUZ program, this reduction would be enough to change a zone from completely unacceptable for housing to completely acceptable.

Technology is available for shielding structures against common, continuous noise sources. However, while the impulse noise problem is not an entirely new area, research into mitigation of this noise has failed to produce effective control methods. Many of these theoretical analyses were done in the late 1960s and early 1970s to study structural

¹Army Regulation (AR) 200-1, *Environmental Quality: Environmental Protection and Enhancement* (Headquarters, Department of the Army [HQDA], 15 June 1982).

²P. D. Schomer, et al., *Blast Noise Prediction, Vol I: Data Bases and Computational Procedures*, and *Vol II: BNOISE 3.2 Computer Program Description and Listing*, Technical Report N-98/ADA099440 and ADA099335 (U. S. Army Construction Engineering Research Laboratory [USA-CERL], March 1981).

³P. D. Schomer and R. D. Neathammer, *Community Reaction to Impulsive Noise: A 10-Year Research Summary*, Technical Report N-167/ADA159455 (Revised) (USA-CERL, 1985); P. D. Schomer, *Predicting Community Response to Blast Noise*, Technical Report E-17/ADA773690 (USA-CERL, December 1973); P. D. Schomer and R.D. Neathammer, *The Role of Vibration and Rattle in Human Response in Helicopter Noise*, Technical Report N-85/14/ADA162486 (USA-CERL, July 1985); P. N. Borsky, *Community Reactions to Sonic Booms in the Oklahoma City Area, Vol II, Data on Community Reactions and Interpretations* AMRL-TR-65-37 (U. S. Air Force, 1965); K. D. Kryster, P. J. Johnson, and J. P. Young, *Psychological Experiments on Sonic Booms Conducted at Edwards Air Force Base*, Final Report, Contract No. AF49(638)-1758 (National Sonic Boom Evaluation Office, Arlington, VA, 1968).

response to sonic booms. In general, the theoretical procedures did not take into account nonlinear effects of large impulse noise and resulted in idealized data. The most complicated structure analyzed was a simple box with an opening.

Techniques are needed for rattle-proofing structures located in areas of high-level impulse noise. The technology should cover both retrofitting of existing structures and preventive measures for new buildings.

Purpose

The overall purpose of this work is to develop methods for preventing rattles inside structures inhabited in areas of blast noise. This report documents the development and refinement of: (1) an experimental test structure that will model the effects of blast noise realistically, allow repeatable source noise testing for reliable results, and support the testing of several promising alternatives for noise mitigation; and (2) systematic procedures for studying the complex issues involved in this problem using an empirical approach. Expedient methods for rattle-proofing certain housing elements as an immediate solution to existing problems are documented in USA-CERL TR N-87/24.

Approach

The USA-CERL Biaxial Shock Testing Machine (BSTM) was modified to use as a giant loudspeaker for producing repeatable, impulse-type sounds. An existing test structure was retrofitted to meet the requirements for this study. Controlled tests were conducted on various building components and the results were analyzed. Based on this initial experience, the test facility's current capabilities were defined.

Mode of Technology Transfer

Information in this report will be used to support future work in developing noise mitigation methods. Once final solutions are recommended, they will be incorporated into the ICUZ program.

2 EXPERIMENTAL FACILITY AND TEST DESIGN

Overview

The test facility was constructed by modifying an existing "house" which had been used in a previous study at USA-CERL. Selected noise and vibration data were collected inside the house while it was subjected to acoustic pulses simulating artillery firing sounds at 2 to 5 mi distance. The data were gathered during 1980-84 at the USA-CERL building which houses a hydraulically actuated "shaketable" platform (the BSTM). For these tests, the shaketable was converted to an acoustic piston that could be driven to produce pulses of 25 to 40 msec duration and overall peak overpressures up to 127 dB. The data consisted of component vibration responses and measured acoustic pressure and intensity fields inside and outside the test house during both pulse and steady-state excitation from auxiliary loudspeakers. All pulse data were recorded on reels of magnetic tape using an FM recorder (see Appendix).

The experimental simulated partial house and the USA-CERL BSTM are located in a high-bay facility. Inside dimensions of this building are approximately 90 ft long by 52 ft wide by 40 ft high. Figure 1* shows the high-bay building layout.

Test House

The test house is intended to simulate one corner room of a single-story house typical of those found in the Midwest. Figure 2 illustrates the front (north) and side (east) elevations.

The house has a cinder-block foundation mounted on a wooden support structure which, in turn, is supported by four felt corner pads (Figures 3 and 4). The gap between the floor and the frame is closed during testing by loose sand and sandbags. The floor framing consists of 2 by 10 in. joists on 16-in. centers with two courses of diagonal bracing. The frame is attached to 2-in.-thick sills which are anchored to the cinder block. The structural floor surface is 3/4-in.-thick particle board over a 1/2-in. plywood subfloor. It is covered with a 3/16-in.-thick carpet installed over a 3/16-in. foam pad.

The walls consist of 2 by 4 in. studs lined with fiberglass insulation blankets. Inside walls are finished with 1/2-in. gypsum board. The two simulated exterior walls (north and east) are covered with 1/2-in. sheathing and clapboards made of particle board (Figures 5 through 7). The south and west exterior walls (i.e., "inner" walls) are faced with the same regular sheathing.

The roof is supported by wooden trusses made of 2 by 4 in. boards spaced on 2-ft centers. The trusses shown in Figures 5 and 6 consist of a basic triangle with a "V" brace connecting the rafter to the center of the joist. The roof consists of 3/4-in. plywood surfaced with tarpaper and mineral fiber shingles.

The ceiling also is composed of 2 by 6 in. joists spaced on 16-in. centers. Lower edges of both the joists and the trusses are connected by 1 by 3 in. batten strips that run east and west. The inner ceiling is 1/2-in. gypsum board nailed to the 1 by 3 in. battens and covered with insulation.

*Tables and figures appear at the end of the report, starting on p 34.

Window units include a small double-sash window on the east side and a picture window flanked by two double-sash windows on the north side (Figure 7). The double-sash windows have single-strength glass and removable storm windows. The picture window is insulated glass with two layers of double-strength glass which are separated by a 3/8-in.-thick airspace. The door has a solid core; a storm door also has been installed.

The south and west walls are shielded by a sand-filled concrete block wall which is separated from the sheathing on the test house by a space of 6 to 8 inches. This gap is filled with loose insulation material (Figures 8 and 9) and is closed in the plane of the of exterior walls with a thick facing of resilient material. The insulation material in the gap on the west wall later compacted and settled to approximately ceiling level at the south end and 3 ft below ceiling level at the north end.

Simulated Blast Acoustic Pressure Pulses

The BSTM is hydraulically actuated and electronically controlled. Its 12 by 12 ft platform can accommodate objects weighing up to 13,200 lb. The machine can produce accelerations of up to 20 Gs in either the vertical or horizontal direction. The minimum time constant is 0.005 msec (200-Hz maximum frequency response); maximum displacements are 2.75 in. vertically and 5.5 in. horizontally.

USA-CERL has taken advantage of the BSTM's speed and size to produce low-frequency acoustic waves that closely simulate blast noise. The shaketable has been converted to an acoustic piston driver by covering the table and pit with a heavy rubber diaphragm (0.5 in. thick and 25 ft in diameter). The diaphragm is bolted to the table through wooden 2 by 4 in. battens and is anchored to the floor by sandbags. Fiberglass batts are mounted in three locations in the high-bay area to reduce the magnitude of reflections of the simulated blast acoustic pulse.

A filtered step function is used to produce the blast noise. Filtering controls the step function rise time and hence the table's rise time. A low-pass filter of 50 to 150 Hz produces pulses with fundamental periods of 25 to 40 msec (40 to 25 Hz). In these tests, peak overpressures of up to 127 dB were produced at the front of the test structure. The maximum peak overpressure capability demonstrated by the facility is 130 dB.

Blast noises produced with the BSTM are quite reproducible in both energy and spectral contents. Within a given set, peak levels vary by only a few tenths of a decibel; 1/3-octave spectral levels never vary more than 0.5 dB. When the free field flat peak exceeds 113 to 115 dB, rattling almost always occurs in the house, but rarely when the peak is less than 108 dB. House elements such as windows, bric-a-brac, and china all rattle when the peak is 121 dB.

Figure 10 shows two examples of the time history for pulses measured at an exterior reference microphone. The pulse in the 1982 test had a nominal duration of 26 msec (approximately 40 Hz fundamental).⁴ The pulse from reel 23 recorded later in the program had a nominal duration of 35 msec, as indicated in Figure 10. Also shown is the onset of the first reflection from either the side wall or ceiling; both have approximately the same time delay (55 to 56 msec) measured from the onset of the direct pulse at the exterior reference microphone. The amplitude of this and subsequent reflections has been reduced significantly by the fiberglass acoustic treatment (Figure 1).

⁴L. C. Sutherland, *Low-Frequency Response of Structures*, Wyle Research Report WR 82-18 (Wyle Laboratories, May 1982).

It is apparent from Figure 10 that most of the sound exposure (mean square pressure integrated over time) is contained in the direct pulse. Also, both pulses appear to be approximately sinusoidal, the earlier pulse having two half-cycles and the later pulse three half-cycles. The flat frequency-weighted sound exposure level (SEL) for a sine wave can be calculated directly from its peak flat sound pressure level (PSPL) and its duration (Δt). The relationship for the direct pulse is (Equation 1):

$$\text{PSPL} - \text{SEL} = -10 \log \Delta t + 3 \text{ in dB} \quad [\text{Eq 1}]$$

If the total sound exposure in the reflected pulses is estimated to be one-quarter of that in the direct pulse, the difference between PSPL and SEL is on the order of 1 dB less than the result indicated in Equation 1.

Figure 11 shows the differences between the measured PSPL and SEL at the reference exterior microphone for 39 pulses on reels 23 and 24. The simple relationship in Equation 1 for the direct pulse gives an upper bound to the data. If it is assumed that reflected sound exposure is 25 percent of the direct sound exposure, adding 1 dB to the SEL provides an approximate lower bound to most of the data. If the assumption is that reflected sound exposure is 60 percent of the direct sound exposure, adding 2 dB to the SEL provides an absolute lower bound to the data.

The mean constant derived from the data is +2.3 dB with a standard deviation of 0.5 dB. This value indicates that the expected value of the reflected sound exposure is approximately 17 percent of the direct sound exposure for this series of pulses.

Figure 12 compares the SEL 1/3-octave spectra of a simulated blast acoustic pressure pulse with average free field spectra obtained for a 4 1/2-lb charge at distances of 2 and 5 mi.⁵ For this presentation, the measured values of PSPL at the exterior microphone were reduced by 6 dB to account for pressure doubling at a distance of about 3/8 to 1 1/4 in. from the house wall. In addition, the measured 1/3-octave band 1/2-sec equivalent sound level (LEQ) values were reduced by 6 dB to account for pressure doubling and by 3 dB to convert to SEL, which has a 1-sec reference.

Figure 13 shows a portion of the dynamic range for the pulse simulation facility. The PSPLs of the two spectra are 120 dB and 105.5 dB (both corrected by -6 dB for pressure doubling) and the corresponding SELs are 102.2 and 83.3 dB. It is clear from the graphic data in Figures 12 and 13 that the facility can simulate a wide range of blast acoustic spectra from 12 through 160 Hz with well controlled fidelity.

The overall controllability range also is evident in Figure 14a, which shows the difference between the two spectra in Figure 13. Their overall differences were 14.5 dB for both PSPL and SEL, which is shown for reference in the figure. The difference spectrum is within approximately +3 dB of the 14.5 overall difference in all frequency bands below 160 Hz, except for an anomaly in the 63-Hz band.

Figure 14b illustrates the effect of changing pulse length while maintaining a constant value of overall PSPL. The data show the difference spectra between a pulse with a 41-msec duration and another with a 24-msec duration after the values were adjusted for the difference of 1.0 dB in their overall PSPLs. The primary effect is to change the relative spectra for frequencies in the 10- to 31.5-Hz range.

⁵P. D. Schomer, et al., *The Statistics of Amplitude and Spectrum of Blasts Propagated in the Atmosphere*, Vols I and II, Technical Report N-13/ADA033361 (USA-CERL, November 1976).

By examining the controllable range, it is apparent that a facility noise floor becomes dominant at and above 100 Hz (Figures 13 and 14a). This floor was believed to be the noise from the hydraulic power supplies that power the shaketable. This possibility can be reinforced by noting that both spectra in Figure 13 appear to have the same noise floor even though the 120-dB spectrum was measured directly from a microphone and the 105-dB spectrum was measured from an FM magnetic tape recording. Further support for this explanation is evident by comparing the pulse and background spectrum in Figure 15. Here, the data are presented as measured without the -9-dB correction contained in Figures 13 and 14 (although the correction is included in the scale on the right-hand side of the figure). Figure 15 shows clearly that the levels above 200 Hz are the result of a noise floor.

Figure 15 also shows a spike in the 63-Hz frequency band. This 60-Hz noise would appear to account for more of the value of 74.7 dB at 63 Hz contained in the lower spectrum in Figure 13 and the corresponding anomaly noted in Figure 14a. (Note that 82.5 dB at 63 Hz in Figure 15 minus a 9-dB correction is 73.5, 1.2 dB less than the 74.7 value shown in Figure 13.) The source of this 60-Hz signal is unknown.

Loudspeaker Steady-State Sound Field

The BSTM facility has two columns of low-frequency loudspeakers located 34 ft from the test house, as shown in Figure 1. Each column is 8 ft high and consists of two loudspeaker units which are 4 by 4 by 2 feet each. These loudspeakers were driven in the frequency range of 2 to 2000 Hz by a pink noise generator at a sound pressure level (SPL) of 94 to 96 dB as measured at the exterior reference microphone.

Figure 16 shows two example spectra measured at the exterior reference microphone and one example measured at a position 5 ft east of the test house's northeast corner. The measurements represent 64-sec averages on a B&K 2131 Analyzer. The January spectrum was filtered above 500 Hz and adjusted to place additional emphasis in the low-frequency region. It also exhibits a marked increase in level above the 16-Hz 1/3-octave band and a peak in the 31.5-Hz band. The increase above 16 Hz may be the result of good coupling of the speakers to the facility's 18.7-Hz longitudinal mode. At this frequency, there are three one-half wavelengths (approximately 30 ft) in the facility and the loudspeakers are situated at one of the facility's antinode lines (60 ft from the south wall). This is the lowest frequency at which the speakers are near an antinode. The peak in the 31.5-Hz 1/3-octave band also appears in exterior measurements of pure-tone sweeps and is believed to be an acoustical wave resonance between the house front wall and some other part of the high-bay facility. It is at the frequency for the five one-half wavelength longitudinal facility mode and the distance between the house and loudspeaker is about one wavelength (36 ft).

Figure 17 shows the difference in levels between the reference position and other measurements of the field at positions not immediately adjacent to the test house surface. The November data show the difference between the reference and a position which is in the plane of the front of the house, but 5 ft east of the northeast corner. The January data demonstrate the difference between the reference and the energy average of three microphones located at 28 in., 106 in. and 164 in. from the center front of the house. The data from both tests have a tendency, at frequencies above 63 Hz, to approach a value which is 3 dB less than that on the surface of the test house. This result indicates that at these frequencies, the positions are in a reverberant field. The data for lower frequencies show the major dips in relative response between 20 and 50 to 63 Hz. These dips appear to be associated with discrete facility modes.

3 MEASURED RESPONSES OF TEST HOUSE COMPONENTS

As discussed in Chapter 1, the main annoyance factor due to blast noise is the vibration and rattle of the house and objects inside it. The test house is designed to evaluate these components' responses to high impulse noise using an empirical, systematic approach. The responses of typical key components of the test house (e.g., windows, walls, and ceiling) were measured in one or more of three ways:

- Acceleration response to pulse
- Acceleration response to pink noise
- Transmission loss estimated from intensity measurements.

Figure 18 shows the standard positions for the geophones, accelerometers, and interior reference microphone used. Data were collected for some of these positions in almost all test configurations, with the selection of positions depending on the purpose of each test. Additional vibration data were taken at supplemental positions for some special tests and additional microphones were used at various positions for many test configurations. Data from these additional positions are described in Chapter 5.

The acceleration data are presented in terms of a 1/3-octave band acceleration transfer function (T_a) defined as (Equation 2):

$$T_a = 10 \log (a/g)^2 / p^2 \text{ in dB} \quad [\text{Eq 2}]$$

where $(a/g)^2$ is the measured mean square acceleration ratio and p^2 is the measured square acoustic pressure in psi.⁶

Acoustic mobility (M_a) is a dimensionless quantity calculated directly from the acceleration transfer function by multiplying the quantities within the transfer function by the density of the vibrating structure in pounds per cubic inch.⁷ Thus,

$$M_a = T_a + 20 \log m - 43.2 \text{ in dB} \quad [\text{Eq 3}]$$

where m is the surface weight of the structure in pounds per square foot and 43.2 is $20 \log 144$ (square inches).

The transfer function allows direct comparison of the magnitudes of vibration on various surfaces. The acoustic mobility enables comparison with measurements on other structures.⁸

The SPL for both pulse and pink noise input spectra were measured at the exterior reference microphone position. At this position, the microphone was about 3/8 in. from the house for the pulse tests and up to 3 in. from the house for the pink noise tests. At these close distances, the sound pressure for the normal incidence wave from the pulse is

⁶L. C. Sutherland, B. H. Sharp, and R. A. Mantey, *Preliminary Evaluation of Low Frequency Noise and Vibration Reduction Retrofit Concepts for Wood Frame Structures*, Wyle Research Report WR-83-26 (Wyle Laboratories, June 1983).

⁷L. C. Sutherland.

⁸L. C. Sutherland.

almost doubled. Therefore, the SPL measured at the surface should be reduced by 6 dB to estimate the SPL of a free field incident wave that causes the same acoustic intensity at the house surface.

If it is assumed that the pink noise field in the facility is essentially reverberant, then the SPL of the reference microphone needs to be reduced by 3 dB to estimate the SPL in the reverberant field. Figure 17 indicates that this relationship applies to these data for frequencies above 63 Hz. At the lower frequencies, discrete wave effects dominate the data for the two areas sampled. At these low frequencies, the simple assumption of "reverberant" is incorrect and much more sophisticated analyses and/or measurements would be required to determine the exact nature of the field. At higher frequencies, when the field does appear to be essentially reverberant, there probably is a significant direct sound component from the loudspeakers to the north wall of the test house. However, its level is masked by the "reverberant sound."

The reverberant SPL also has to be reduced by 6 dB if it is to be compared with a free field wave and to cause the same incident acoustic intensity at the surface of the test house as that in the free field wave. Finally, the response of a structure to sound averaged over various angles of incidence (field incidence) is about 5 dB higher than its response to sound arriving at normal incidence.⁹ Consequently, to compare the acceleration transfer functions and the acoustic mobility functions measured from pulses (P) and steady-state reverberant pink noise (R), the SPL measured at the exterior reference microphone must be corrected using Equation 4 for pulses and Equation 5 for the reverberant field:

$$\text{SPL} = \text{SPL}_{\text{PM}} - 6 \text{ in dB} \quad [\text{Eq 4}]$$

$$\text{SPL} = \text{SPL}_{\text{RM}} - 4 \text{ in dB} \quad [\text{Eq 5}]$$

where SPL_{PM} is the equivalent SPL measured for 0.5 sec in 1/3-octave bands at the exterior reference microphone for the pulse; SPL_{RM} is the SPL measured in 1/3-octave bands at the exterior reference microphone for the pink noise; and the value of the constant (-4) represents the sum of these corrections:

- -3 dB (surface to reverberant)
- -6 dB (reverberant to intensity comparable to free field wave)
- +5 dB for greater response to random.

With these corrections, both the pulse and the pink noise forcing functions have been approximately normalized to a free field acoustic wave. This approximation is believed to be most valid at frequencies above 63 Hz. In this frequency range, the corrections remove most of the differences in spatial characteristics between these two acoustic fields in the facility and the outdoor field to be simulated.

The intensity transmission loss is calculated from intensity measurements on the inside of the test house when driven by external pink noise. Intensity was measured with the B&K 2134 Intensity Analyzer at a probe spacing of 1.97 in. (for 32.5 to 1250 Hz). Data were obtained by moving the microphones over each surface at a distance of about 3/4 to 3 in. to obtain three 64-sec measurements which were then averaged.

⁹L. C. Sutherland, B. H. Sharp, and R. A. Mantey.

The pink noise measurement was the "volume average" of the sound between the rail and the pit (Figures 1 and 17). This value was the result of averaging four 64-sec measurements wherein the microphone was moved through a volume for which the height extended from the facility floor almost to the roof eaves at the test house.

The intensity transmission (ITL) is (Equation 6):

$$ITL = SPL_V - I - 6 \text{ in dB} \quad [Eq 6]$$

where SPL_V is the volume average SPL, I is the measured intensity, and -6 is the correction to obtain the intensity on any plane in the reverberant field.

Acoustic Modes Inside Test House Room

Table 1 lists the frequencies for the first 17 acoustic modes in the room inside the test house. The fundamental length (19.25 ft) mode is at 29.1 Hz. The fundamental width (13.25 ft) mode occurs at 42.3 Hz, and the fundamental height mode (7.92 ft) is at 70.9 Hz. It is clear from Table 1 that the four 1/3-octave bands of 31.5 through 63 Hz each contain only one mode. Considerably more modes are contained in the 80- and 100-Hz bands; there are seven modes in the 80-Hz band and six in the 100-Hz band.

Figure 19 shows the relative 1/3-octave band spectra of the acoustic response in the room for positions along a three-dimensional diagonal. This diagonal extends from the lower northeast (exposed) corner of the room to the upper southwest (shielded) corner.

The data are tightly clustered for 1/3-octave band frequencies above 100 Hz. This result indicates that the field in the room is reasonably reverberant and diffuse in this frequency range, as would be expected with the increased density of potential modes. The field is also fairly uniform at frequencies below 25 Hz where the room acts essentially as a uniform pressure volume stiffness element. However, from the frequency of the first room mode at 29.1 Hz in the 31.5-Hz band through the second width room mode in the 80-Hz band, the room response is controlled by only a few discrete modes.

The most dramatic effect of acoustic modes on sound field measurement can be observed at the center microphone. This position has a null at both the fundamental length and width modes, which are in the 31.5- and 40-Hz bands, respectively. The relative amplitudes for these modes suggest that the 40-Hz mode has the greater excitation. It is well coupled to the first piston-like mode of the north wall. These results also suggest that there may be more intensity on the north than on the east wall at this frequency. This may be the result of direct sound adding to reverberant sound on the north wall and/or acoustical wave effects in the high-bay facility.

The center microphone position also has the highest level in the 80-Hz band where it is at an antinode of the second width mode at 84.3 Hz. This mode is also well coupled to the fundamental mode of the north wall.

Because of these room acoustic response characteristics, it should not be expected that formulas for noise reduction and transmission loss which are based on statistical behavior will be valid in the frequency range below approximately 125 Hz. Rather, in this frequency region, calculations would have to account for the joint acceptance of vibratory and acoustic modes and their magnitude frequency response functions. A

vibroacoustic finite element model would probably be the most useful approach, particularly if future tests were to explore the effects of altering any of the test house's response characteristics.

Windows and Doors

As mentioned earlier, the test house has a picture window, flanked by sash windows, and a door in the north wall and a sash window in the east wall. There are no penetrations in the shielded south and west walls. The response characteristics of these components were analyzed using the basic concepts introduced in the next section with the picture window as an example. Table 2 summarizes key parameters and dynamic characteristics.

Picture Window

The picture window is 4.08 ft wide and 3.67 ft high and is constructed as described in Chapter 2. Its fundamental natural frequency (f_{11}), assuming the window to be simply supported, is calculated to occur at 11.3 Hz.

In the 1:1 mode, there is $1/2$ wavelength in both the longer and shorter directions. In the 2:1 mode, there would be two $1/2$ waves in the longer direction (i.e., a full sinewave) and one-half wave in the shorter direction. Note that the response at the center of the window is theoretically zero for any mode which has an even number of one-half waves in either or both directions. Conversely, for modes in which there is an odd number of one-half waves in both directions, the response at the center is maximum since the center is at an antinode.

Because this window is made of homogeneous, uniform material, it can be expected to exhibit resonances at some of the calculated higher order panel modes. The calculated frequencies in Hz, assuming simple supports, for the first few series of modes for the window are:

- $f_{11} = 11.3$
- $f_{21} = 26.5, f_{12} = 30.1, f_{22} = 45.5$
- $f_{31} = 51.9, f_{13} = 61.4, f_{33} = 102$
- $f_{32} = 70.6, f_{23} = 76.7$
- $f_{41} = 90.6, f_{14} = 105.3.$

Figure 20 shows the response to pink noise at two locations on the picture window ($L_x/3, L_y/3$ (one-third), and $L_x/4, L_y/4$ (one-quarter) relative to the response at the center of the window.

When the window is responding in its 1:1 mode, the response is greatest at its center followed by the response at the one-third position with the lowest response at the one-quarter position. This characteristic is exhibited for the 1/3-octave band data below the 25-Hz band. The theoretical relative response for the one-third position is -2.4 dB and, for the one-quarter position, it is -6 dB--almost exactly as measured in the 12-Hz band. The order of response magnitude by position is changed in the 25- and 31.5-Hz bands, where the window is responding in its 2:1 and 1:2 modes as well as the 1:1 mode.

Here, the response is least at the center, which is at a node for the 2:1 and 1:2 modes, greatest at the one-third position, and least at the one-quarter position. The response in the 80-Hz band, which should contain some energy in the 2:3 and 3:2 modes, shows a similar order of response at the three positions.

The response in the 50- and 63-Hz bands is dominated by the 3:1 and 1:3 modes which have maxima at the center. The response at the one-third position is least because it is theoretically zero at these two higher modes, and thus, presumably is responding only to excitation in the 1:1 mode.

Between 80 and 500 Hz, the relative responses at these two positions remain within about ± 2.5 dB, indicating a multimodal response. Above 500 Hz, the relative responses increase, which might indicate that the mass of the accelerometer is reducing the response of the window at its center.

Figure 21 shows the acceleration transfer function measured in the same test for the accelerometer at the center of the window. Here, the response is greatest in the 12 and 16 $1/3$ -octave bands from the 1:1 mode, and in the 50-Hz band where the 1:3 and 3:1 modes become dominant. The response is least in the 25- and 30-Hz bands and in the 80-Hz band where the even modes are important (1:2 and 2:1 in the 25- and 30-Hz bands and 3:2 and 2:3 in the 80-Hz band).

In theory, the response to sound of an "ideal," simply supported panel is zero for all modes except odd-odd modes at frequencies below the coincidence frequency. This situation is due to the fact that there is no net volume displacement if either of the mode numbers is even. For this same reason, the ideal simply supported panel cannot radiate sound in this frequency region except at odd-odd modes. However, because panels are almost never exactly simply supported, they often exhibit some small response when zero is predicted, although they behave generally as expected for simple supports.

The lower curve in Figure 21 is the intensity transmission loss (ITL) measured with pink noise. It was estimated from the difference between the space average intensity measured over the surface of the picture window (three 64-sec averages) and the volume average (four 64-sec averages) of the sound between the rail and the pit. Note that the "sense" of this curve is opposite that of the response curve. Higher values of ITL are associated with lower values of panel response and transmission.

The ITL shows three minima, at the 40-, 80- and 250-Hz $1/3$ -octave bands. The minima in ITL at 40 and 80 Hz probably are related to the modal response characteristics of the room inside the house (see Table 1). The fundamental width mode (north-south) is in the 40-Hz band and the second is in the 80-Hz band. Thus, although the window does not have resonant responses at these frequencies, the fact that the 1:1 mode couples well into a room acoustic mode's resonant response produces a low apparent value of ITL (also see the discussion on intensity measurement in Chapter 5).

The ITL minima at 250 Hz probably are caused by the double-panel resonance of the two windows. The calculated frequency for this resonance, assuming a one-dimensional airspace (thickness only), is 300 Hz. However, the first lateral acoustic mode in the inner space occurs at 137 Hz and the first vertical mode is at 152 Hz. Consequently, the airspace is actually three-dimensional, acoustically, and is somewhat less stiff than was assumed in the calculation.

It should be noted that the window and other components which are less than a complete wall cannot radiate effectively when they are small compared with an acoustic

wavelength. Consequently, their effective transmission loss (TL) at very low frequencies will be greater than that computed from simple theory. For one of these components, the critical radiated frequency (f_r) is given by Equation 7:

$$f_r = C/\sqrt{S}\pi \text{ in Hz} \quad [\text{Eq 7}]$$

where C = speed of sound (1120 ft/sec) and S = the panel area in square feet. For the picture window, the radiation frequency is 163 Hz. Below this frequency, the TL is increased by up to 6 dB per halving of frequency.

Figure 21 also shows the random incidence mass law TL calculation for the picture window behavior as a single panel. Equation 8 was used for this calculation:

$$\text{TL} = 20 \log (mf) - 33.5 \text{ in dB} \quad [\text{Eq 8}]$$

where m is the surface weight in lb/sq ft and f is frequency in Hz. This calculated TL is greater than that computed for the intensity measurements for all components. The possible cause and significance of this result are discussed in Chapter 5, where the ITL for the entire test room is compared with other measurements of room TL.

Figure 21 includes an acceleration transfer function calculated from the pulse measurements. This function was calculated from the estimated SEL of the incident acoustic pulse and the acceleration exposure level for the response. For most component responses, the acceleration transfer function from the pulse experiments is similar to that from the pink noise steady-state loudspeaker tests.

Sash Window on North Wall

There is a double-hung sash window on each side of the picture window. Each pane is made of single-strength glass and measures approximately 1.97 by 1.65 ft. Each unit has a storm window, spaced at approximately 2 in., which can be opened. The fundamental natural frequency calculated for a sash window pane, assuming simple supports, is 39.6 Hz, and its calculated double-panel resonant frequency is 150 Hz.

Both the acceleration transfer function and the ITL data in Figure 22 show a significant effect from the double-panel resonance which occurs in the 160-Hz 1/3-octave band. The fundamental panel resonance shows up in a maximum of the pulse acceleration transfer functions in the 40-Hz band, but not in the pink noise acceleration transfer functions.

The "zero" data shown in the 40- to 63-Hz 1/3-octave ITL curve indicate that the measured power flow was from inside to outside. Thus, within these frequency bands, the window appears to absorb acoustic power from the room inside the test house rather than transmitting additional power to the inside.

Sash Window in East Wall

The sash window in the east wall is similar to those in the north wall except that it is wider and shorter, with each pane measuring approximately 2.64 by 1.31 ft. The fundamental resonance frequency calculated for a pane, assuming simple supports, is 46 Hz, and the double-panel resonant frequency is 150 Hz.

Front Door

The front door is a standard, well gasketed, solid-core design measuring approximately 6.65 by 3.00 ft. It has an aluminum storm door with movable glass panels and an airspace of approximately 3 in. between the other door. The solid-core door's resonant frequency ranges from 12.7 Hz for simple supports at top and bottom to 75.2 Hz for simple supports all around. However, since this door's edge conditions are controlled primarily by the gaskets and their state of compression, it is not possible to make a reasonable estimate of the actual resonant frequency. Its double-panel resonant frequency is estimated to be less than 96 Hz because this frequency is above the first vertical acoustic mode with airspace, estimated at 84 Hz. The coincidence frequency is an estimated 560 Hz; this is the frequency at which the propagation speed of the bending waves in a panel equals the speed of sound in air.

The acceleration transfer functions show a first peak value at 20 Hz, which probably is the resonant frequency of the north wall (Figure 23). The "zero" data in the ITL curve represent negative (outward) acoustic intensity flow.

Walls, Floor, and Ceiling

Walls

The walls are constructed of 2 by 4 in. studs with fiberglass insulation in the inner space between the studs and 1/2-in. gypboard on the inside surface. The wall exteriors (south and west) are covered with 1/2-in. regular sheathing; north and east walls have clapboards made of pressed composite wood. The south and west walls are shielded from the high-bay facility by an 8-in., sand-filled cinder-block wall, separated from the sheathing by a 6-in. airspace. The airspace is filled with a loose mineral fiber absorbing material and gasketed at its outer edges. The absorbent material later became compacted. For example, in the west wall gap, the top of the absorbent material was about even with the ceiling at the south end and 3 ft below the ceiling at the north end.

The exterior walls have several penetrations and are therefore dynamically complex. However, their normal fundamental mode should be dominated by the simple bending of a typical stud together with the added weight and stiffness of the exterior and interior sheathing. The typical fundamental resonance frequency for the exposed north and east walls is calculated to be approximately 20 Hz; this value is the mean of 17.2 and 23.4 Hz, which were calculated for a range of assumptions about the stiffness of the stud and its sheathing. This frequency is in the range for the "midwall" resonance frequencies (11 to 25 Hz)¹⁰ found in measurements of approximately 40 houses which had a variety of designs.

Figure 24 shows the acceleration transfer functions and the ITL for parts of the north wall. The fundamental resonance of 20 Hz appears in both the pulse and loud-speaker acceleration transfer functions. The ITL shows dips at 40 and 80 Hz, the first two fundamental acoustic resonances in the inner room based on the width of the room.

¹⁰D. E. Siskind, et al., *Structure Response and Damage Produced by Airblast From Surface Mining*, Bureau of Mines Report of Investigation RI 8485 (U.S. Bureau of Mines, 1980).

Figure 25 shows the pulse acceleration transfer function for the south wall which is shielded from the high-bay facility. It would appear that the shielding is effective for this location on the south at low frequencies but a significant response maximum occurs in the 63-Hz band. The 63 Hz might be the frequency of the double-panel resonance between the inner wall and the shielding wall; however, preliminary calculations indicate that this frequency is 30 Hz, assuming the construction is as described earlier.

Floor, Ceiling, and Roof

The floor is faced with 3/4-in. particle board over 1/2-in. plywood subflooring and supported by 2 by 10 in. joists 16 in. on center with two courses of diagonal bracing. It is covered with a 3/16-in.-thick carpet over a 3/16-in.-thick foam pad. The crawl space between the underside of the subfloor and the concrete floor of the high-bay facility is approximately 3 ft 2 in. high. It contains no acoustic absorption and has length and width acoustic modes at approximately the same frequencies as in the room, e.g., beginning at 29 and 40 Hz. The frequency of the fundamental height acoustic mode is 176 Hz. The crawl space is separated from the facility by the concrete block foundation which is floated on a wood box structure supported by felt pads at the four corners. The opening under the box beam supports is closed by sandbags on the outside during testing.

Figure 26 shows the acceleration transfer function measured at one location on the floor for pink noise. Above 25 to 30 Hz, its response is clearly less than that of other major structural components.

The ceiling surface is 1/2-in. gypboard fastened to 1 by 3 in. wood battens which are attached to the underside of 2 by 6 in. joists on 16-in. centers. The ceiling is covered with fiberglass insulating blankets. A typical fundamental resonant frequency for this structure is calculated to be 16.1 Hz, assuming that the only significant stiffness is in the direction of the joists.

However, the 1 by 3 in. ceiling battens are also attached to the wood trusses that support the roof. These trusses, shown in Figures 5 and 6, are made of 2 by 4 in. wood and are spaced on 2-ft centers. They consist of a triangle formed of a joist, stud, and rafter, with a "V" brace in the center. This center "V" brace effectively couples the roof and ceiling structures in their low-frequency vibrating response modes. The roof is 3/4-in. plywood covered with tar paper and asphalt shingles. The approximately typical fundamental frequency for this linked ceiling-roof structure is calculated as 12.3 Hz. The double-panel resonance for this structure is estimated to be 15 Hz, so that, except for the coupling of the "V" brace, there should be significant isolation at frequencies above 15 Hz.

Figure 27 gives the acceleration transfer function for one point on the ceiling. The resonance in the 12-Hz frequency band is clearly evident in the pink noise transfer function but its significance is masked by the pulse transfer function. The acceleration transfer function for the pulse appears to be approximately 8 dB greater than the function measured with pink noise at frequencies above the 16-Hz band. The reason for this difference is unknown. However, it may result from spatial differences in the pulse and pink noise acoustic fields as they relate to the surface of the roof. As will be seen in Chapter 4, the 12.5-Hz resonant frequency dominates the ceiling's velocity response when measured by a geophone.

Figure 28 compares the pulse acceleration transfer functions of the north wall, south wall, and ceiling. The ceiling and north wall appear comparable, but the south wall shows evidence of shielding below 30 Hz.

4 ACOUSTIC RESPONSE OF TEST HOUSE

The test house's acoustic response is the summation of its component responses, allowing for these responses' relative weightings and interactions. The overall response to both steady and impulsive sounds is summarized and effects of configurational changes such as removal of furniture and various states of window openings are described.

Transmission Loss of the House

Several experimental techniques were used to define the house's acoustic transmission characteristics, including:

- Volume averaging with pink noise
- Single fixed-position microphones with both pink and impulsive sounds
- Arrays of 5 to 15 fixed-position microphones with both pink and impulsive sounds
- Acoustic intensity differences.

Results from the first two techniques are discussed in this chapter. Chapter 5 describes results from the last two methods in an examination of experimental techniques.

The transmission loss of the test house was computed from "volume average" data measured with steady pink noise generated by the loudspeakers. The exterior and interior averages were the average of four 64-sec spatial averages of the sound field. For the inside measures, the microphone was moved continuously throughout the volume of the test house room. For the outside measurements, the microphone sampled the sound field between the railing and the shaketable pit up to the height of the house's roof eaves. The transmission loss was computed from the measured noise reduction under the assumption that the sound fields were reverberant both inside and outside the house. The calculation was based on the standard equation (Table 3) using the area of both exposed walls.¹¹ The calculation for 1/3-octave bands above 50 Hz used the values of the room constant R shown in Figure 29. These values were derived from volume average measurements of the sound in the test house room resulting from operation of an ILG standard reference sound source which was located in one corner of the room. Below 63 Hz, the ILG data appear invalid. Therefore, the correction assumed that the room constant was approximately equal to the room's exposed wall area (256 sq ft).

It is believed that the rapid rise in the value of room constant as the frequency is decreased below 200 Hz is the result of the decreasing number of room modes in the 1/3-octave band. Thus, the increase in room constant is not a measure of room absorption. Further, it should be noted that the coupling between the north wall and the 42- and 84-Hz room acoustic cross modes is strong and is not duplicated by the coupling of the corner-mounted ILG. Consequently, at low frequencies, certainly below 100 Hz, the acoustic response of the whole test house is dominated by discrete modal effects which are not accounted for by ILG data.

¹¹L. L. Beranek, *Acoustics* (McGraw-Hill, 1954).

Figure 30 shows the TL calculated from the volume averages. The TL has two distinct minima in the 42- and 84-Hz bands as expected. It is compared with a simple calculation based on mass law TL for the windows, walls, and door. This simple calculation agrees with measurement at 200 Hz but is a few dB higher than measurement at higher frequencies. Below 200 Hz, the measured data decreases more rapidly than the mass law calculation, partially due to the increase in room constant from 200 to 63 Hz in Figure 29.

The estimated noise reduction of the test house is compared with data for actual houses in Figure 31. The results for the test house are similar to the average values measured in 20 owner-occupied homes in Los Angeles¹² at frequencies above 250 Hz. The Los Angeles data represent the average difference between aircraft noise measured outdoors in the free field and the sound measured at several positions in each of the rooms that was on the side of the house exposed to the aircraft noise.

Figure 31 also shows the bounds measured for noise reduction at single positions in a few rooms in each of four houses located in Virginia and California.¹³ These data are included because they extend to low frequencies, although the interior sound data have an unknown relationship to the actual spatial average. It appears that, above 125 Hz, the acoustic transmission characteristics of the test house are within the bounds found with the four houses. However, the results at lower frequencies, particularly in the 80-Hz 1/3-octave band, show the test house to have lower noise reduction. This is believed to be the result of strong coupling with the 84-Hz resonant acoustic mode, its probable low acoustic absorption, and the lack of interior interconnections to other rooms.

Transmission Loss for Impulsive Noise

The "volume average" is believed to give the most accurate estimate of the spatial average 1/3-octave sound pressure levels within the room. However, it cannot be calculated for the impulsive sounds when reliance must be placed on a finite number of fixed microphones. The inside reference microphone, channel 6, was used in all tests. It was placed at 40 in. above the floor, at one-third the room length from the east end, and at one-half the room width (Figure 18). Therefore, the sound measured at this location had a minimum at the 42-Hz width fundamental resonant acoustic mode and a maximum at the 84-Hz second width mode (for example, see Figure 19 for the center position).

Similar results are evident in Figure 31 which gives the noise reduction (NR) calculated between corrected values of the outside and inside reference microphones. The high apparent NR at 42 Hz is simply the result of a very low response in the room at this reference position.

It should be noted that the NR measured for impulsive sound based on the difference in 1/3-octave SELs is almost the same as that obtained from differences in the 1/3-octave sound pressure levels for the steady noise. This correspondence is even more striking in the data of Figure 32. These data were obtained from a microphone located in the upper southwest corner of the room at approximately 1 ft from each wall surface. Here, the results for the pulse and steady-state sounds are almost identical as a

¹²K. E. Eldred, et al., *Home Soundproofing Pilot Project for the Los Angeles Department of Airports*, Wyle Laboratories WCR 70-1 (Wyle Laboratories, March 1970).

¹³H. H. Hubbard, "Noise Induced House Vibrations and Human Perception," *Noise Control Engineering Journal*, Vol 19, No. 2 (September-October 1982).

function of frequency. The average difference between the two measures in Figure 33 is -0.055 dB with a standard deviation of 4.5 dB. The average difference in the A-weighted SEL for the two positions in Figure 33 is 0.55 with a standard deviation of 1.5 dB. These results are consistent with the similarity noted earlier between the acceleration transfer function measured with steady-state and impulse excitation. This finding is a central result of these tests because it means that the vibration and acoustic transmission characteristics of a house found with steady-state sound excitation can be applied directly to the outdoor SEL spectrum of an impulsive sound to calculate the resulting interior SEL spectrum and overall value.

These results apply only to impulse data for which the analysis sample contains substantially all of the impulse or impulse response. In the current tests, both the sample length and measurement time were 1/2 sec.

Figure 34 illustrates one test pulse and some of its resultant responses. The principal frequency in b-e is 13.3 Hz. When the traces are aligned in time, considerable correspondence is evident between the response of the corner microphone and the ceiling, suggesting that the ceiling may be the main driver of the room at the apparent resonant frequency of the coupled ceiling-roof.

Effect of Furnishings

The test house contained several items of furniture including a small sofa, stuffed chair, table, cabinet, lamps, and drapes that could be removed from the room. However, the rug remained in place at all times. Figure 35 shows the effects of the furniture on the room's absorption characteristics. For all practical purposes, the furniture contributed negligible acoustic absorption at frequencies below 200 Hz. However, at higher frequencies, the absorption of the furniture was high enough to reduce the sound level in the room by 2 to 3 dB.

Effect of Attic Vents

The test house has three ventilator openings in the roof and three in the eaves. When these vents were sealed, the sound level from impulses, as measured inside the test house, decreased by an average of 1 dB in the frequency range 12 to 100 Hz (Figure 36). USA-CERL calculations indicate that the Helmholtz resonance of the vents with the attic volume would be about 4.3 Hz for the roof units and 6.5 Hz for the eave units.

Effect of Opening Windows

Figure 37 displays the noise reduction between the inside and outside reference microphones minus 5 dB for three window conditions: closed (winter conditions), one sash window open, and all windows removed. The effect of opening the sash window is to lower the noise reduction by a few dB at almost all frequencies between 10 and 125 Hz. For higher frequencies, the calculation based on weighted mass law indicates that the decrease in noise reduction should be approximately 5 dB. USA-CERL's calculated Helmholtz resonant frequency for this single-sash window is 5.6 Hz.

When the windows are entirely removed, there is a substantial decrease in the noise reduction. In fact, in the 10- and 12.5-Hz frequency bands, the sound levels inside the room exceed those outside by 10 to 12 dB. This result appears to be due to a Helmholtz resonance, calculated by USA-CERL to occur at 9.6 Hz. For higher frequencies, the calculation based on weighted mass law indicates that the decrease in noise reduction when the windows are closed should be about 12 to 13 dB. This calculation is consistent with the noise reduction measured at 100 and 125 Hz.

5 ADDITIONAL EXPERIMENTAL RESULTS

During these initial tests at USA-CERL, several findings were recorded that were not part of the specific objectives. These results are related to intensity measurement, background, and microphone averaging and will be considered in refining the test facility and procedures.

Intensity Measurement

In the discussion of component transmission characteristics in Chapter 3, several figures showed intensity transmission loss (ITL) data. These data were computed from differences in the reverberant field level determined from one-fourth of the volume average mean square sound pressure between the rail and the pit and the average transmitted acoustic intensity. In most cases, the ITL was lower than the mass law estimate. Also, dips in transmission loss were observed in the 40- and 80-Hz 1/3-octave bands.

Figure 38 illustrates the ITL computed for the entire north wall including all of its components. This computation involves multiplying the area of transmitted acoustic intensity for each component by the area over which the intensity was averaged, adding each of these component transmitted sound powers, then dividing by the total area to obtain the average intensity.

A comparison of the ITL for both walls with the volume average transmission loss (VATL) shows that both methods give nearly identical results above 315 Hz. For 160 to 250 Hz, the ITL is below the VATL; below 125 Hz, the ITL is generally higher. For most frequencies above 160 Hz, the east wall appears to be absorbing sound power, i.e., the intensity is flowing into the wall from the room inside the house. Thus, in this frequency range, almost all the energy in the room appears to enter through the north wall.

At low frequencies, three points are evident. First, there are some frequency bands in which no ITL points are plotted. For these bands, the net intensity for the configuration (north wall or both north and east walls) was measured to be flowing into the wall rather than through the wall into the room.

Second, there is evidence of a dip in the transmission loss at 80 Hz, just as in the VATL. The dips in "measured transmission loss" in the 40- and 80-Hz 1/3-octave bands probably are due to experimental error. In the case of the VATL, the error is due to an underestimate of the effective absorption for the first and second room widths' acoustic modes which are strongly coupled with the fundamental mode of the north wall. For the ITL, the appearance of this dip, both here and in some of the earlier component data, results from the inadequacy of the intensity measurement device to discriminate between the pressures related to actual acoustic power flow and those related to the highly reverberant acoustic modes.¹⁴ Correct ITL measurements in this condition would require good absorption in the room within this frequency range and might also require separation of the noise transmitted through the north and east walls.

¹⁴J. Buffa and M. Crocker, "Background Noise Effects on the Measurement of Sound Power of Small Machines Using Intensity Techniques," *Noise Control Engineering Journal*, Vol 25, No. 1 (July-August 1985).

Third, the ITL values are significantly higher than the VATL values at frequencies below 100 Hz. This frequency region is the one in which the VATL-based noise reduction values appeared to be lower than those found in four actual homes (see Figure 31). The room constant determined using the ILG source in the corner probably is not a measure of absorption in the single acoustic modes coupled to the north wall. Consequently, the calculated volume average TL is lower than it should be. Also, the formulas that relate sound power transmission to reverberant field sound pressure in the statistical modal region do not apply to discrete modes and contribute to the apparent low values of VATL in this frequency region. Finally, the presence of high Q resonant acoustic modes makes it difficult to measure intensity.

Another suggestion emerging from these analyses is that the low-frequency room modes in the test house may have a higher Q value than found in actual homes. Also, the apparent stiffness of the room in this frequency range may contribute to lower values of noise reduction at frequencies between the high Q modes than would be found in actual houses. Both phenomena, if they exist, could result from the fact that the entire house is a single, sealed room, rather than a series of rooms which are acoustically coupled through open doorways and archways. These factors related to discrete acoustic modes need additional investigation if the test house is to be developed for maximum experimental utility.

An alternative, or perhaps complementary, possibility is that the shielding walls are inadequate in the low-frequency range. The estimated double-wall resonance frequency of these walls is about 30 Hz, assuming the walls are sand-filled. The walls could provide fairly effective transmission paths between approximately 10 and 60 Hz if they are exposed to a noise level similar to that existing on the north wall. They also are partially flanked by the voids left by the settling of insulation in their inner spaces. These possibilities should be investigated (Figure 28).

Intensity was measured outside the house as well as inside. If the house wall were a single layer of "lossless" homogeneous material, the intensity measurements on the outside should be identical to those on the inside. These two measures of intensity on the north wall are compared in Figure 39. From 315 Hz and higher, the two measurements are almost the same. Below 315 Hz, the "inside" intensity is higher than the "outside" intensity; note the peak "inside" at 80 Hz. If this "outside" measure of intensity were used to estimate the TL, the ITL would be close to the VATL from about 160 Hz to 1000 Hz. However, the ITL would still be significantly higher than the VATL at lower frequencies.

Background Noise

In Chapter 2, the background noise in the high-bay facility was found to be similar to the levels generated by an impulse at frequencies above the region of 125 to 200 Hz (Figures 13 through 15). The inside data in Figure 40 show a similar result. It is not known whether the peaks in the 63- and 125-Hz bands are electrical or from the hydraulic power supply. They should be investigated and reduced, if possible. Then the pulse data should be usable to at least 200 Hz.

Averaging Microphones

During several tests, the microphones' outputs were directly connected and averaged, typically for 64-sec averaging periods. This technique was used in the five-microphone diagonal array and in the 15-microphone "random" array in which three banks of five microphones were averaged. The results in Figure 41 show that the average values computed by direct electronic averaging differ from those computed by averaging the levels for individual microphones on an energy basis. This difference ranges from 12.7 dB at 10 Hz to -7.1 at 40 Hz with smaller variations at higher frequencies. Note that if five microphones are in phase, the direct electrical average should be 7 dB greater than the energy average. If two microphones are out of phase with the others, then the electronic average would be at least 7 dB lower than the energy average. These values cover all of the data from 12 Hz to 1000 Hz, but do not explain the anomaly at 10 Hz.

6 CONCLUSIONS AND RECOMMENDATIONS

A test facility and empirical methods have been developed for studying a structure's response to blast impulse noise. The test facility is intended for laboratory simulation of responses by residential houses located at a distance of 2 mi or more from an artillery firing range. The characteristics of the sound field outside the test house and the house's responses are similar to those found in an actual situation, making the facility useful for studying effects and methods for their control. The data analyzed from initial tests have led to several conclusions about the facility. Based on these conclusions, recommendations have been generated toward improving the facility and developing increased confidence in understanding the house's response characteristics.

Overall Findings

The acoustic pulse produced by the USA-CERL facility has amplitude and spectrum characteristics that simulate the sounds from explosive charges at a 2- to 5-mi range and beyond. The peak flat amplitude is controllable up to approximately 124 dB free field and the pulse duration can be controlled between approximately 25 and 40 msec. The duration variation enables control of the spectrum at frequencies in the 10- to 31-Hz range. The pulse is very repeatable, although some change in its shape may have occurred between the early data from 1980 and those recorded in 1984.

Rattles are almost always present in the house when the free-field flat peak exceeds 113 to 115 dB, but rarely when the peak is less than 108 dB. When the peak is 121 dB, windows, bric-a-brac, and china all rattle.

The pulse appears to be similar to a single sine wave or 1 1/2 sine waves, depending on duration and perhaps experimental technique. Its flat SEL can be reliably estimated from its duration (Δt) and flat PSPL using Equation 1 with the constant changed to +2.3. This figure was derived from the mean of the data and is within 0.7 dB of the value that would be calculated for a sine wave signal.

The 1/3-octave band noise reductions (NR) measured at two locations within the test house were almost identical for SELs of both the acoustic pulse and steady pink noise from a loudspeaker (after appropriate adjustments). Therefore, the results obtained using steady-state noise to evaluate the vibration and acoustic response characteristics of a structure can be applied directly to estimate the comparable sound or vibration exposure level spectra and overall values.

The lowest frequency acoustic mode in the test house occurs at 29 Hz. There is only one mode per 1/3-octave band in the range 31 to 63 Hz. The two most dominant acoustic modes are the fundamental and first harmonic "width" modes at 42 and 84 Hz. These modes appear to be tightly coupled with the fundamental vibrating mode of the north wall, which appears to have the greatest excitation.

The low-frequency region below approximately 100 Hz appears to be totally characterized by discrete vibration and acoustic modes. High responses within the room at 12 Hz appear associated with the resonant frequencies of the picture window and the coupled roof-ceiling system; they are associated with the wall resonance at 20 Hz and, in the 40- and 80-Hz 1/3-octave bands, with the "width" acoustic resonances. These complex coupled discrete modes could be analyzed best using a finite element vibro-acoustic model designed to stimulate significant modes at frequencies below 100 Hz and

supplemented by a careful experimental exploration of the mode shapes and damping in the significant acoustic and vibration modes.

The steady-state NR is best evaluated by a "volume average" technique in which the microphone is moved continuously throughout the volume being sampled while its output is accumulated in an integrating sound level meter or filter.

The 1/3-octave band noise reduction of the test house at frequencies above 125 Hz compares well with the average NR of 21 occupied homes measured in Los Angeles as part of a home soundproofing pilot project.

The test house NR at frequencies below 125 Hz appears to be less than that in four test houses measured by NASA. It is particularly low at 80 Hz, where the north wall is well coupled to the first harmonic width acoustic mode. The reason for the apparent low value of NR is not known, but may be due to (1) very high Q acoustic resonances for which effective absorption is improperly estimated from a corner-mounted ILG reference sound source and/or (2) flanking sound through the south and west shielding walls which have an estimated double-wall resonance frequency of 30 Hz, assuming complete sand-filling.

Transmission loss estimated from internal measurements of acoustic intensity on the two exposed walls produced results that were almost identical to those from the volume average at frequencies above 315 Hz. At frequencies below 125 Hz, the acoustic intensity method produced transmission losses that were above those estimated from the volume average data. Although the direction of this change appears correct, the magnitudes are questionable because the highly reactive sound field inside the test house may have caused errors in intensity measurement. Substantially more acoustic absorption than is now present will be required to eliminate these effects.

Effects of Experimental Manipulation

The effect removing the furniture (except for the rug) was to reduce acoustic absorption in the test house room and increase the reverberant levels by 1 to 3 dB in the frequency range 200 to 1000 Hz. The effect was negligible at frequencies below 200 Hz.

The effect of sealing the attic vents was to reduce the acoustic levels in the test house room by 1 to 2 dB at most frequencies between 16 and 100 Hz.

The removal or opening of windows appeared to increase acoustic levels inside the room at the higher frequencies, as expected, and to produce a marked increase at the opening's Helmholtz resonant frequency.

An effect due to closing the storm windows could be seen in data involving the windows themselves but did not significantly change the reverberant sound level within the test house because of the windows' relatively small total area.

The data indicated that all responses were linear.

There is some evidence that the accelerometer at the center of the picture window was "mass loading" the window at frequencies near 1000 Hz.

The background noise for the external pulse measurement system shows a spike at 60 Hz which affects the magnitude of the pulse spectrum in the 63-Hz 1/3-octave

frequency band and other noise from 200 Hz believed to be from the hydraulic power supply. The internal spectrum for the pulse tests shows noise spikes in both the 63- and 125-Hz 1/3-octave bands plus an elevated noise floor at higher frequencies. Again, this background noise may be from the hydraulic power supply. Its amplitude limits the validity of much of the pulse NR data to frequencies below 125 Hz.

Recommendations for Improving Test Methods and House

Based on the conclusions, the following improvements are recommended to the test facility and experimental methods:

Review the signal-to-noise level on both the exterior and interior data. Evaluate both electrical and mechanical potential causes and attempt to reduce signal-to-noise magnitude through 200 Hz.

Review the time history of the impulse signal to learn if it has changed over the years; alter the curve as required to optimize its shape.

Add two permanent external microphones to the center of the east wall and roof at about 1 in. from the surfaces. Add two temporary external microphones to the center of the south and west cinder-block shielding walls at about 1 in. from the surfaces.

Check the level of the reverberant field using volume averaging between the rail and pit and outside each of the four walls and relate to the permanent and temporary fixed microphones. Then use pulse excitation to determine the relative levels at all of the fixed microphone positions.

Consider developing a vibroacoustic finite element model for frequencies below 100 Hz. Such a model would use existing or available off-the-shelf software together with the structural definitions appropriate to the test house in this frequency range.

Install an additional internal reference microphone in one of the room corners (perhaps the lower northeast corner) at a distance of about 1 in. from the wall surfaces. Also, add microphones adjacent to the walls as needed for defining the acoustic mode shapes in the following experiments.

1. Using a loudspeaker pure tone sound, a movable microphone, and a handheld accelerometer, check the fundamental vibration and acoustic resonances inside the test house to estimate both mode shape and Q for winter conditions, vents sealed, and no furniture. Repeat the volume average for pink noise inside and outside to relate to all fixed microphones and vibration transducers.

2. Install 6-in.-thick type 703 or 705 fiberglass on the south wall, west wall, and under the ceiling. Repeat the pink noise test at the corner microphone, determine the revised frequency and Q for damped acoustic modes, and explore any anomalies observed in vibration data from fixed vibration transducers. Repeat pulse tests to compare adjusted pulse TL with adjusted pink noise TL.

3. Measure the acoustic intensity for all components within the north and east walls and the ceiling using a pink noise source. Then reconfigure fiberglass to cover the north and east walls and most of the floor. Measure the acoustic intensity for the south and west walls and the ceiling, subdividing as appropriate for "hot spots" or other anomalies.

4. Fill the empty inner spaces between the test house and shielding wall with type 705 fiberglass. Then add at least 4 lb/sq ft of leaded vinyl gaskets to the existing gasketing, ensuring that the gaskets have considerable slack. Recheck the acoustic intensity at the south and west walls and ceiling and correct or otherwise act on all anomalies found. If excessive noise is coming through the shield walls, correct the problem and repeat the tests.

5. If roof-ceiling coupling at low frequencies is confirmed, consider decoupling the trusses from the 1 by 3 in. batten strips supporting the 1/2-in.-thick gypsum board ceiling. One method would be to drop the existing ceiling, nail the batten strips along the underside of the 2 by 6 in. joists, and then nail the gypsum board to the underside of these extended joists. Then recheck the acoustic intensity through the ceiling using pink noise and check the new resonant frequency and mode shape of the ceiling.

6. Change the interior fiberglass to its original configuration on the south and west walls and the ceiling. Place fiberglass insulation under the floor between the joists. Then remeasure acoustic intensity through the floor using pink noise. Check the pink NR using the corner microphone and then check pulse NR.

7. Assuming that the low-frequency NR is now more than adequate with respect to other houses, remove the ceiling absorption and all but a small amount (3 to 6 ft horizontally) of the vertical treatment. Alternatively, consider designing a low-frequency sound absorber that leaves the appropriate absorption at frequencies above 125 Hz; then recheck acoustic mode Q values at low frequencies and results with ILG at higher frequencies. Note: place the ILG in several positions--the corner, the center of the floor, and the centers of the north and east walls--to evaluate the effect of positioning.

8. With the final configuration, repeat the pink noise volume average and pulse TL tests and compare results with those found previously. Consider adding a controlled low-frequency leak to better represent leakage found in real houses.

9. Investigate the potential for exciting rattles with a loudspeaker, either by limiting the pink noise bandwidth to one low-frequency octave, such as 12 to 25 Hz, or by using pure tones in this frequency range to excite wall vibration. If necessary, move the loudspeaker close to the walls that are to be vibrated. When these procedures have been completed successfully, the facility should be reasonably validated and ready for new experiments.

METRIC CONVERSIONS

1 in.	=	2.54 cm
1 ft	=	0.305 m
1 mi	=	1.6 km
1 lb	=	0.45 kg
1 psi	=	6.9 Pa
1 sq ft	=	0.09 m ²

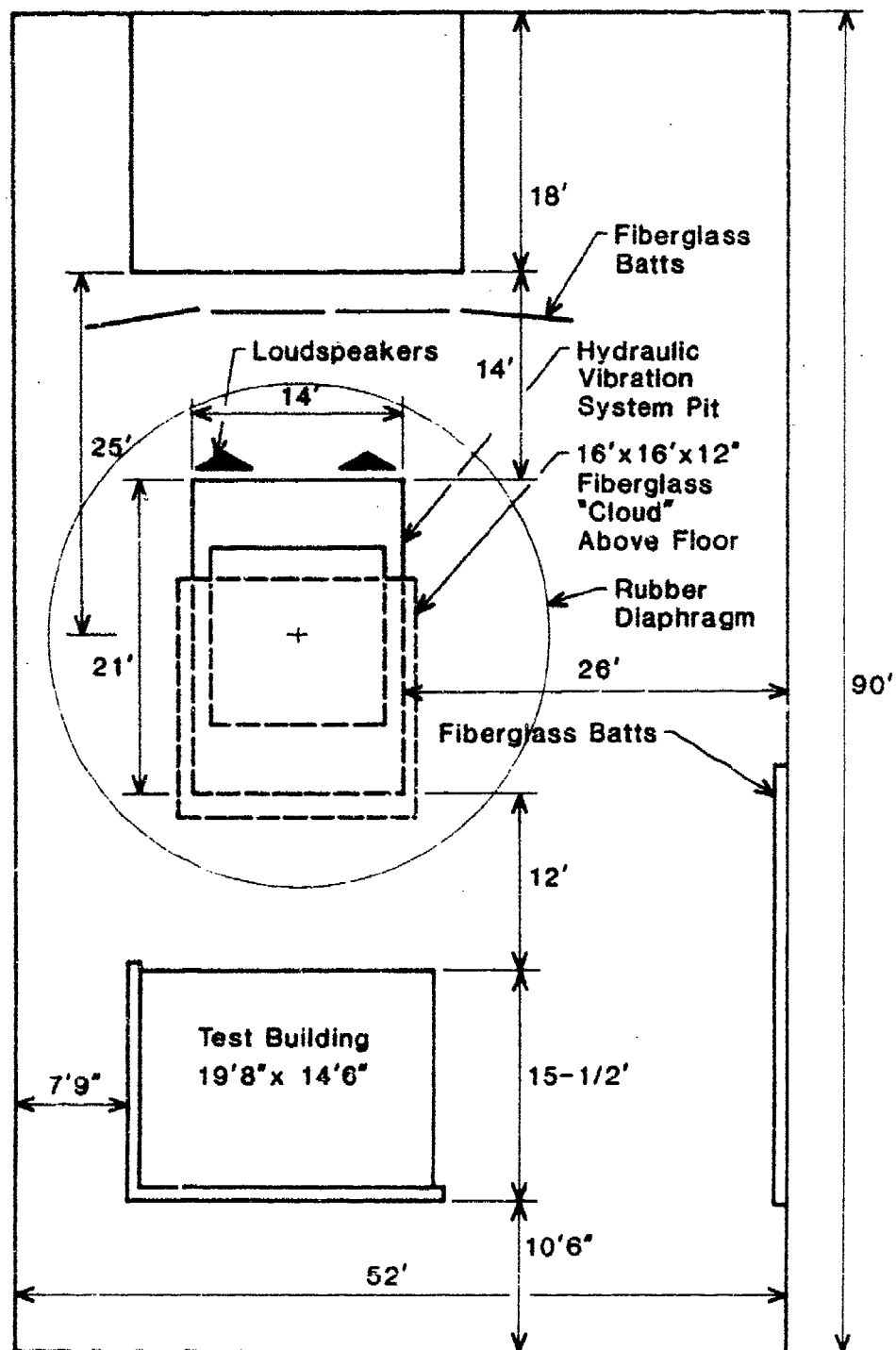


Figure 1. Test facility layout.

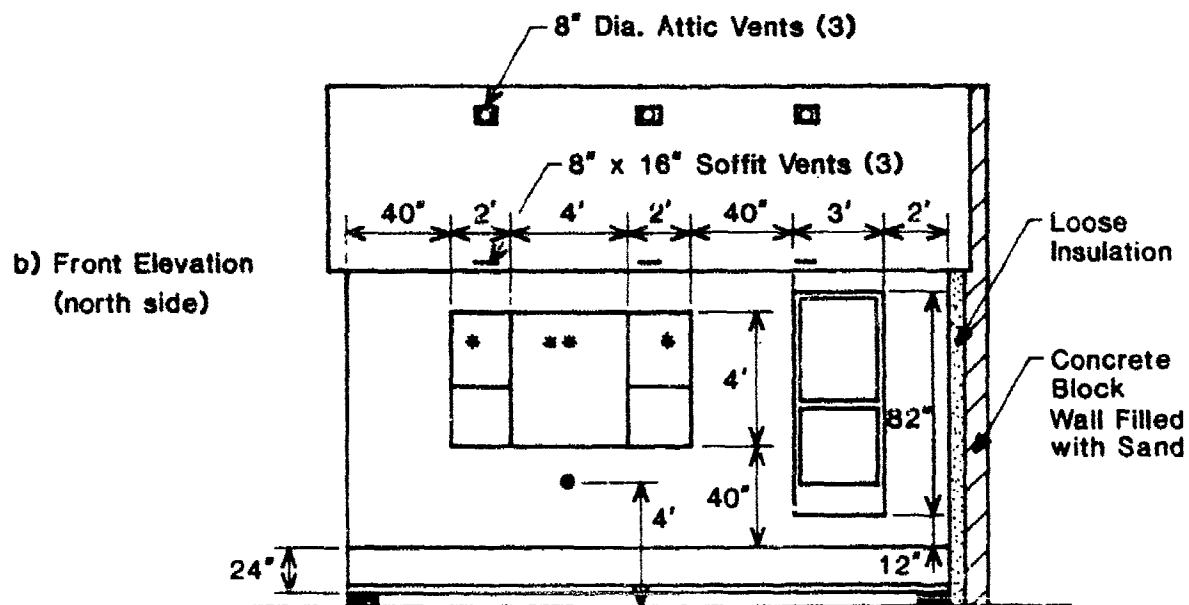
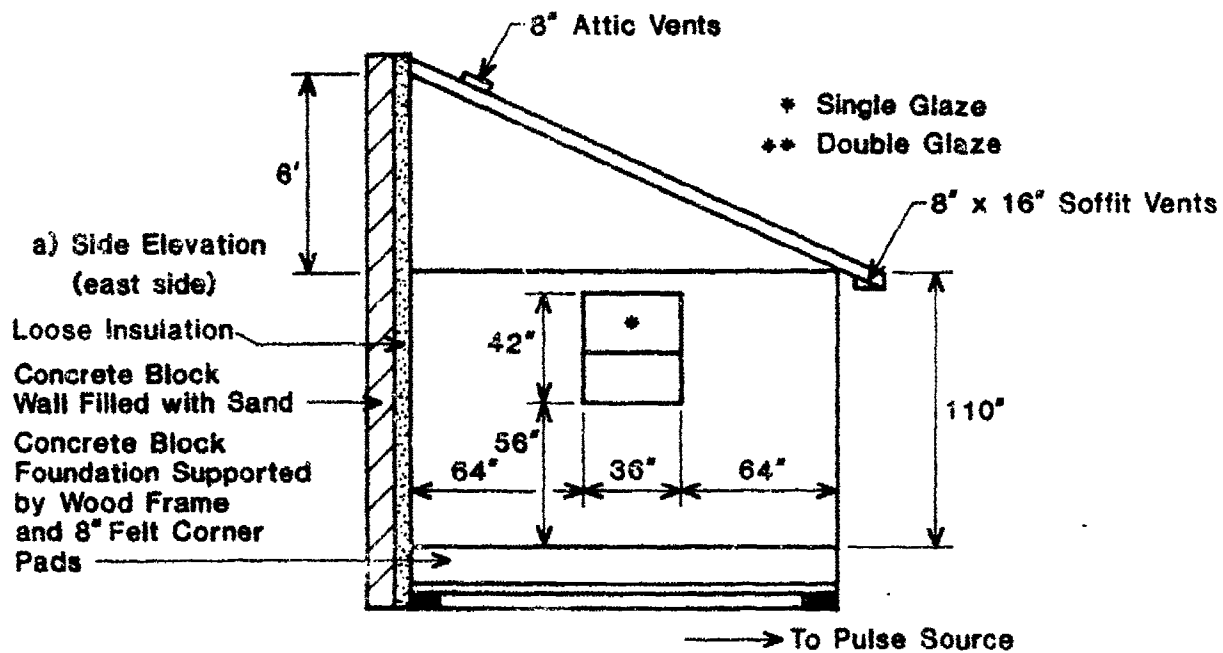


Figure 2. Test house exterior elevations. (Note: interior dimensions are 19 ft 3 in. by 13 ft 3 in. by 7 ft 11 in.)



Figure 3. Test house foundation detail showing corner felt pad, foundation support frame box, and two courses of cinder block.

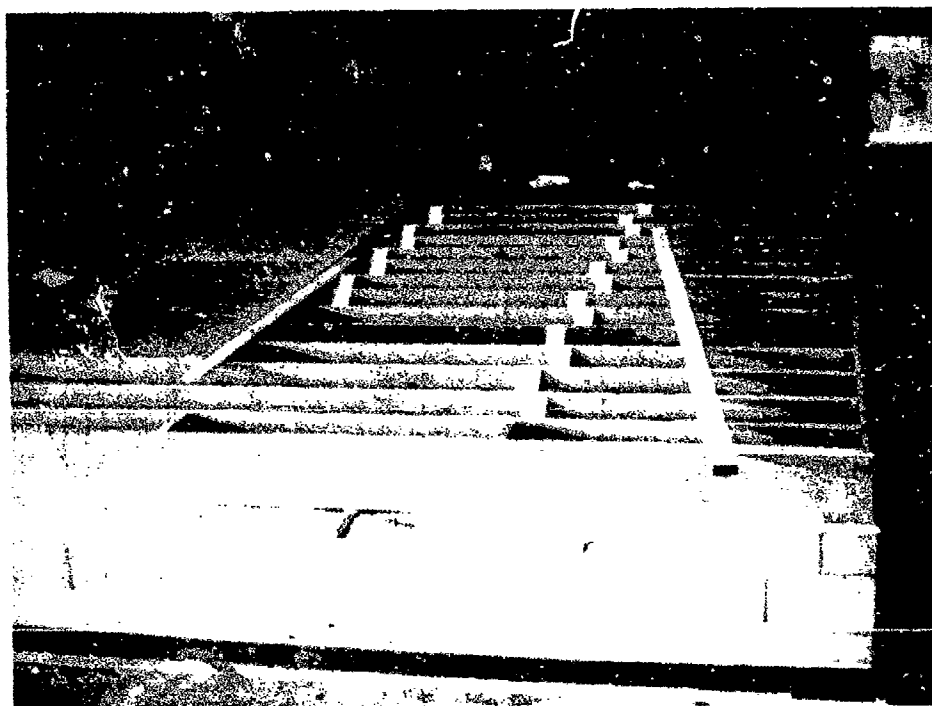


Figure 4. Test house floor framing on floating foundation.



Figure 5. Test house exterior sheathing showing window and door openings and roof trusses. (Note: arrows point to "v" brace in the easternmost roof truss.)

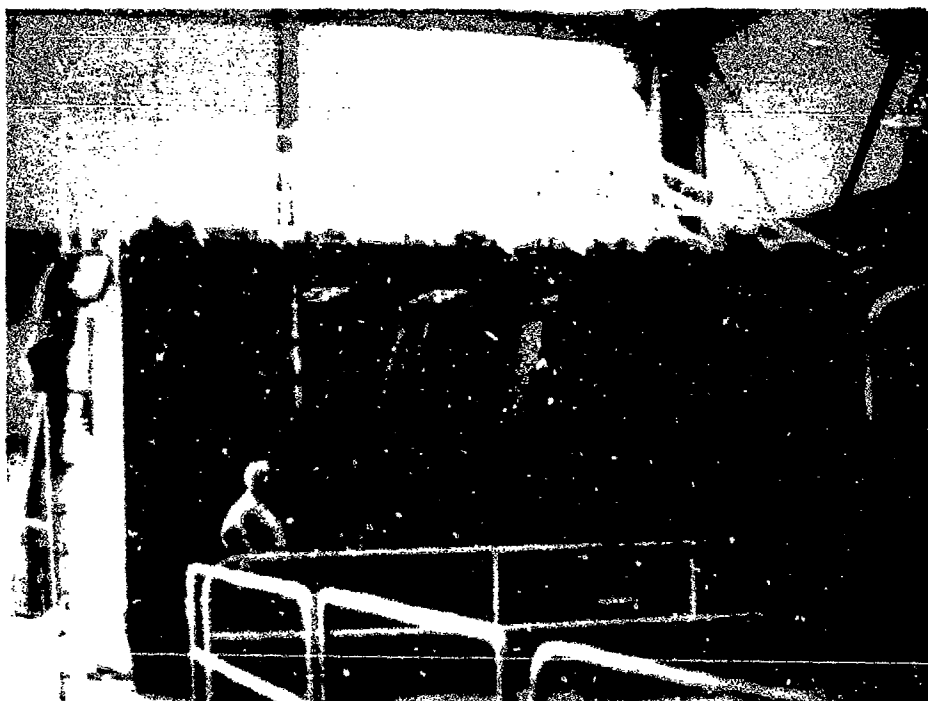


Figure 6. Test house exterior with foundation, sheathing, and roof trusses.



Figure 7. Test house exterior with clapboards and shingles before concrete block shielding walls were constructed.

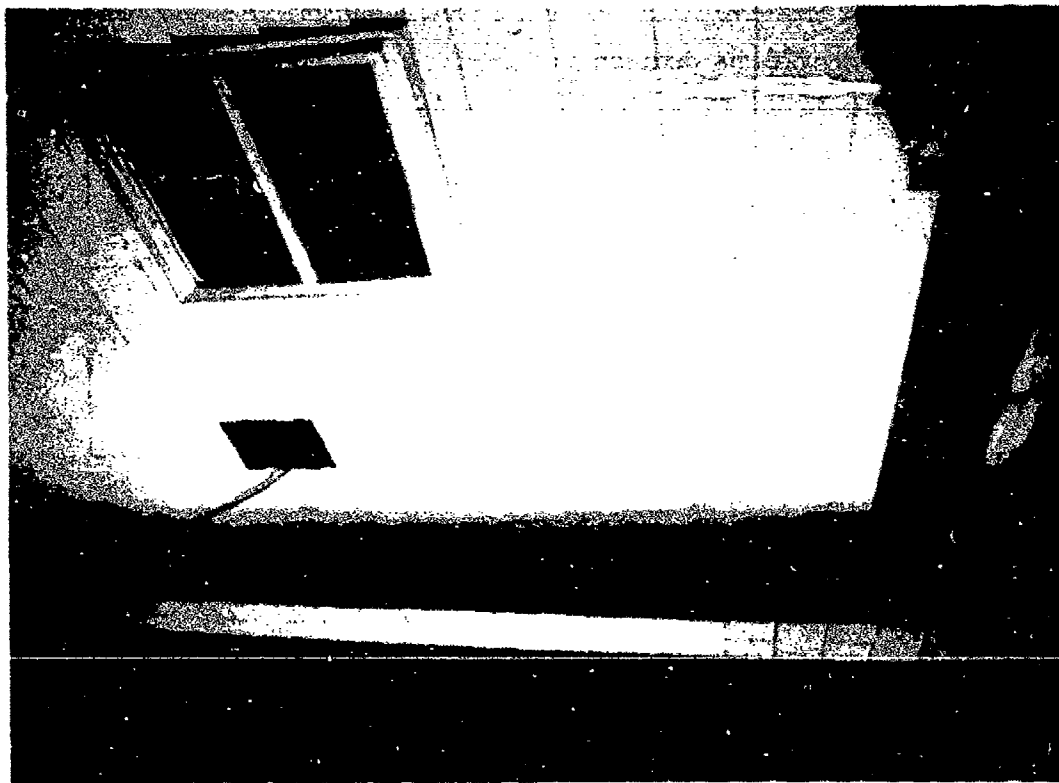


Figure 8. Test house west side finished exterior with concrete block shielding for south wall extending beyond west wall outer surface.

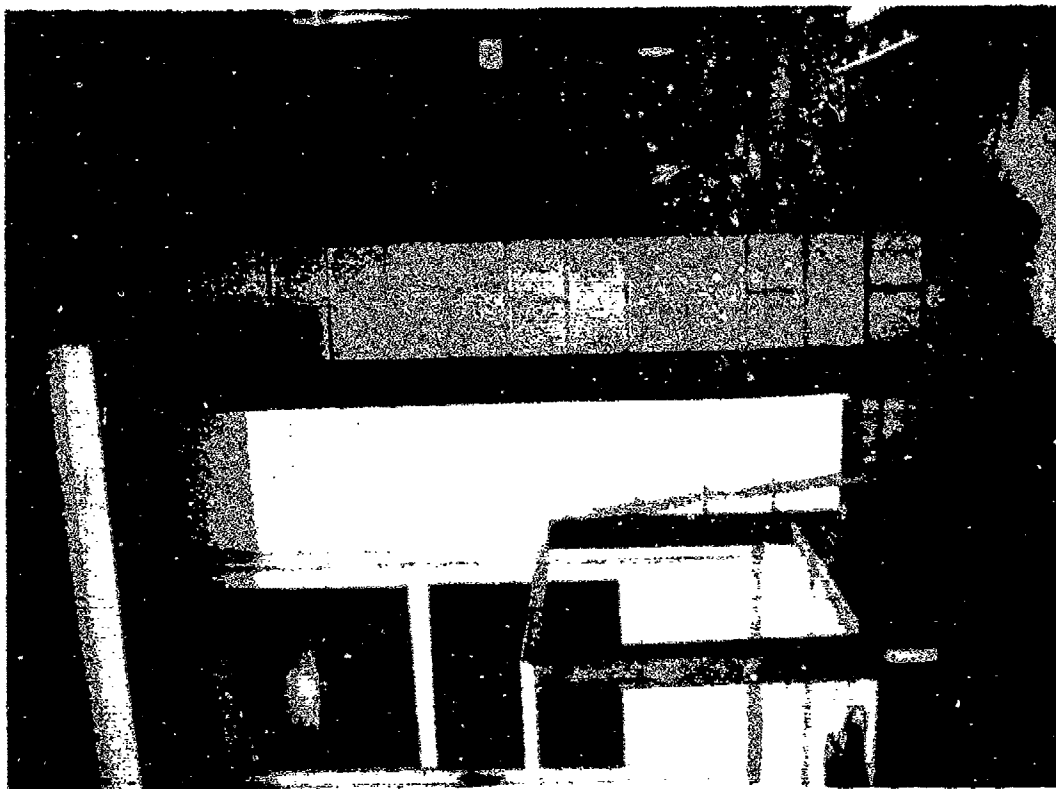


Figure 9. Test house northeast corner with finished exterior and concrete block shielding for east wall and beginning of loose insulation in gap between house and shield wall.

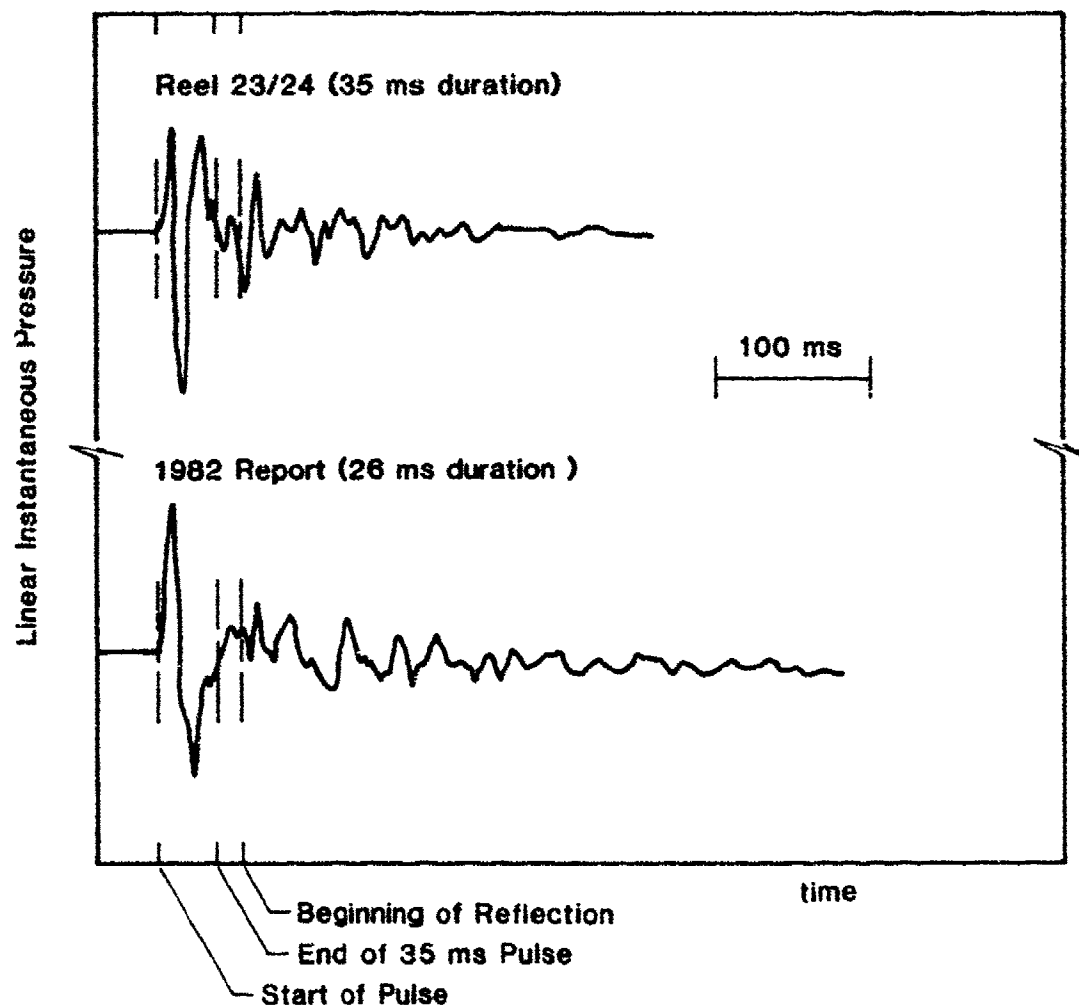


Figure 10. Time history of two simulated blast acoustic pressure pulses, one representing the data in reels 23 and 24 and the other from early tests in the program.

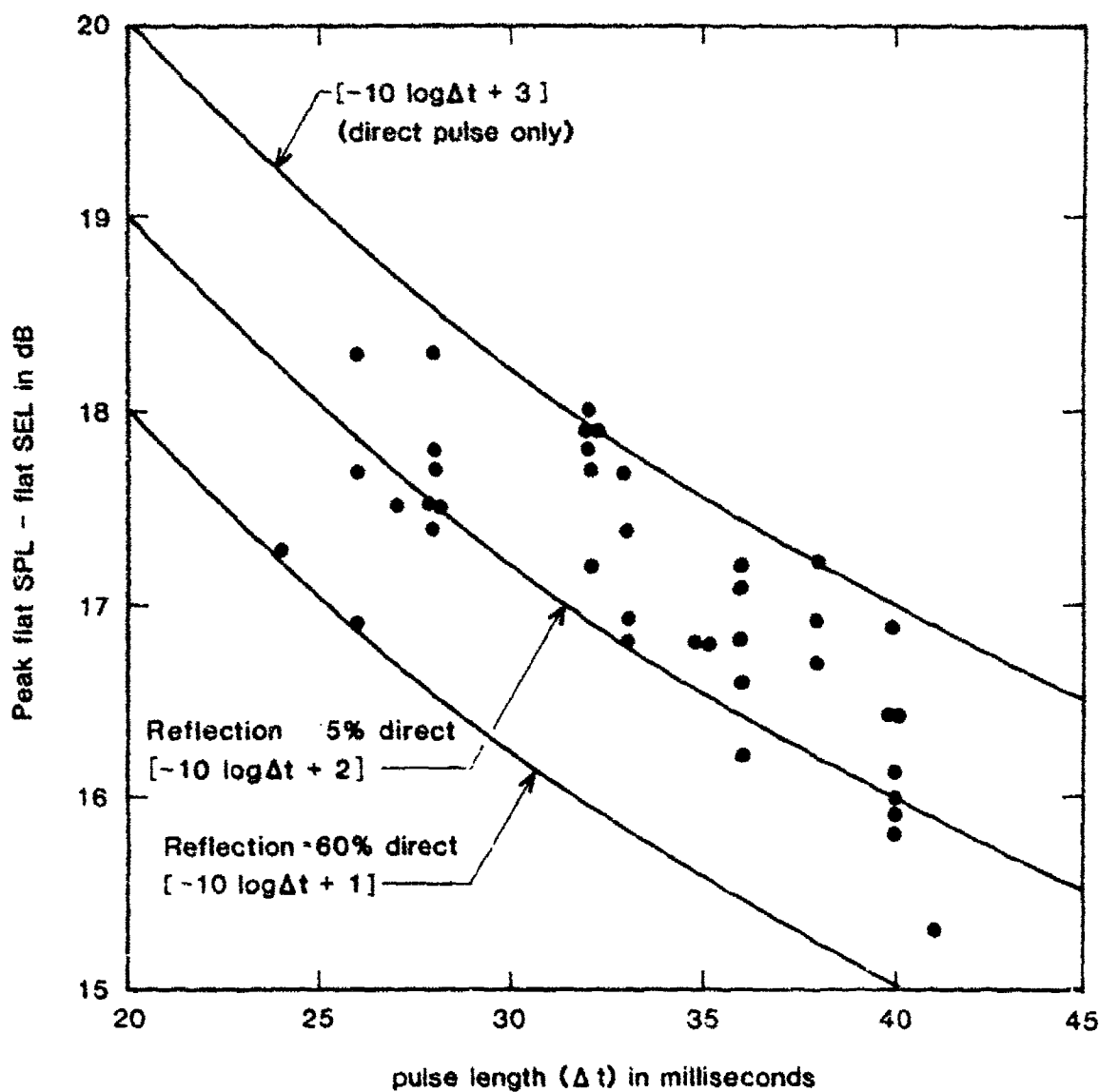


Figure 11. Difference between flat peak sound pressure level (PSPL) and flat sound exposure level (SEL) of simulated blast pulses from reels 23 and 24. The curves bracket a simple approximate theoretical relationship, with the upper curve accounting for the sound exposure estimated for the direct pulse only, and the lower curves allowing for the reflected pulses to have 25 percent and 60 percent of the sound exposure in the direct pulse.

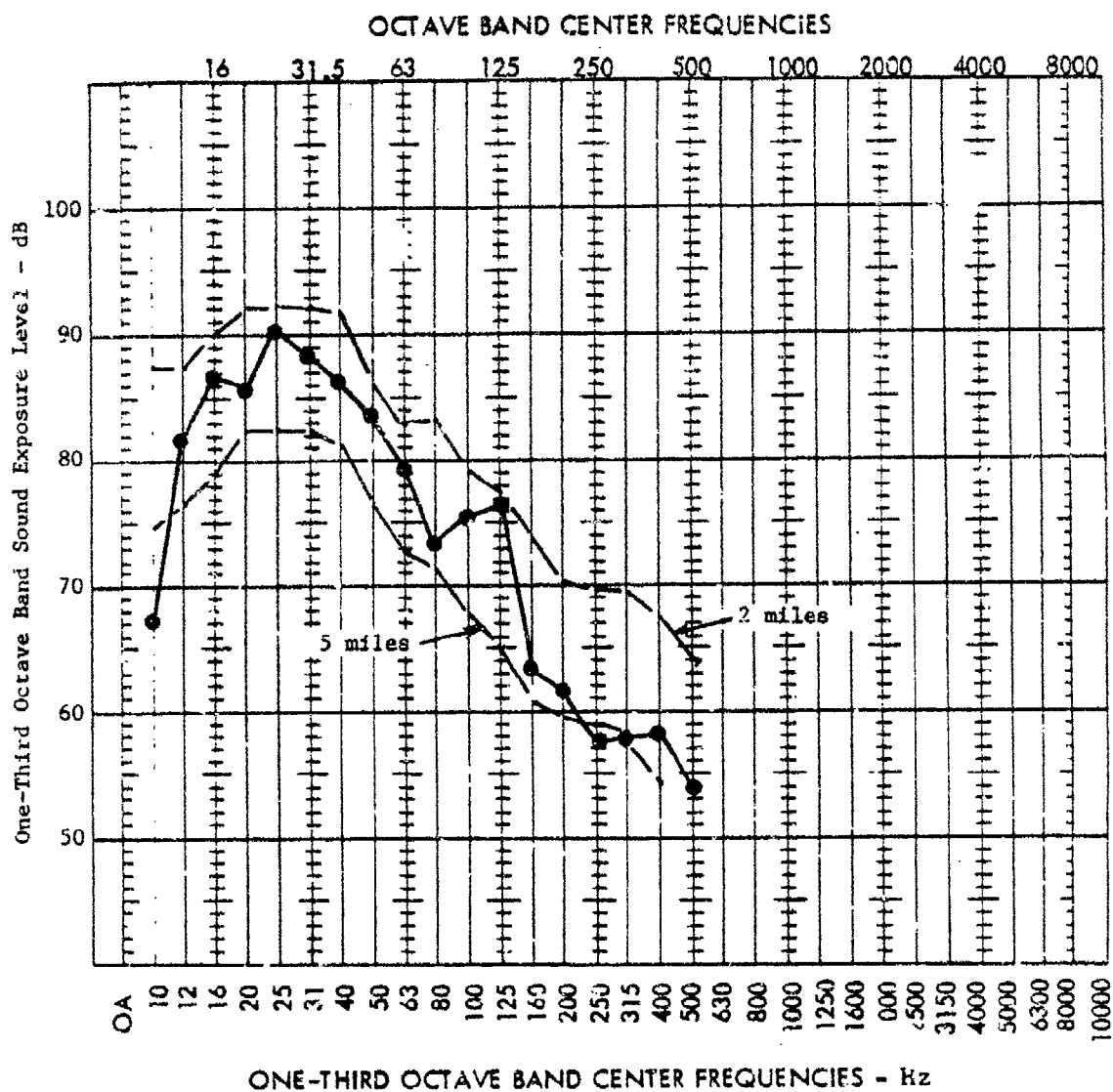


Figure 12. Comparison of 3EL spectrum of simulated blast acoustic pressure pulse with average values from 2-kg charges at 2- and 5-mi distances. The simulated pulse (reel 23, test 10) has 112.4 dB peak SPL, 95.8 dB SEL, and a 37-msec duration after correction by -6 dB for pressure doubling at the reference exterior position.

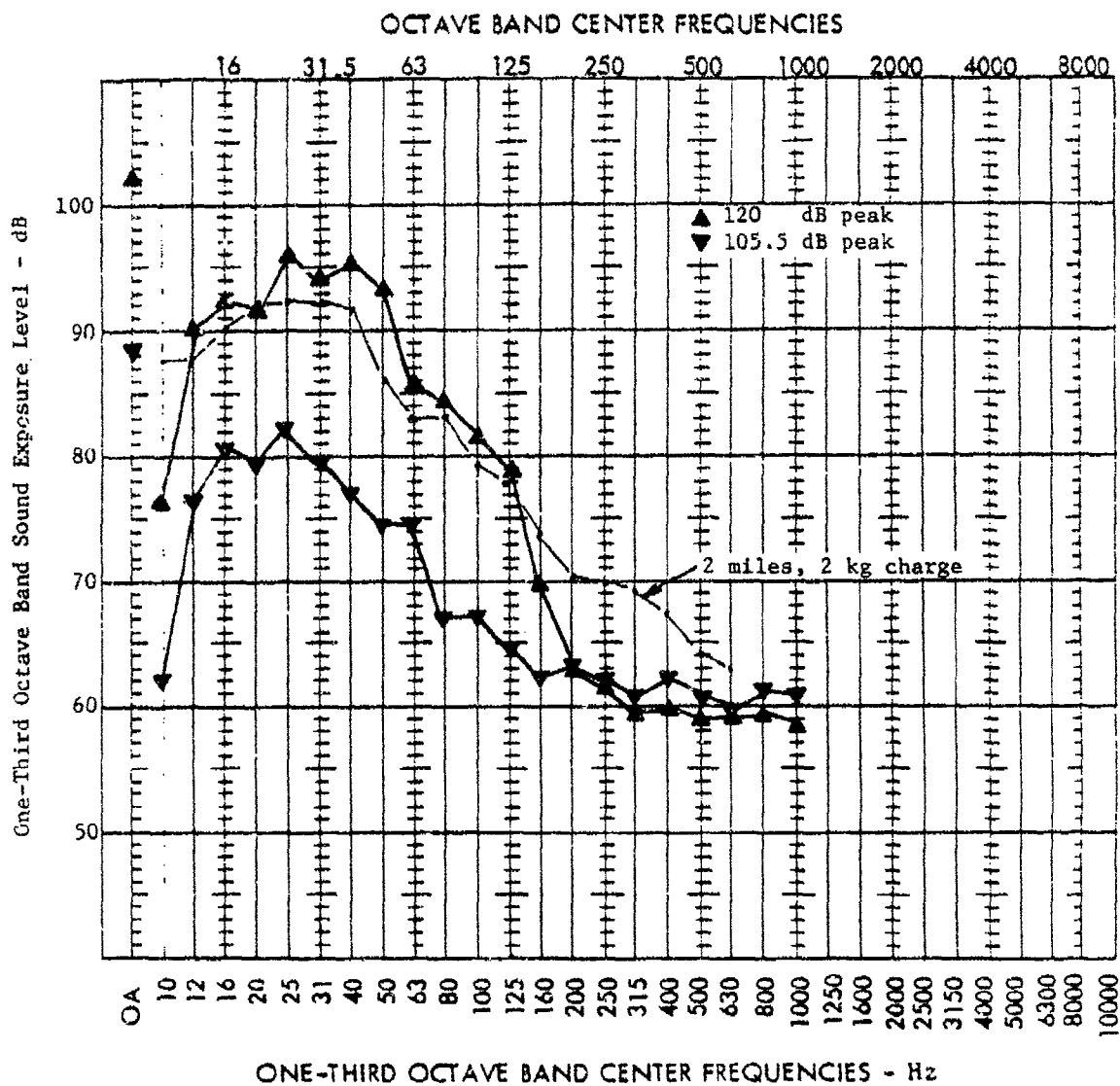


Figure 13. Example of the range of SEL spectra for simulation of blast acoustic pressure pulses with the average spectrum at 2 mi from a 2-kg charge for reference. The 120-dB peak spectrum was measured directly from the microphone in 1984 and the 105.5-dB spectrum was test 5 on reel 23. Both were corrected by -6 dB for pressure doubling at the reference exterior position.

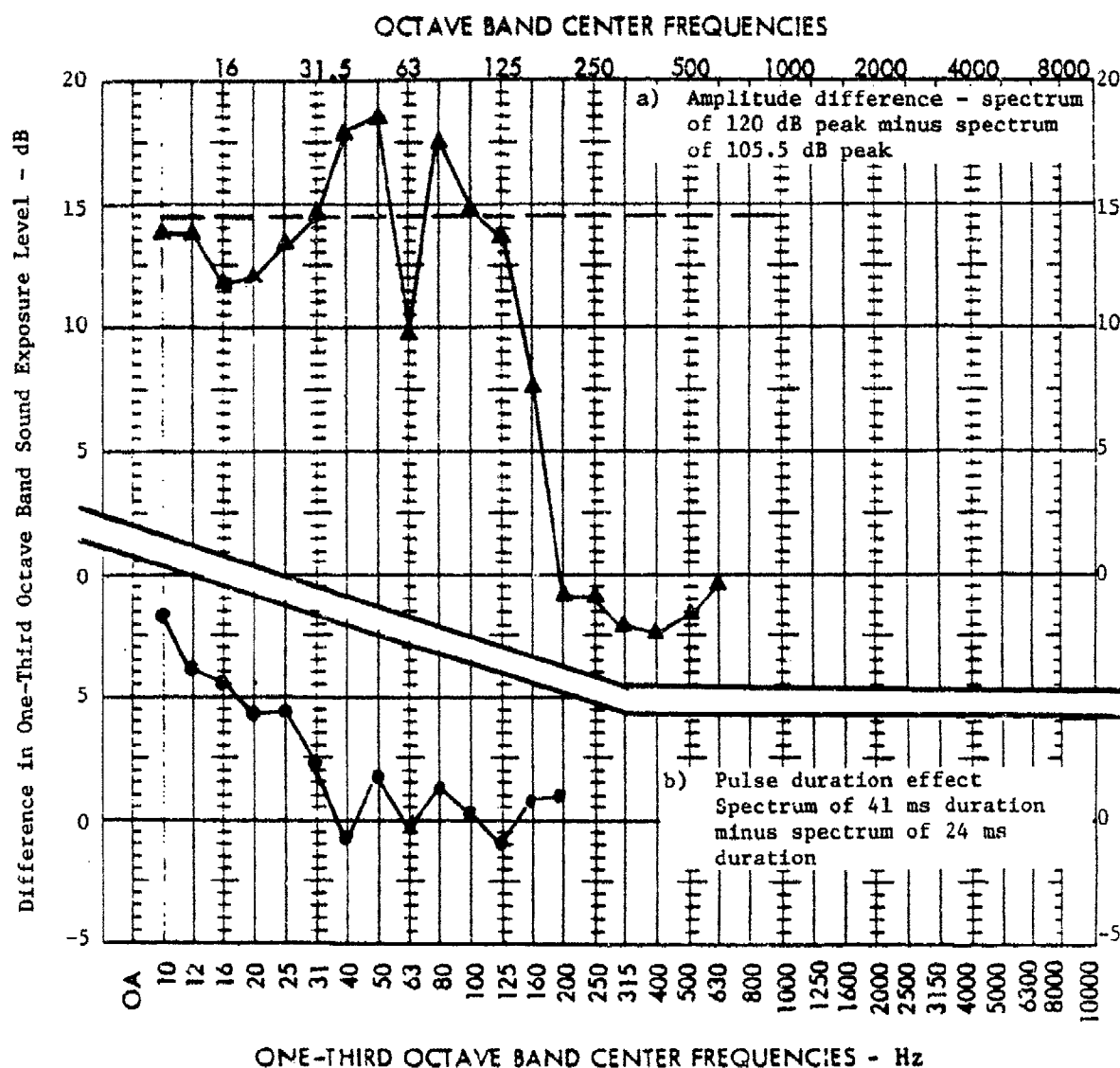


Figure 14. Example range of control over SEL spectra for simulated blast acoustic pulses for: (a) difference of spectra in Figure 13 and (b) difference between a spectrum with 41-msec duration (reel 24, test 8) and a spectrum with 24-msec duration (reel 24, test 9) after adjustment to to the same peak level.

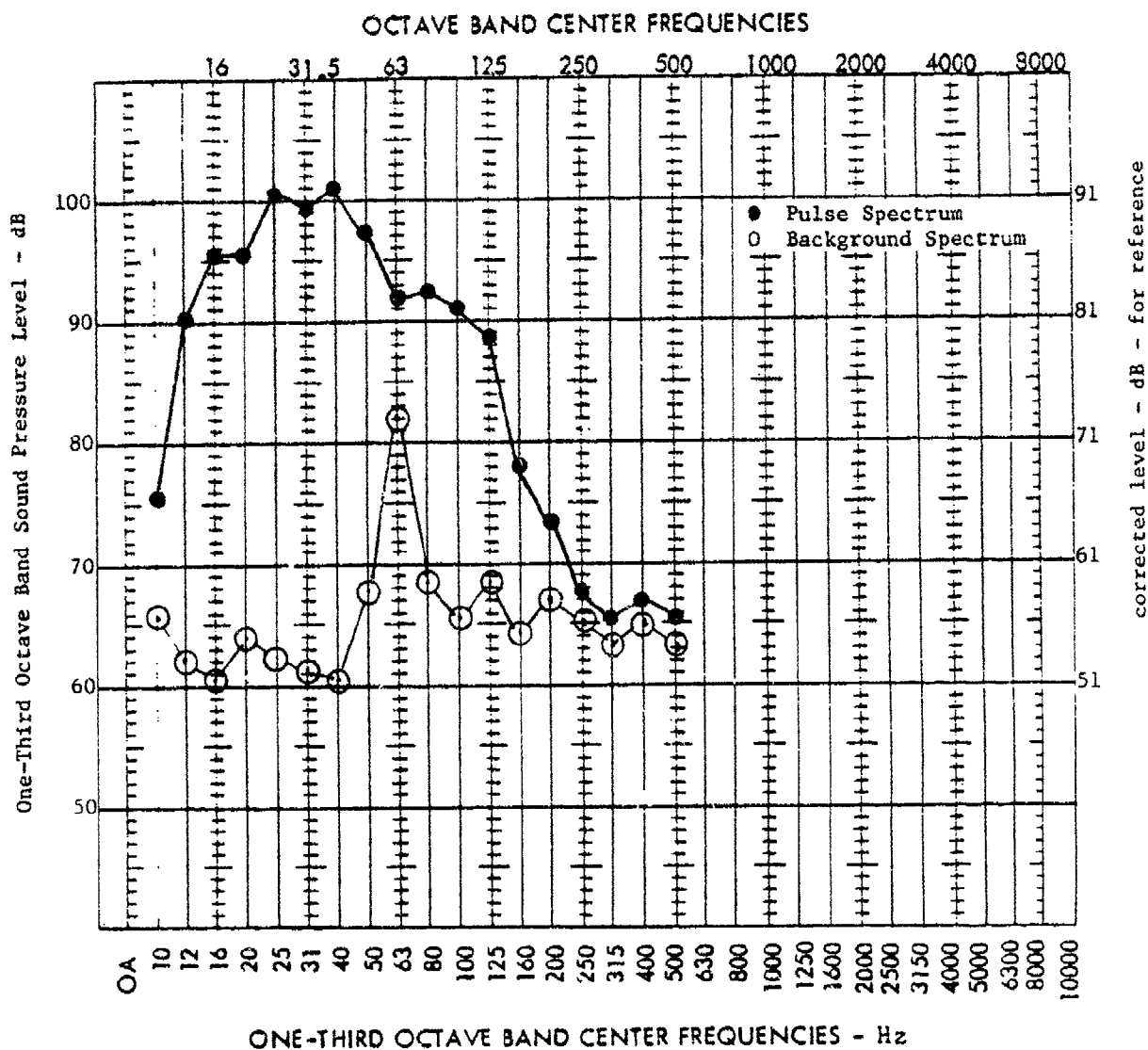


Figure 15. Comparison of measured spectrum of simulated blast acoustic pressure pulse with measured background noise immediately following pulse (reel 24, test 2). The levels are "as measured" without correction to SEL (-3 dB) or pressure doubling (-6 dB).

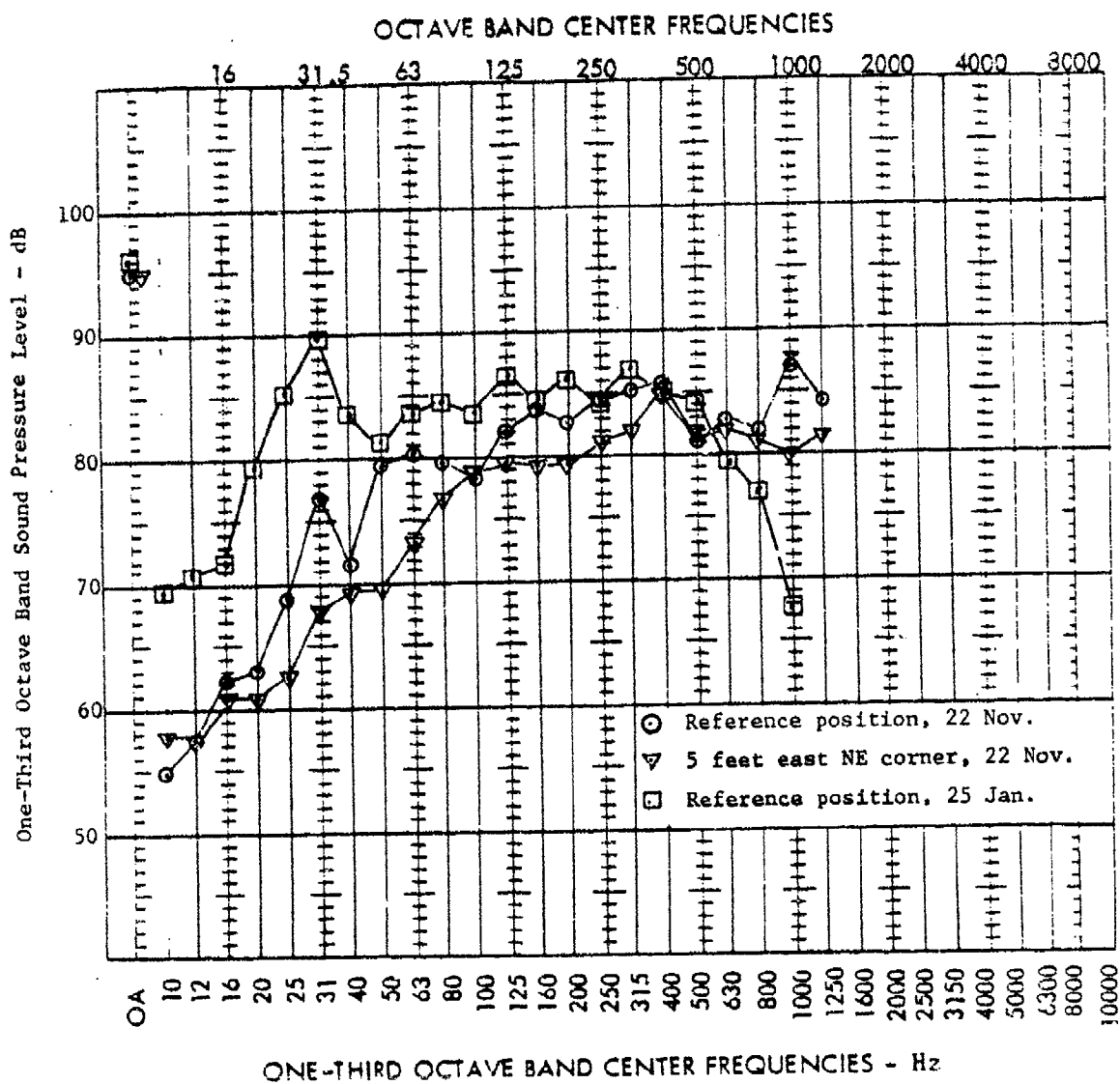


Figure 16. Loudspeaker spectra for the reference exterior position and a location 5 ft east of the northeast corner of the test house on 22 November 1983 and for the reference exterior position on 25 January 1984.

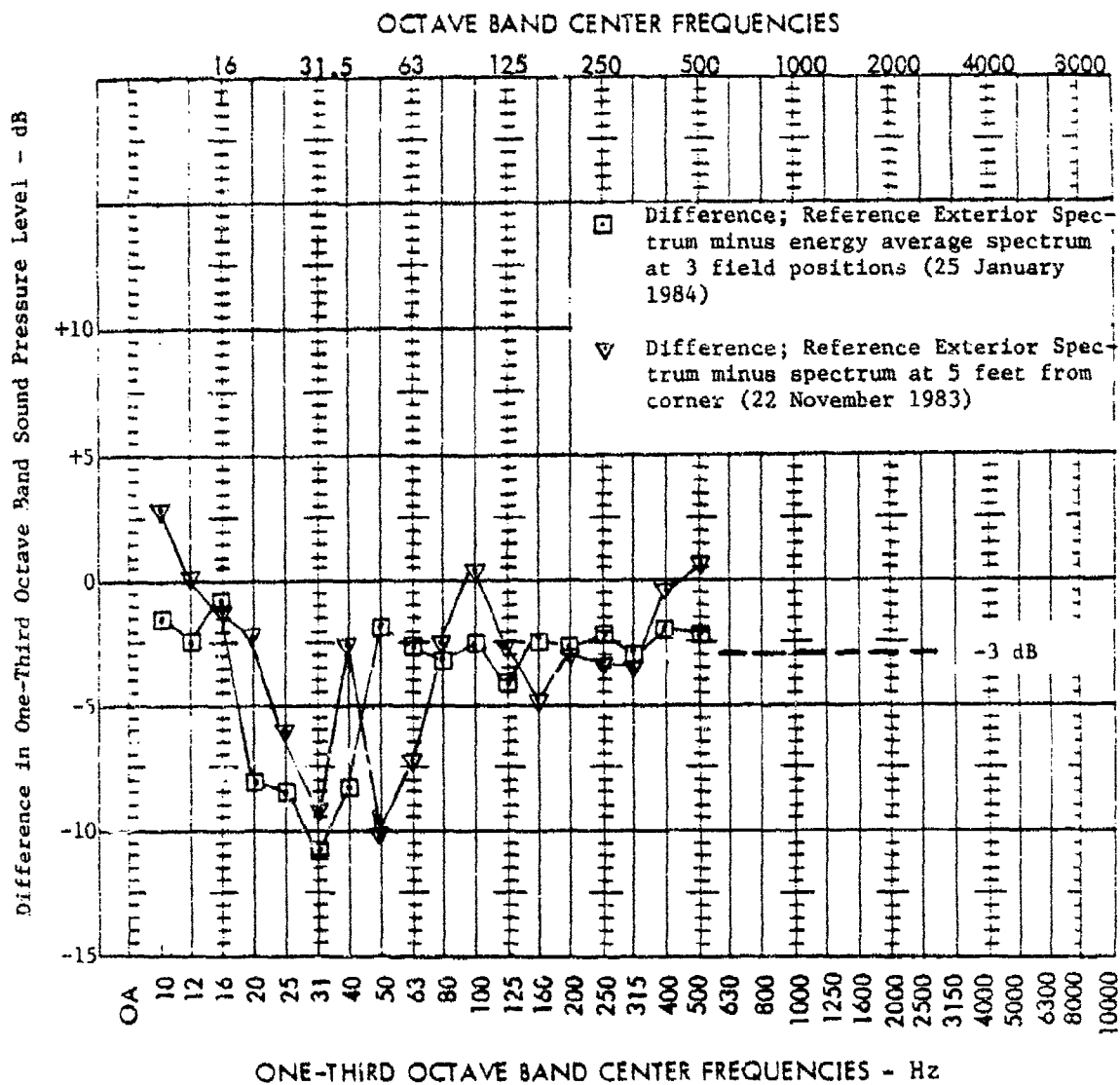


Figure 17. Loudspeaker comparison of differences between spectra at the reference exterior positions and positions away from the house surface.

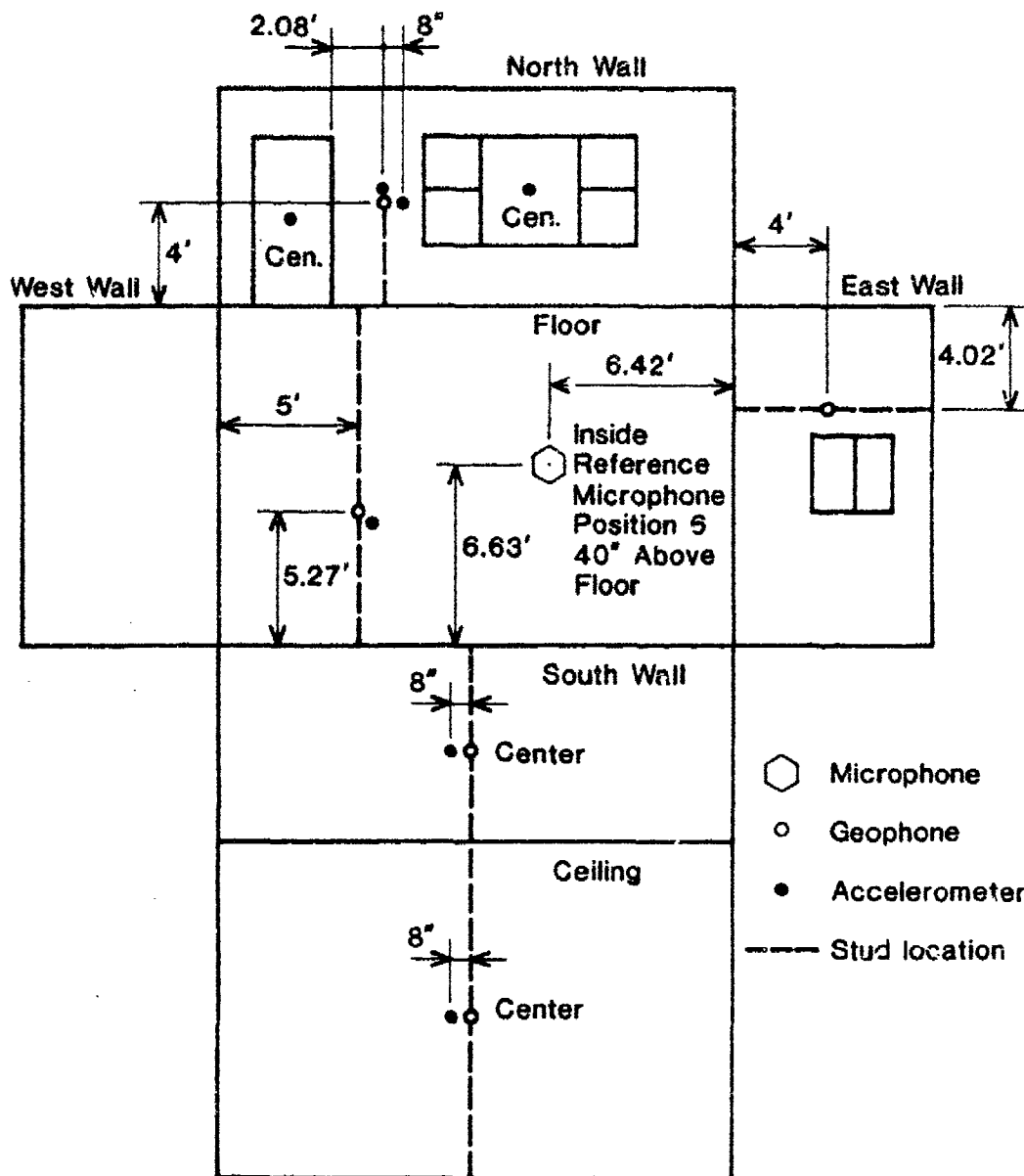


Figure 18. Inside room in test house unfolded to indicate principal standard transducer locations. Note: microphone position 6 was moved 6 in. west, 6 in. south, and 6 in. up for pink noise and reel 23/24 tests.

Table 1

Low-Frequency Room Modes for Test House Interior*

Frequency		Mode Number			1/3-Octave Band (Hz)
No.	Hz	L	W	H	
1	29.1	1	0	0	31.5
2*	42.3	0	1	0	40
3*	51.3	1	1	0	50
4	58.3	2	0	0	63
5	70.9	0	0	1	80
6*	71.9	2	1	0	80
7	76.5	1	0	1	80 (28.1 - 35.4)
8	82.4	0	0	1	80 (35.4 - 44.5)
9*	84.3	0	2	0	80 (44.5 - 56.1)
10	87.3	3	0	0	80 (56.1 - 70.7)
11**	87.4	1	1	1	80 (70.7 - 89.1)
12**	89.4	1	2	0	100
13	91.6	2	0	1	100
14*	97.0	3	1	0	100
15*	100.9	2	1	1	100
16*	102.6	2	2	0	100
17*	110.2	0	2	1	100 (89.1 - 112.2)

*Length = 19.25 ft, width = 13.25 ft, height = 7.92 ft.

**Modes coupling well to north wall or its components (e. g., picture window or door).

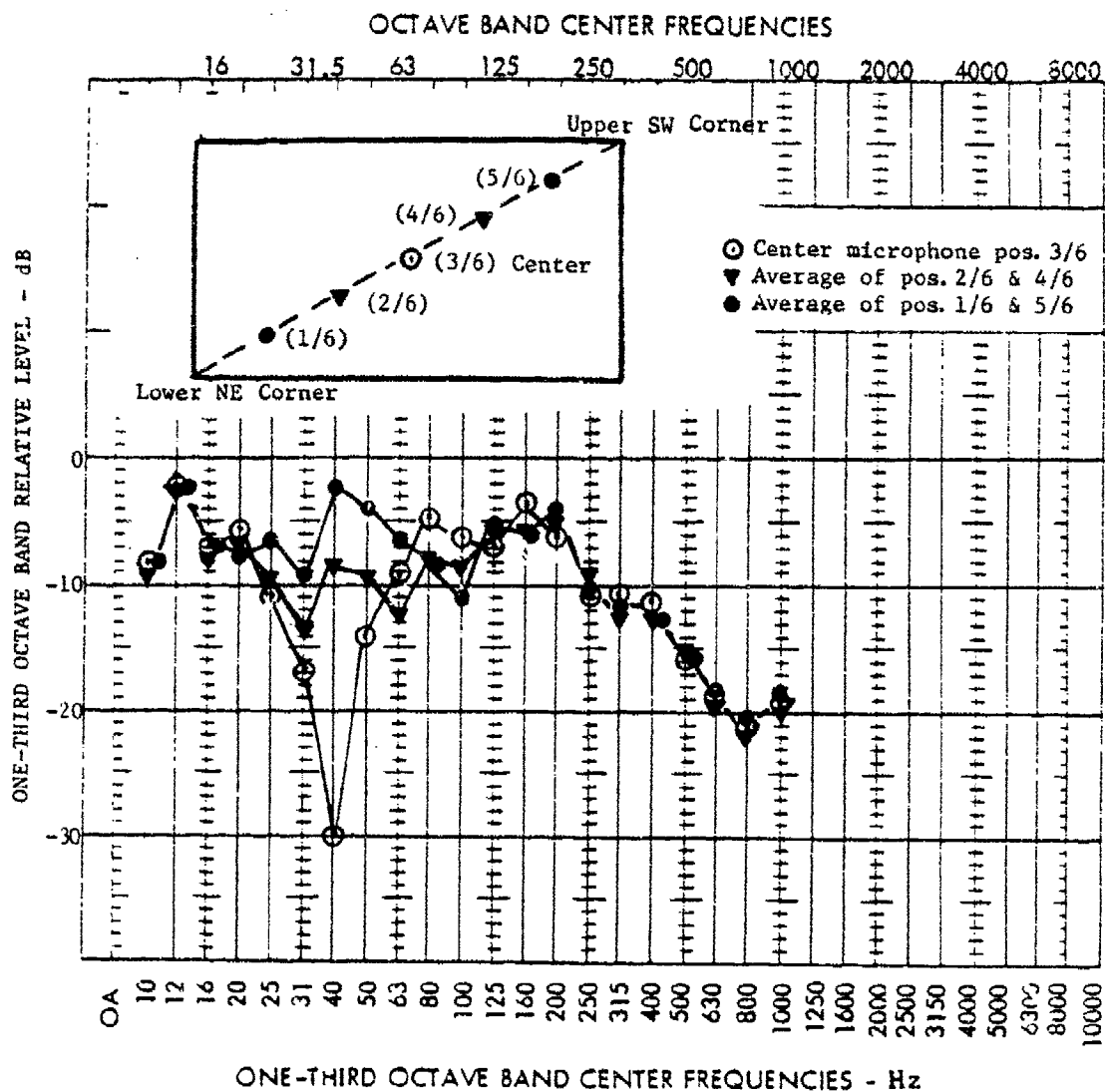


Figure 19. Relative response to external pink noise inside test house at five positions (1/6. . . and 5/6) along a diagonal that extends from a lower northeast (NE) exposed corner to the upper southwest (SW) shielded corner.

Table 2

Estimated Test House Component Parameters and Dynamic Characteristics

Component	L (ft)	W (ft)	Surface Mass (lb/sq ft)	f_{11}^* (Hz)	f_D (Hz)	f_c (Hz)	f_r (Hz)	Comments
Picture window	4.08	3.67	1.63 (ea.)	11.3**	<300	3750	163	2 layers double-strength glass with 1/2-in. airspace.
N. sash with storm	1.97	1.65	1.22 (ea.)	39.6**	150**	5000	350	Sash and storm window panes are single-strength with 2 in. airspace.
E. sash with storm	2.64	1.31	1.22 (ea.)	46.0	150**	5000	340	Same as N. sash above.
Door with storm	6.65	3.0	3.9*** and 1.4***	12-75	<96	~560**	141	Solid-core door and storm door with glass and approximately 3-in. airspace.
N. & E. walls (typical vertical section)	19.25 13.25	7.92 7.92	8.0	20** (Avg.) 197 (Gyp.)	N/A	3150 (Gyp.)	N/A	2x4 inch studs with insulation and with 1/2-in. gypboard on inside and 1/2-in. regular sheathing covered with particle board clapboards on outside and insulation.
S. & W. walls (shielding)			53 (CB) 6.0 (inner)	Various	30		N/A	Same as north wall except no clapboards, with 6-in. fiberglass-filled airspace and sand-filled 8-in. cinder-block wall.

Table 2 (Cont'd)

Component	L (ft)	W (ft)	Surface Mass (lb/sq ft)	f ₁₁ * (Hz)	f _D (Hz)	f _c (Hz)	f _r (Hz)	Comments
Ceiling	19.25	13.25	4.83	16.1	N/A	3160 (Gyp.)	N/A	2x6 inch joists on 16-in. centers with 1x3 battens surfaced with 1/2-in. gypboard (without truss).
Roof	19.25	14.55	5.36	6.7 - 26.8	N/A	N/A	N/A	Asphalt shingles and tar paper on 3/4-in. plywood and 2x4 in. rafters in trusses on 2-ft centers
Ceiling and roof				12.3**	15	N/A	N/A	Combining ceiling and roof at low frequencies, assuming "v" brace is a simple link.
Floor	19.25	13.25	9.65	24**		N/A	N/A	3/4-in. particle board over 1/2-in. plywood subfloor with 2x10 in. joists 16-in. on center.

*With pinned supports.

**Confirmed by experiment.

***Data are from L. C. Sutherland, Low Frequency Response of Structures, Wyle Research Report WR 82-18 (Wyle Laboratories, May 1982), and L. C. Sutherland, et al., Preliminary Evaluation of Low Frequency Noise and Vibration Reduction Retrofit Concepts for Wood Frame Structures, Wyle Research Report WR 83-26 (Wyle Laboratories, June 1983).

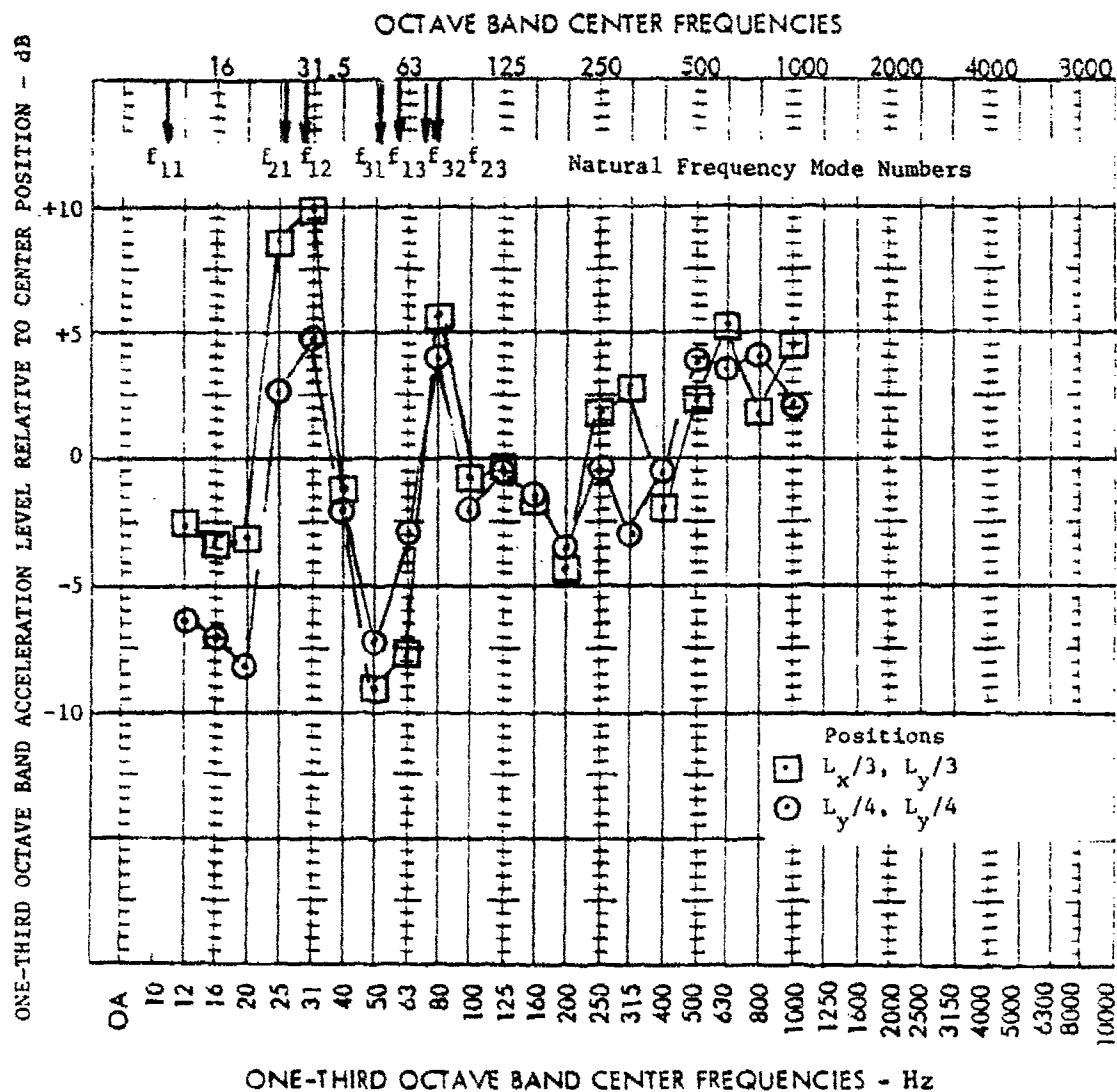


Figure 20. Picture window inner pane: 1/3-octave band acceleration levels at two off-center positions minus the level at the position at the center ($L_x/2, L_y/2$) of the window from pink noise tests in February 1984.

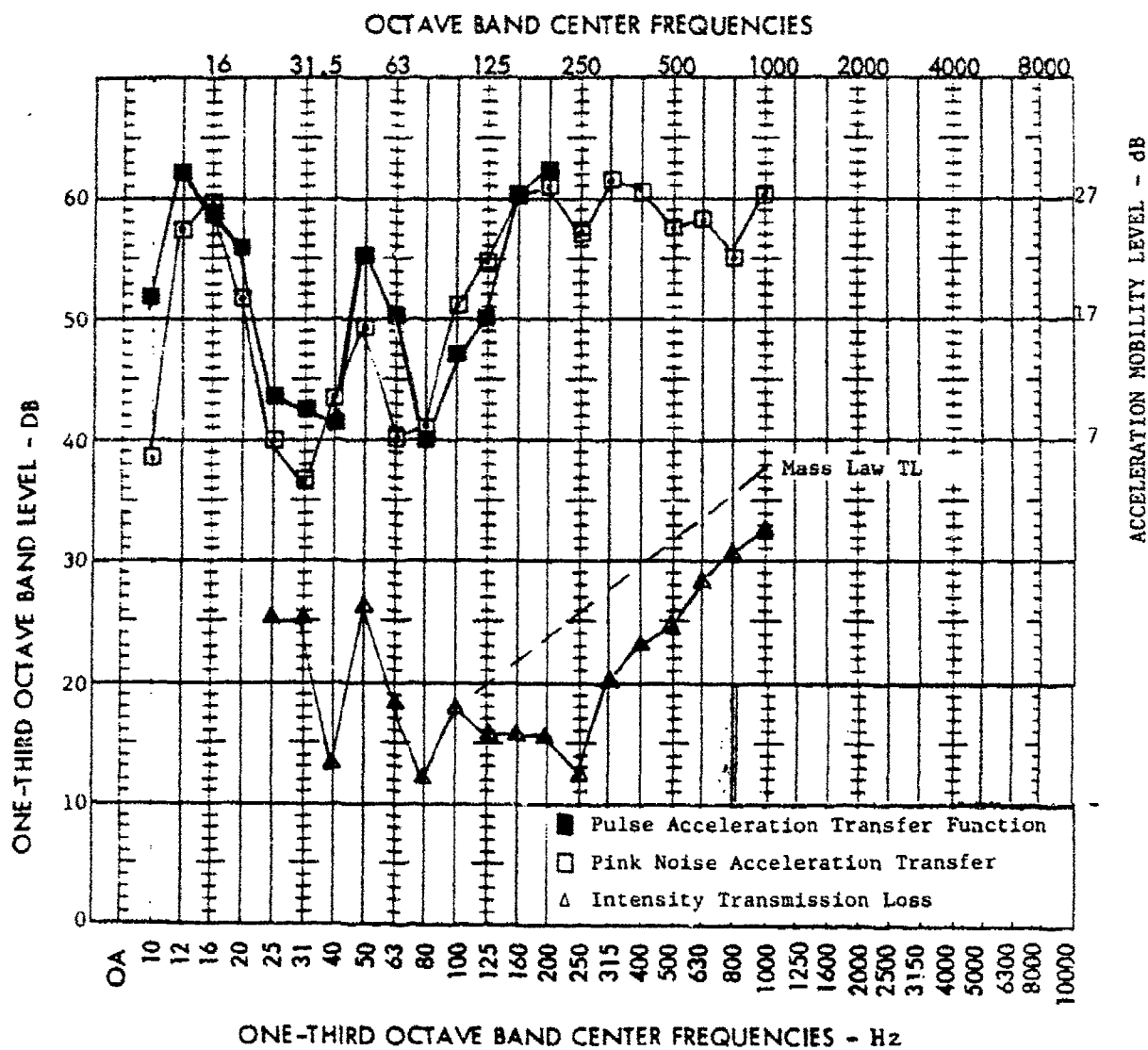


Figure 21. Picture window: (a) acceleration transfer function (acceleration in gravities [a/g] per psi) for a pulse at the center of the window (from reel 23, test 20) and pink noise at the center of the window (16 November 1983); (b) intensity transmission loss (18 January 1984).

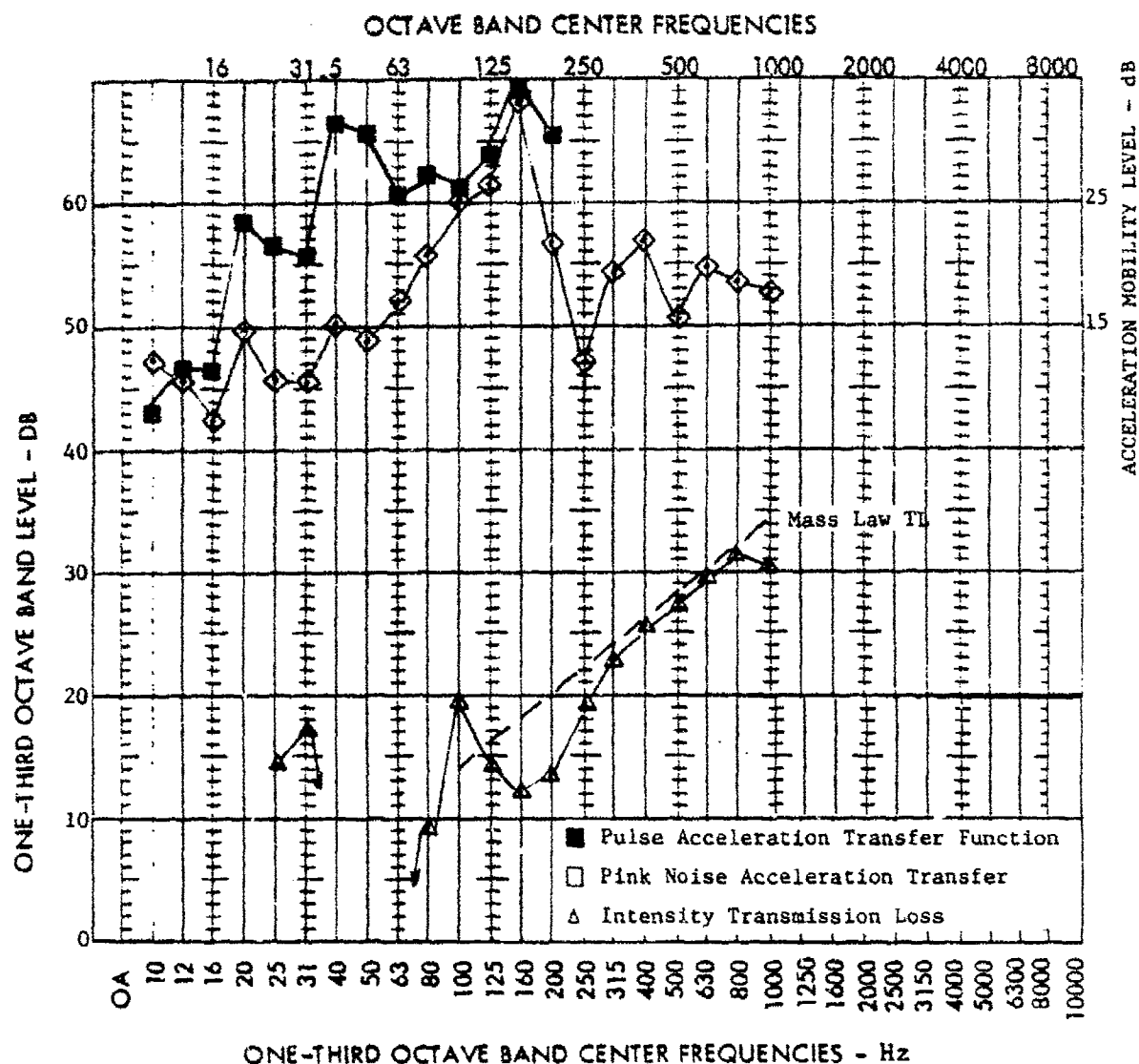


Figure 22. North wall sash windows with storm windows closed: (a) acceleration transfer function (a/g per psi) for a pulse at the center of one of the four panes (from reel 23, test 20) and pink noise at the center of one of the four panes (16 November 1983); (b) intensity transmission loss energy average for both north sash windows (18 January 1984).

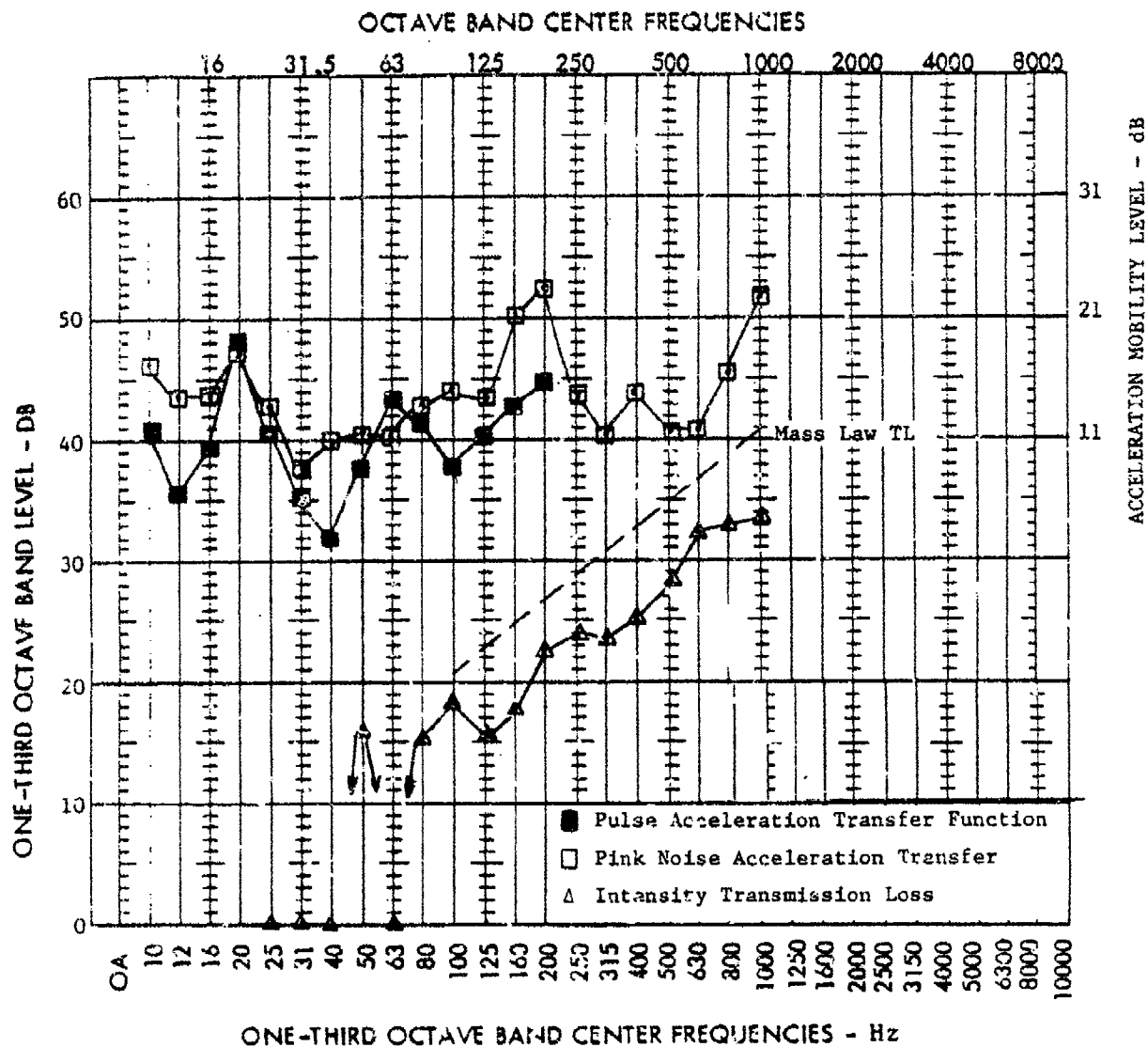


Figure 23. Front door with storm door closed: (a) acceleration transfer function (a/g per psi) for a pulse at the center of the door (from reel 23, test 20) and pink noise at the center of the door (16 November 1983); (b) intensity transmission loss (18 January 1984).

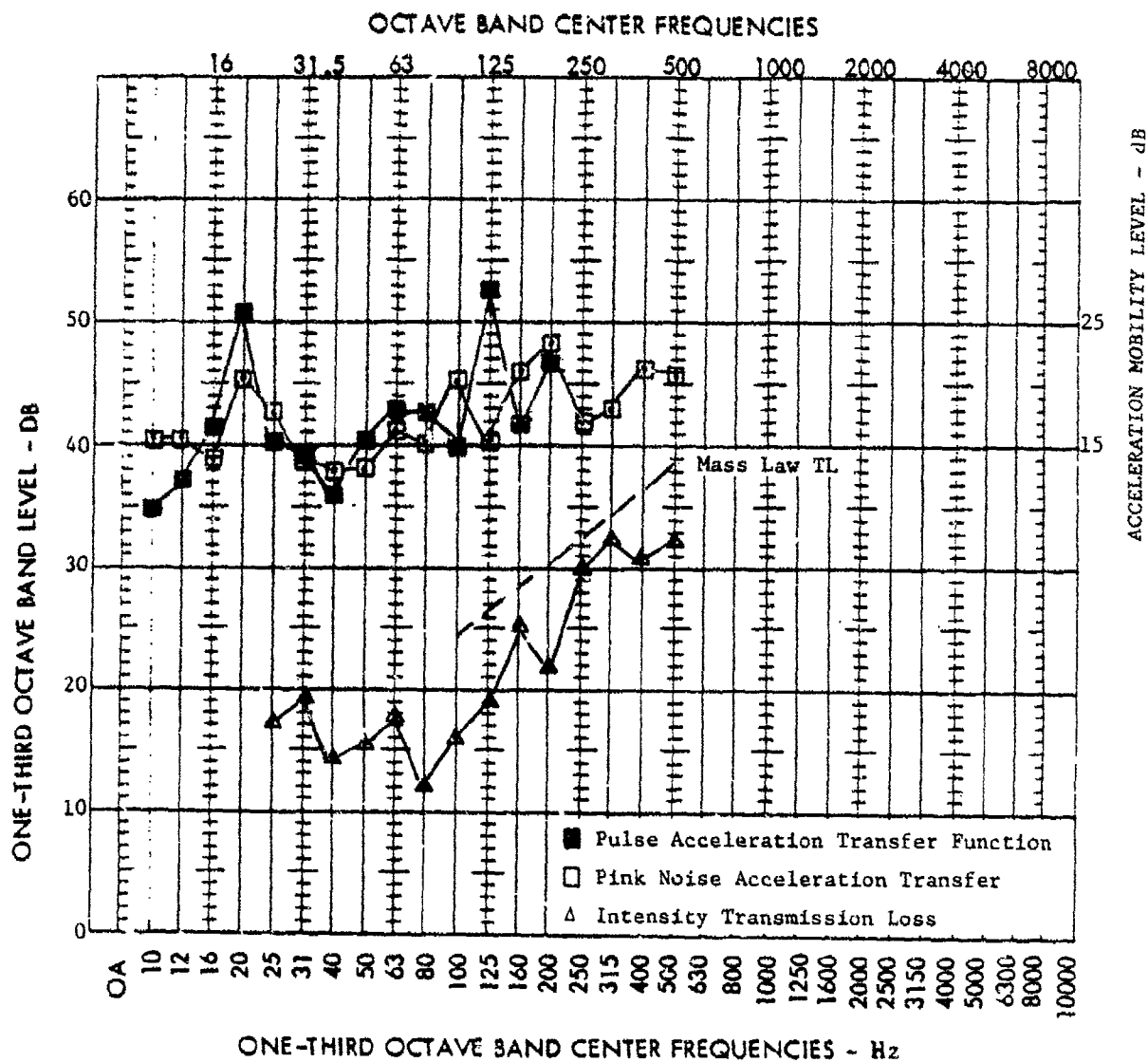


Figure 24. North wall: (a) acceleration transfer function (a/g per psi) for a pulse at a location on the stud (from reel 23, test 20) and (b) pink noise at a location on the stud (16 November 1983), intensity transmission loss for east panel (18 January 1984).

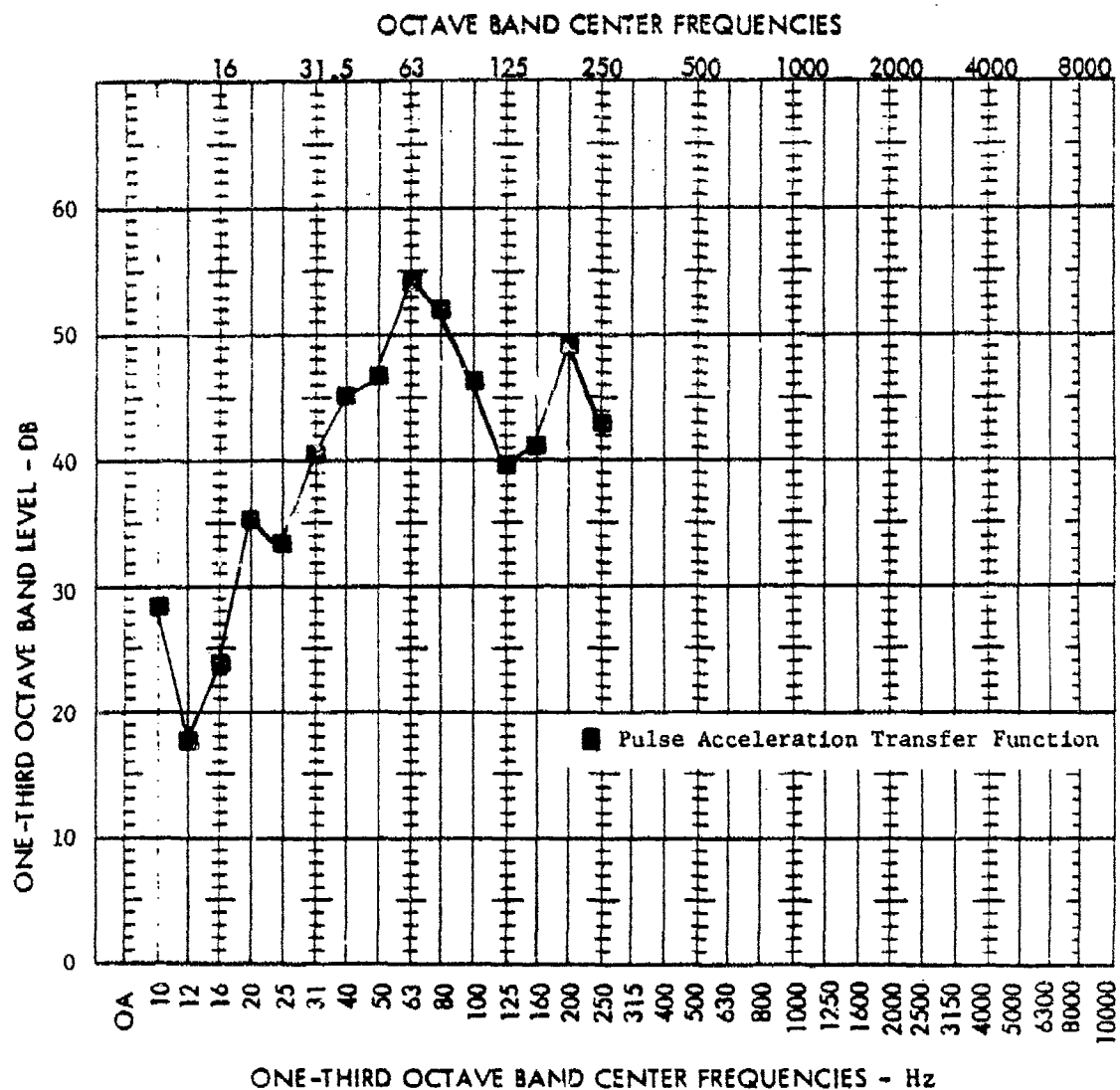


Figure 25. South wall: acceleration transfer function (a/g per psi) for pulse at a location between the studs (from reel 7, test 1).

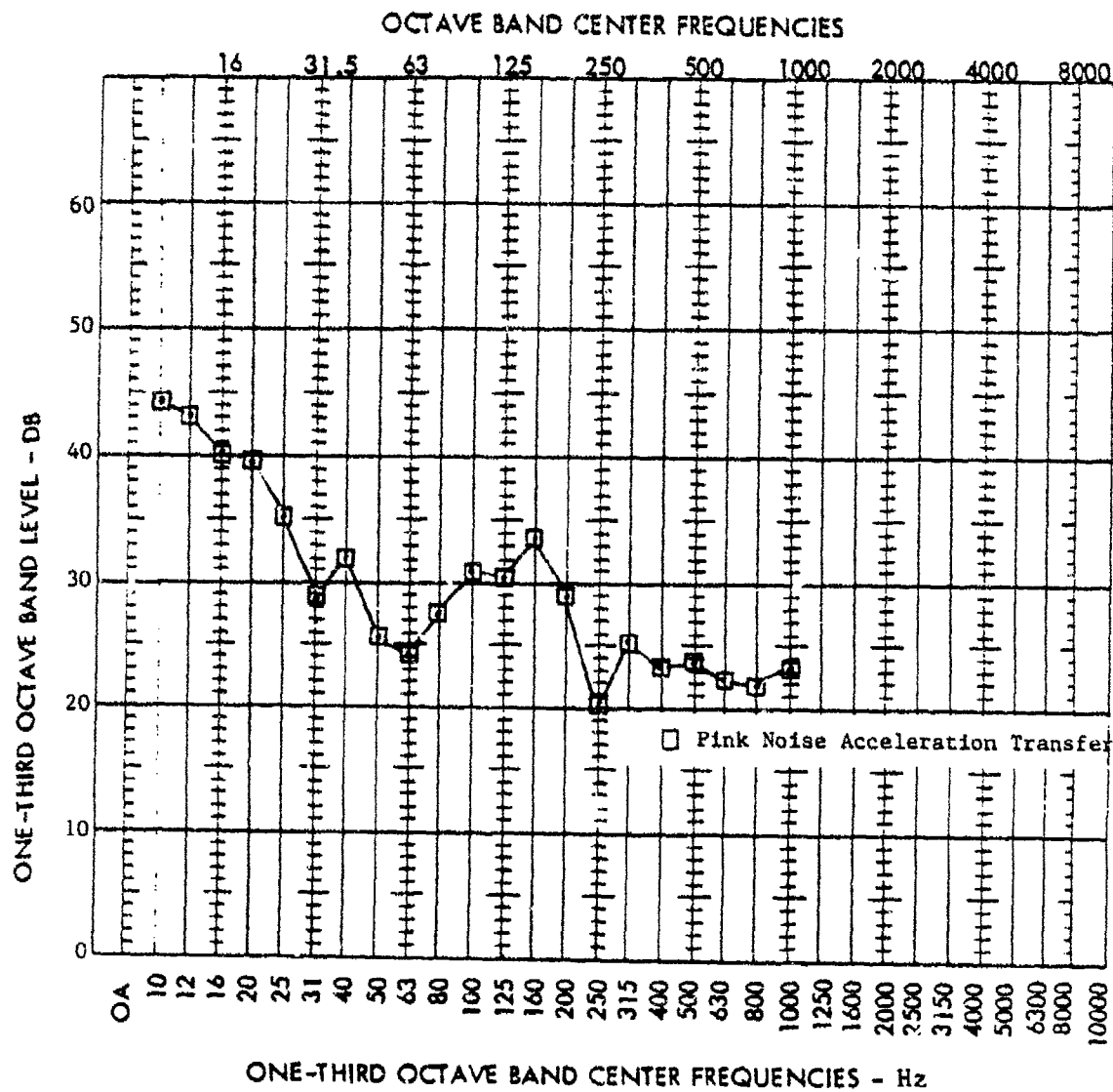


Figure 26. Floors: acceleration transfer function (a/g per psi) for pink noise at a location over the joist (16 November 1983).

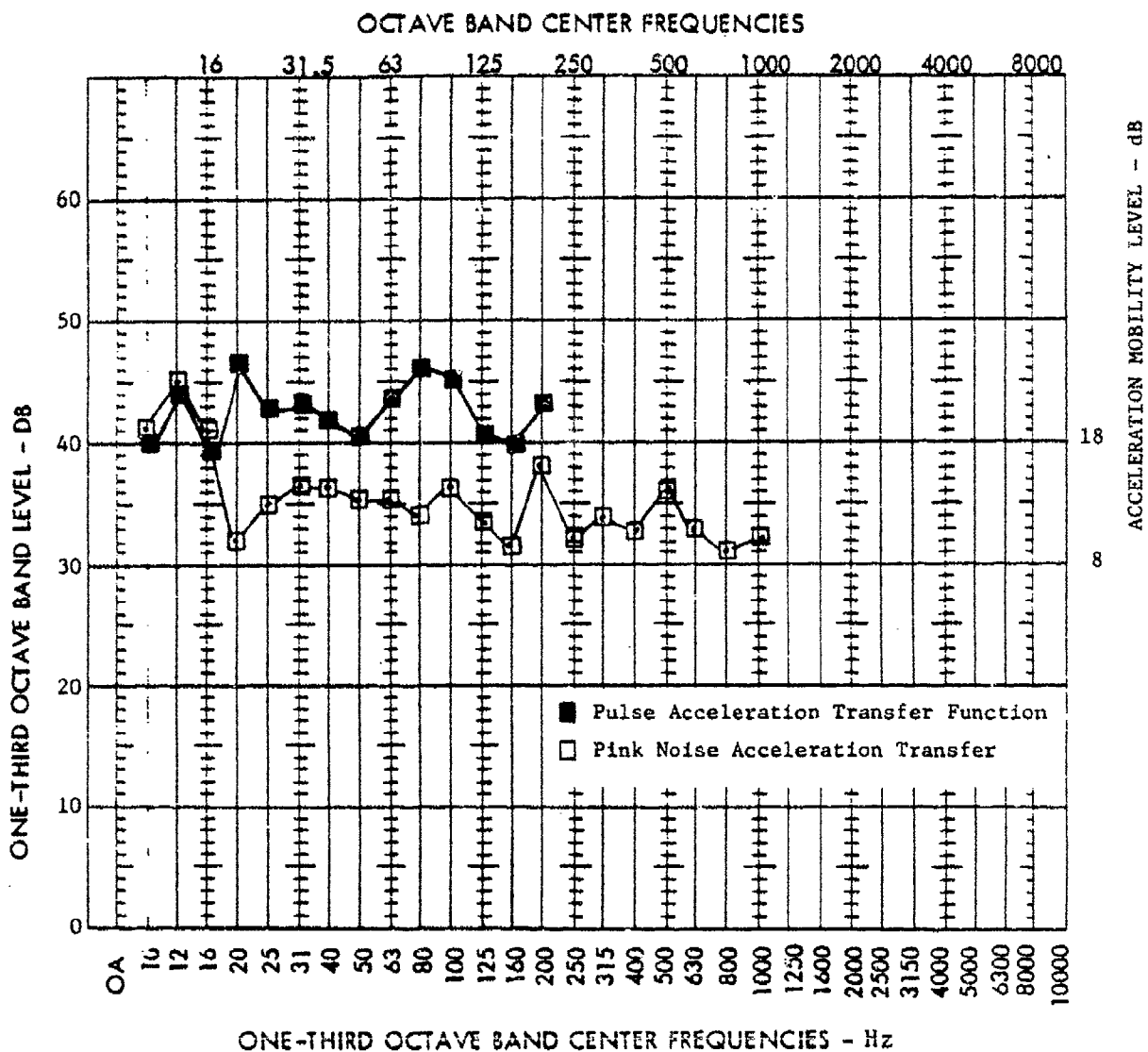


Figure 27. Ceiling: acceleration transfer function (a/g per psi) for a pulse at a location between joists (from reel 7, test 4) and pink noise at a location between joists (16 November 1983).

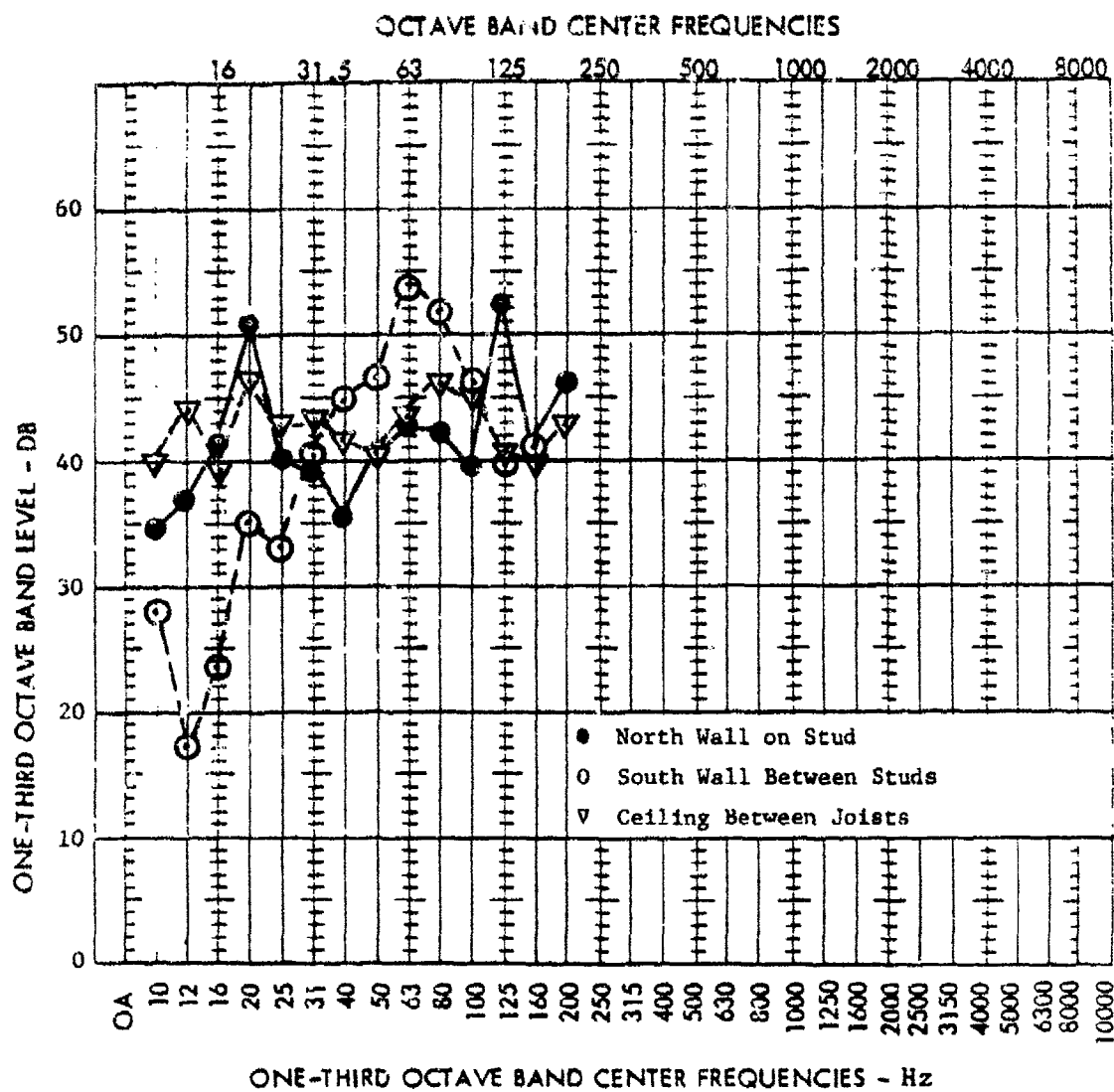


Figure 28. Comparison of pulse acceleration transfer functions for north and south walls and ceiling from Figures 23, 24, and 25.

Table 3

Partial Summary of Formulas Used for Response Calculations

1. Simply Supported Panel:

$$f_{nm} = 0.45 C_L h \left[\left(n/L_x \right)^2 + \left(m/L_y \right)^2 \right]$$

$$= 2\pi \sqrt{B/m/\gamma_b^2}$$

- where: f_{nm} = the frequency of the n:m mode in Hz
 C_L = the speed of sound in the material
 h = the thickness of the panel
 L_x, L_y = the length and width of the panel
 γ_b = the bending wavelength
 B = EI (Young's modules times the moment of inertia)
 m = the surface mass.

2. Room Acoustic Modes:

$$f_{ijk} = \frac{C}{2} \sqrt{\left(\frac{i}{L_x} \right)^2 + \left(\frac{j}{L_y} \right)^2 + \left(\frac{k}{L_z} \right)^2}$$

- where: f_{ijk} = the frequency of the i:j:k mode in Hz
 C = the speed of sound in air
 L_x, L_y, L_z = the room dimensions.

Table 3 (Cont'd)

3. Transmission Loss:

(a) For normal incidence:

$$TL_o = 20 \log \left| 1 + \frac{z}{2\rho c} \right|$$

where: TL_o = the normal incidence transmission loss ($= 10 \log 1/\tau$, where τ is the ratio of the power transmitted to the power incident on the panel)

z = panel impedance

ρc = the characteristic impedance of air.

(b) For random incidence:

$$TL_m = 20 \log (1 + \omega m / 3.6 \rho c)$$

$$\approx TL - 5$$

$$\approx 20^\circ \log (mf) - 33.5$$

where: TL_m = the random incidence transmission loss

m = the surface weight in lb/sq ft

f = frequency in Hz.

(c) General formula between two reverberant rooms:

$$TL = NR + 10 \log \left(\frac{1}{4} + \frac{S_w}{R_2} \right)$$

where: NR ($= SPL_1 - SPL_2$) = the noise reduction between rooms 1 and 2

S_w = the area of the intervening wall

R_2 ($= S_2 \bar{\alpha}_2 / 1 - \bar{\alpha}_2$) = the room constant of room 2 where α is the average statistical absorption coefficient and S is the room wall area.

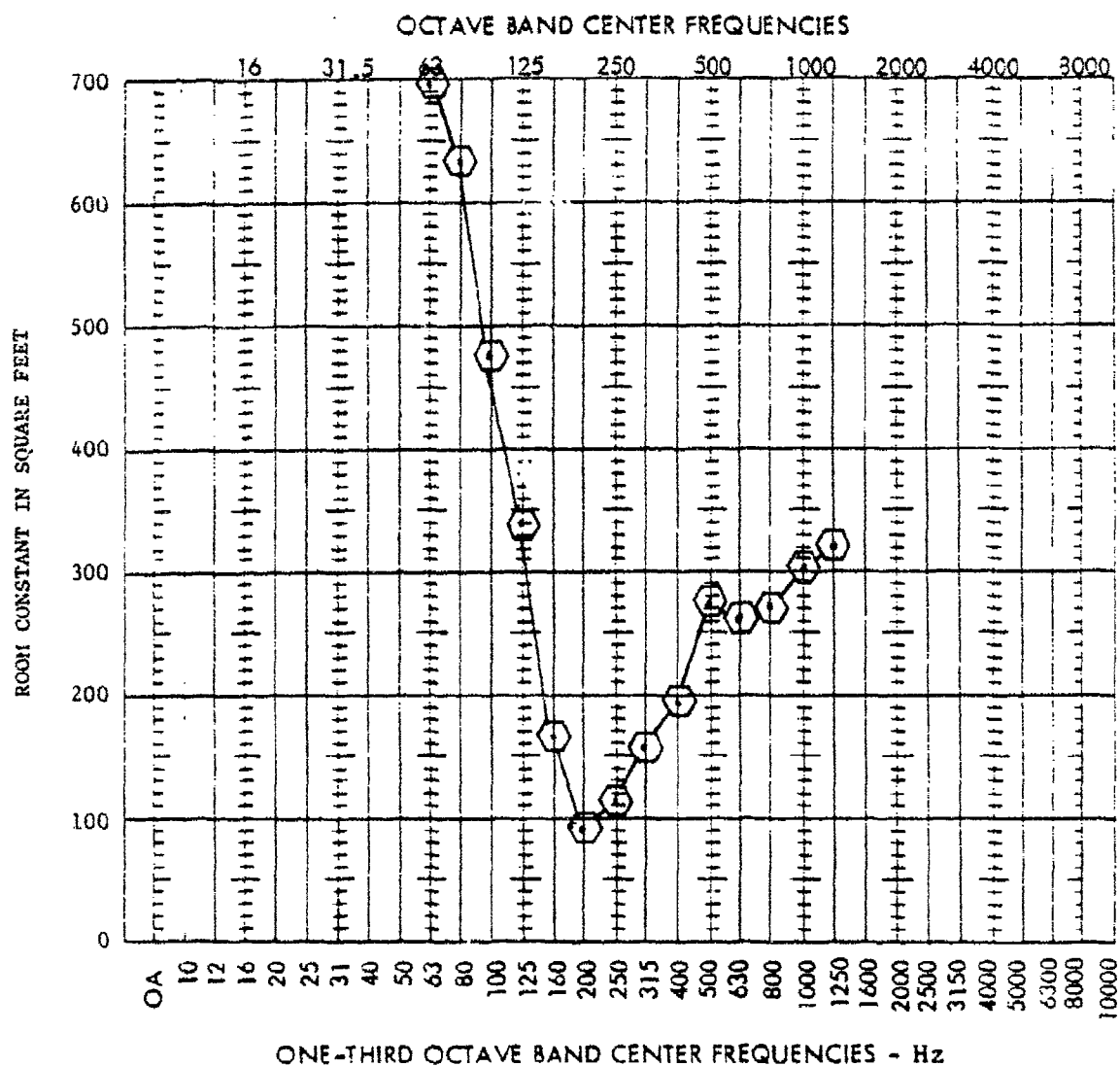


Figure 29. Room constant derived from "volume average" sound levels measured on February 7, 1984, with ILG reference source; furniture remained inside the test house room.

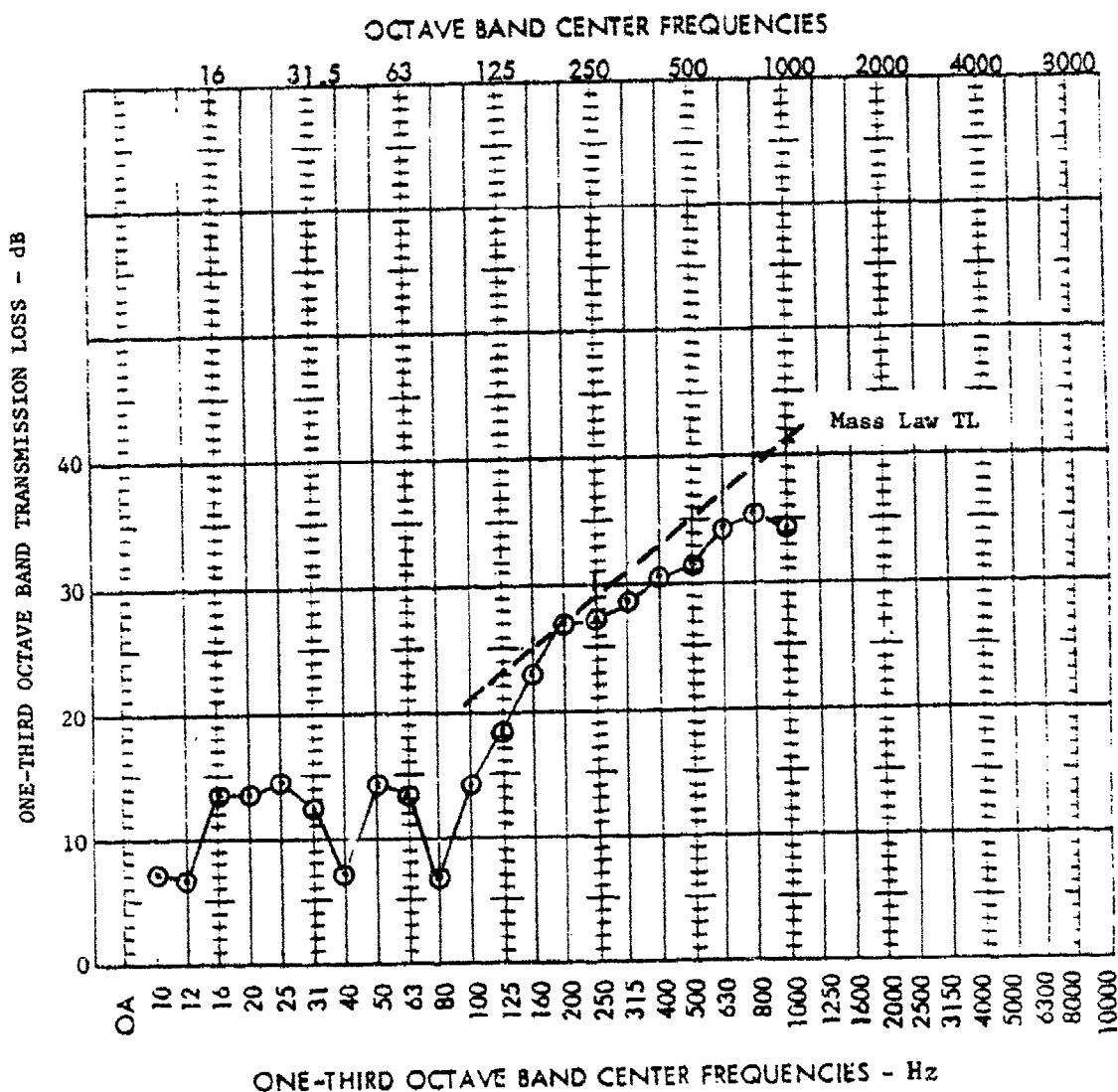


Figure 30. Transmission loss calculated from "volume average" sound level measurements with pink noise (February 3-6, 1984). The data consist of four 64-sec inside averages with the microphone moved throughout the test room and four 64-sec outside averages with the microphone moved between the rail and pit from the floor to the height of the eaves. The room constant data from Figure 29 were applied to the measurements from 63 Hz up and no room constant correction was applied below 63 Hz.

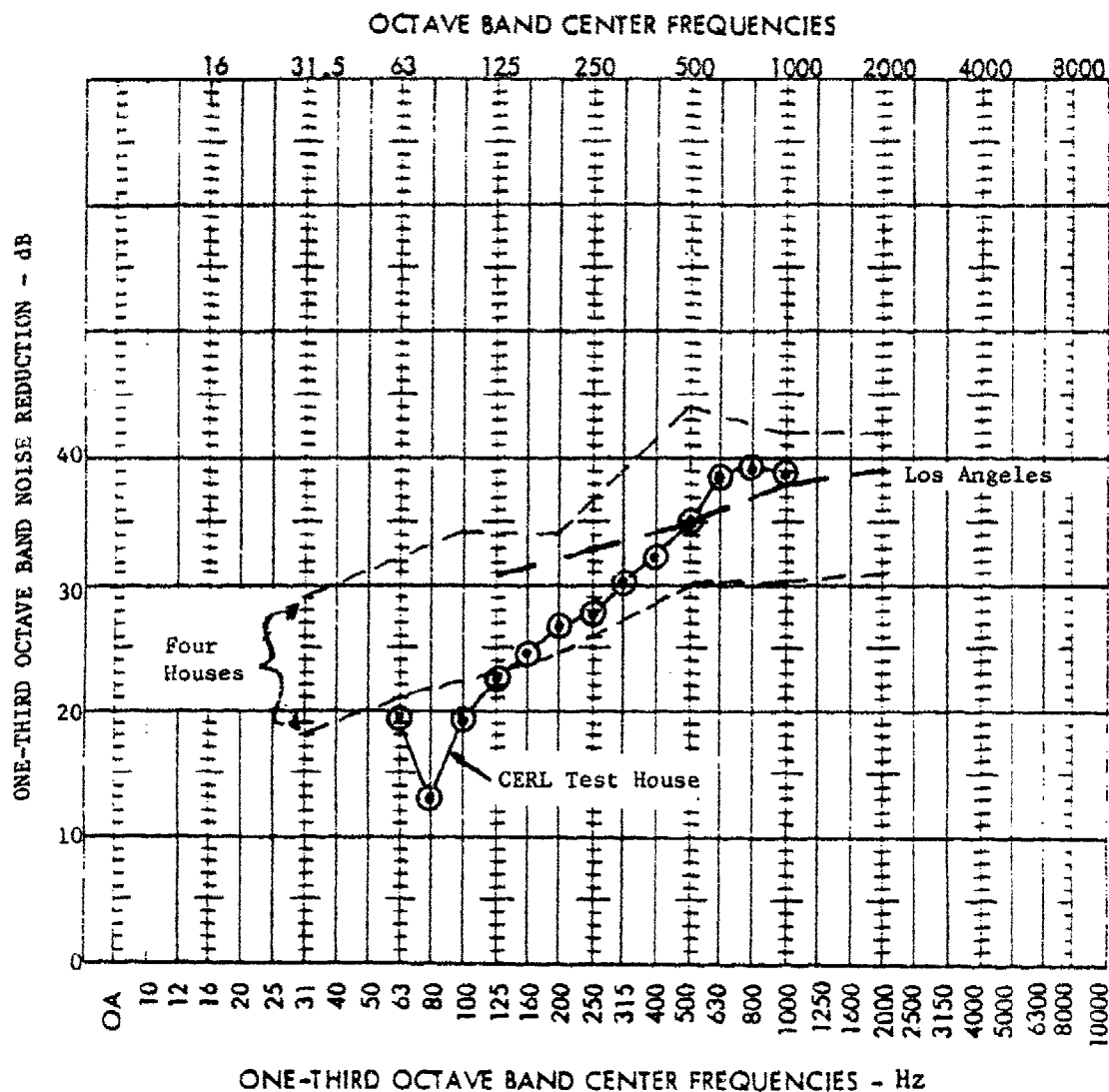


Figure 31. Comparison of estimated noise reduction for free field excitation of test house (furniture inside and winter conditions) with estimated values for 20 houses in Los Angeles and four in California and Virginia. (Los Angeles data are from K. E. Eldred, et al., *Home Soundproofing Pilot Project for the Los Angeles Department of Airports Wyle Research Report WCR 70-1* [Wyle Laboratories, March 1970]. The California/Virginia data are from H. H. Hubbard, "Noise Induced House Vibrations and Human Perception," *Noise Control Engineering Journal*, Vol 19, No. 2 [September-October 1982].)

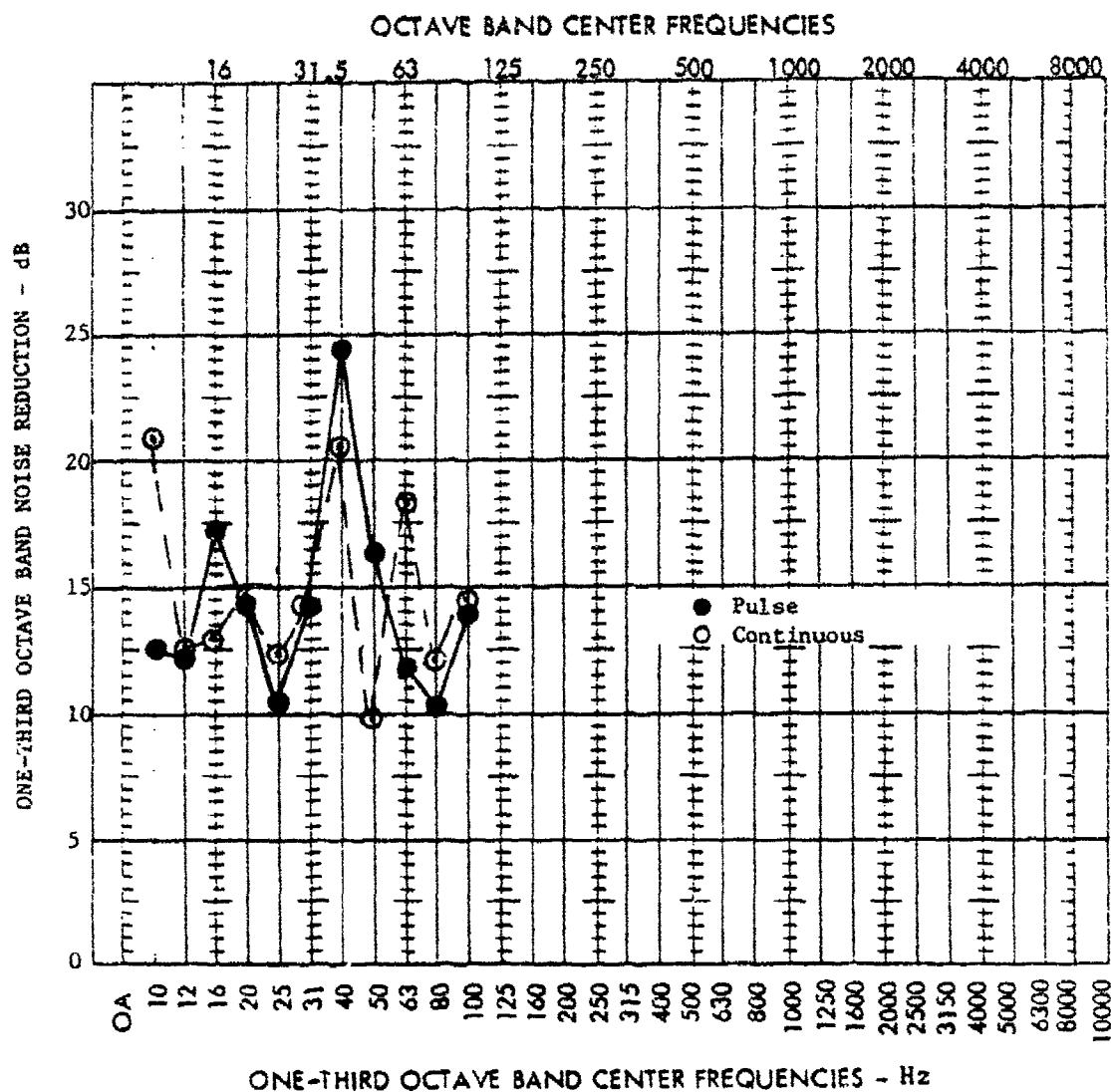


Figure 32. Reduction of SEL for simulated blast pulse (reel 24, test 2) and for continuous noise. Inside measurements were made at the SW corner microphone and exterior measurements were made at the standard reference position and corrected (-5 dB for pulse and -4 dB for continuous noise). Both tests were for winter conditions with attic vents sealed; the pulse data are with furniture out and continuous data are with furniture in.

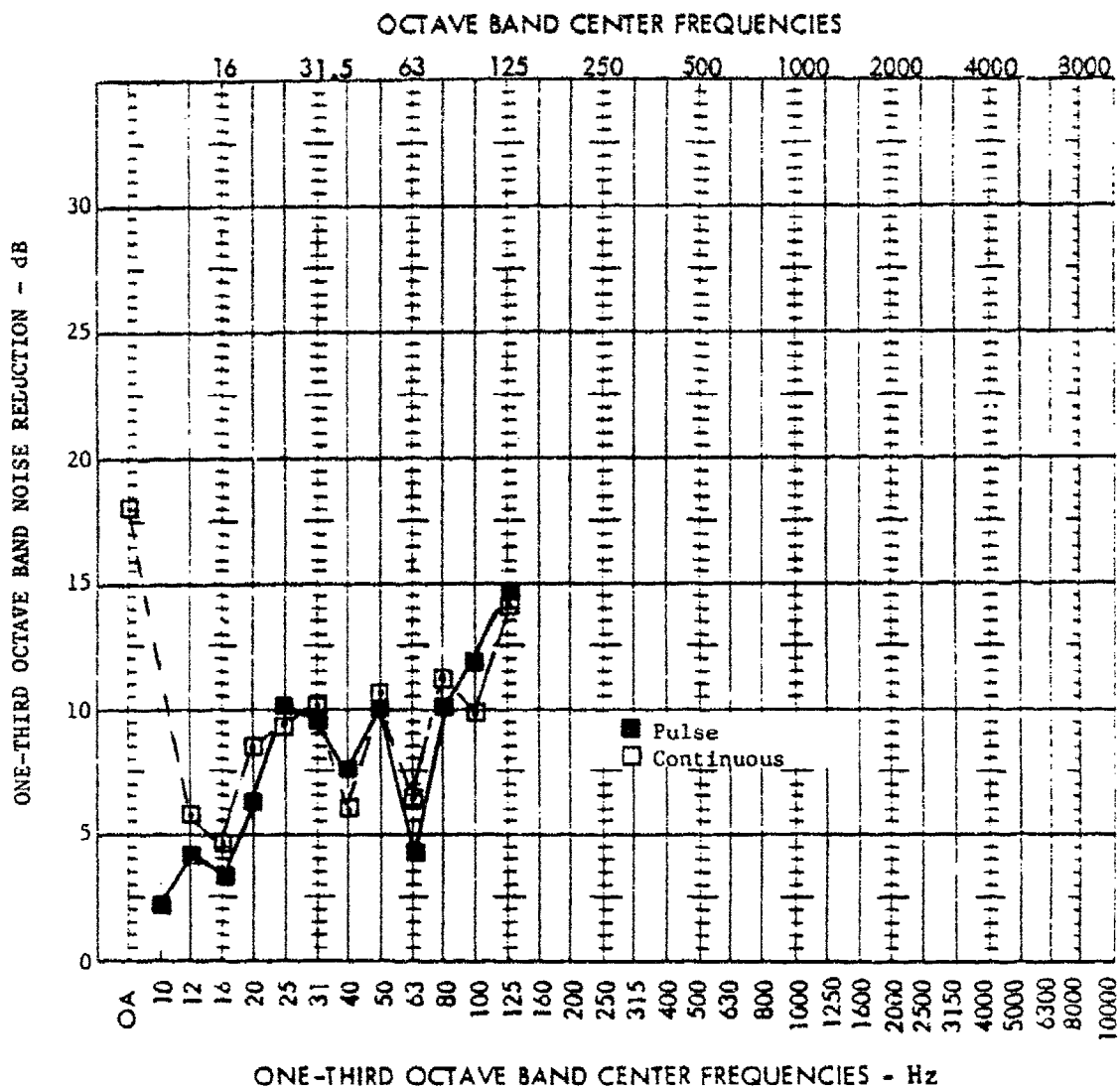


Figure 33. Reduction of SEL for simulated blast pulse (reel 24, test 2) and for continuous noise. Inside measurements were made at the standard interior reference microphone and exterior measurements were made at the standard reference position and corrected (-5 dB for pulse and -4 dB for continuous noise). Both tests were for winter conditions with attic vents sealed; pulse data are with furniture out and continuous data are with furniture in.

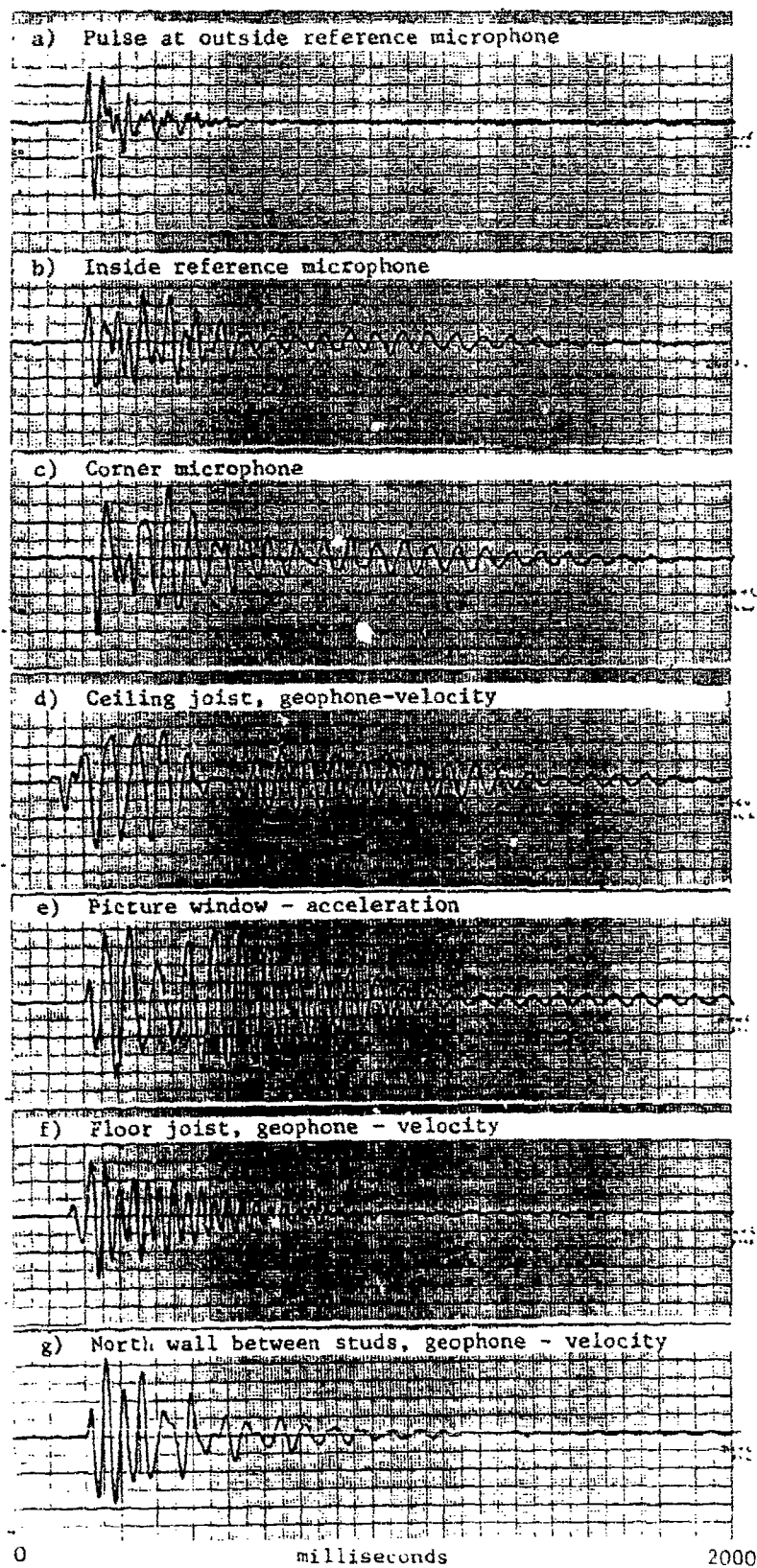


Figure 34. Time histories for an impulsive sound (reel 23, test 16).

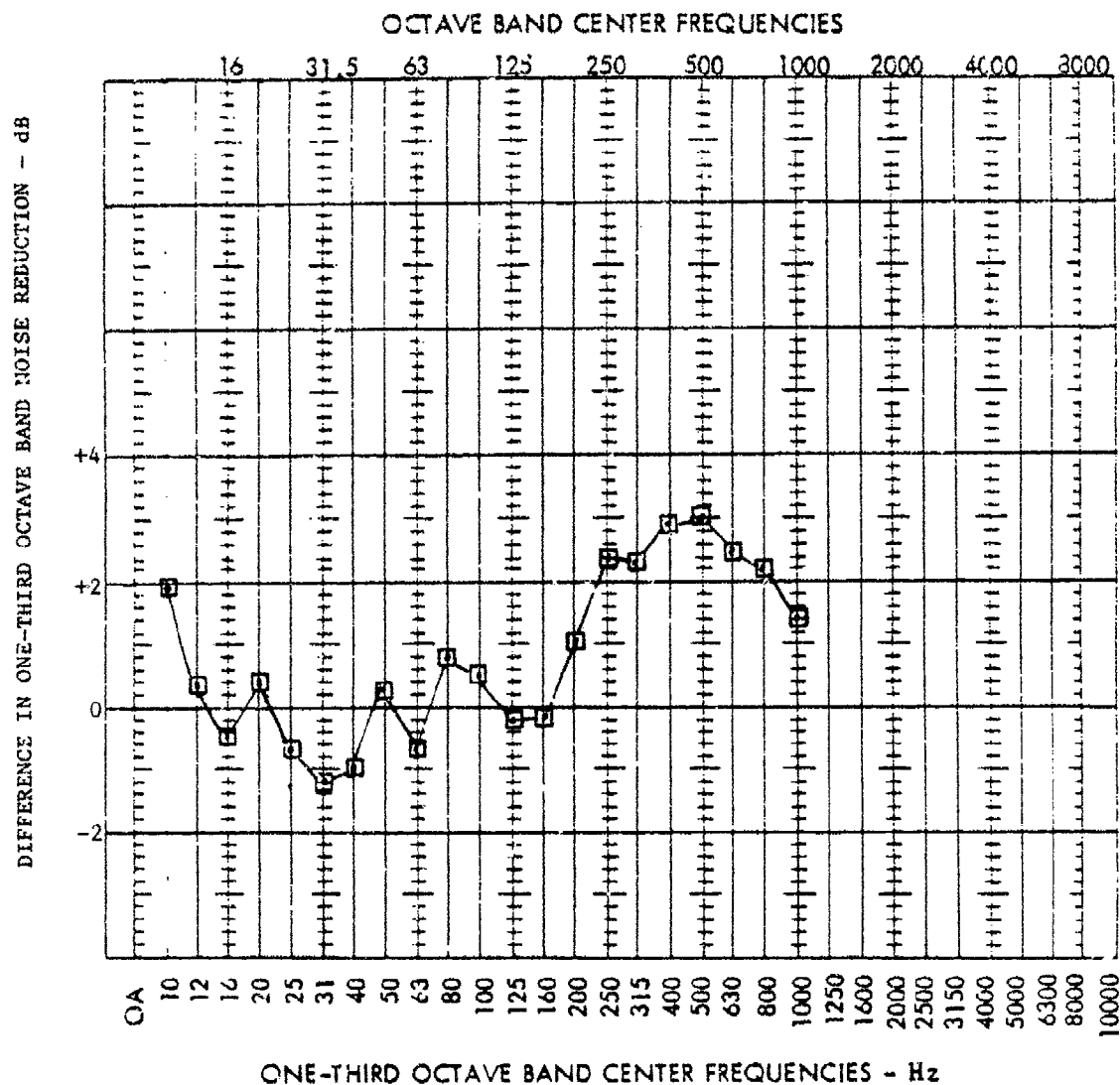


Figure 35. Difference in 1/3-octave band noise reduction between inside and outside reference microphones with and without furniture in the room. Data are from four 64-sec volume averages measured on February 3, 1985. A positive value denotes that furniture increased the room's acoustic absorption.

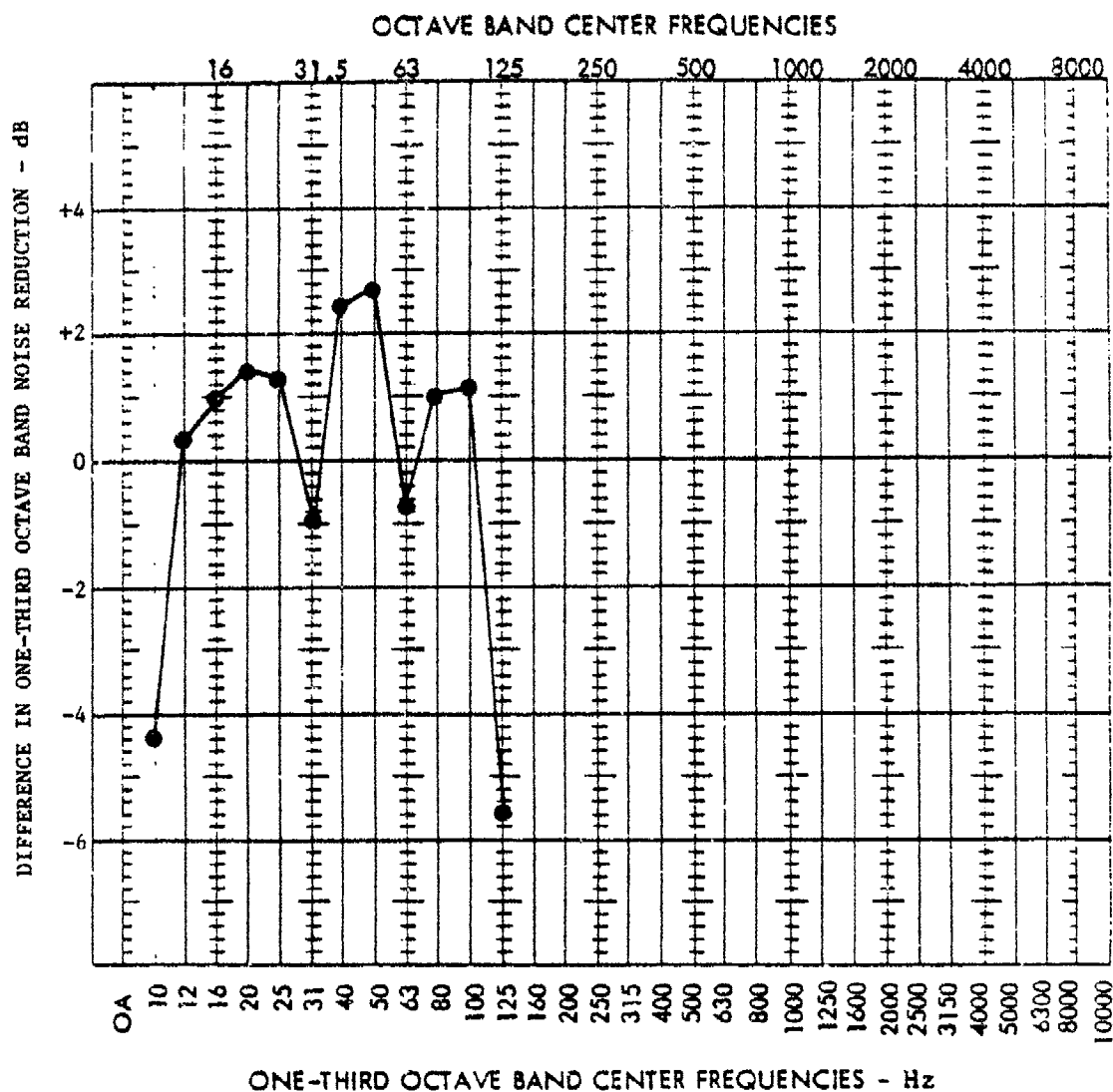


Figure 36. Difference in 1/3-octave band noise reduction between inside and outside reference microphones when the attic vents are sealed. Data are averages from reel 21, tests 1, 3, 5, and 7 for vents closed and from reel 23, tests 12, 14, 16, and 18 for vents open. Both cases were for winter conditions without furniture. A positive value denotes that sealing the vents increased the noise reduction.

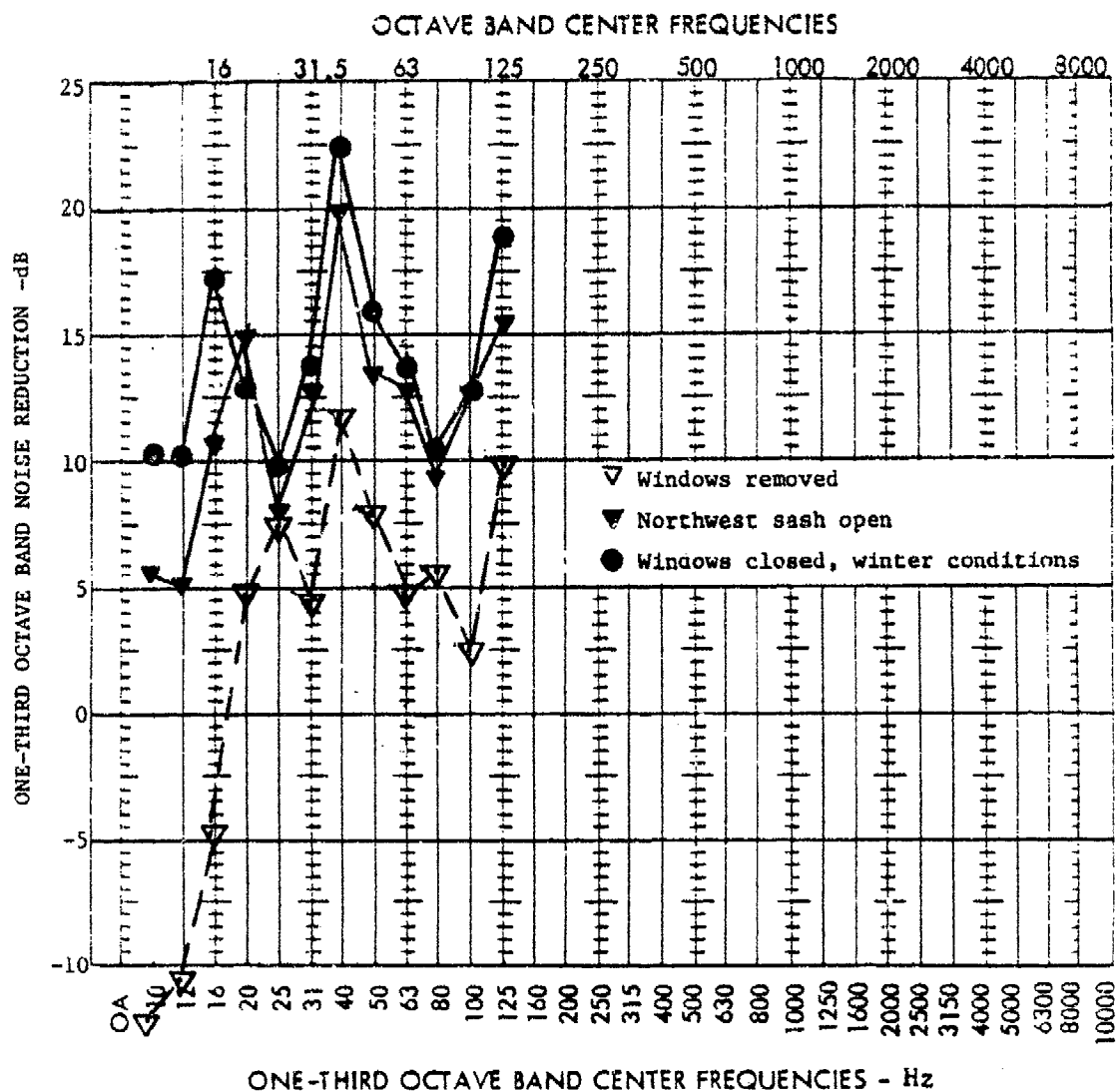


Figure 37. Noise reduction between inside and outside reference microphones minus 5 dB for three states of window closure. Data for window unit removed were from reel 14, test 10, with a 25-msec pulse. Open-sash data were from reel 23, test 23, with a 28-msec pulse and the windows-closed data were from reel 23, test 20, with a 28-msec pulse. The attic vents were not sealed and there was no furniture in the room.

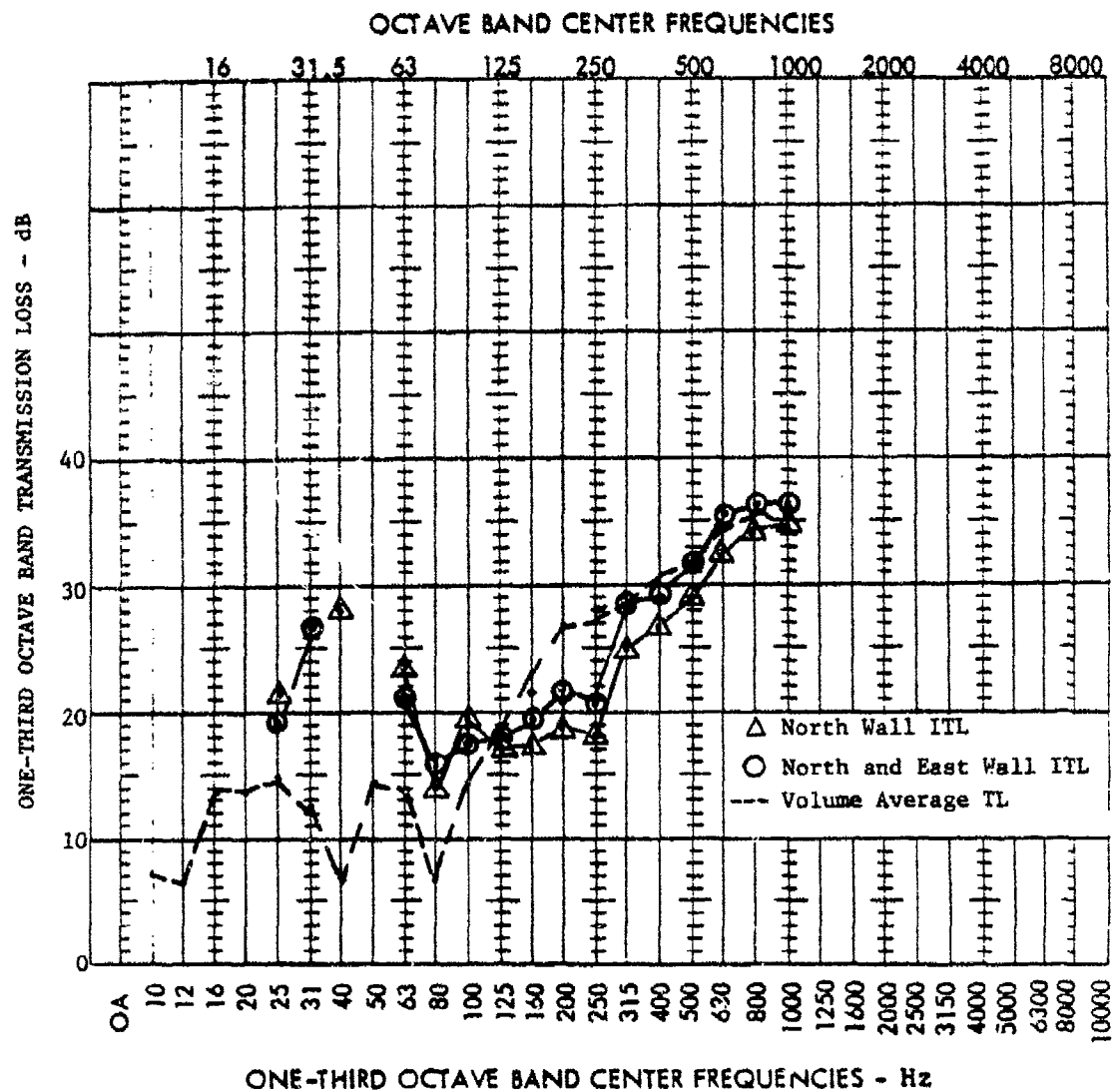


Figure 38. Comparison of volume average TL curve from Figure 30 with ITL calculated for the north wall and the north plus east walls using acoustic intensity methods.

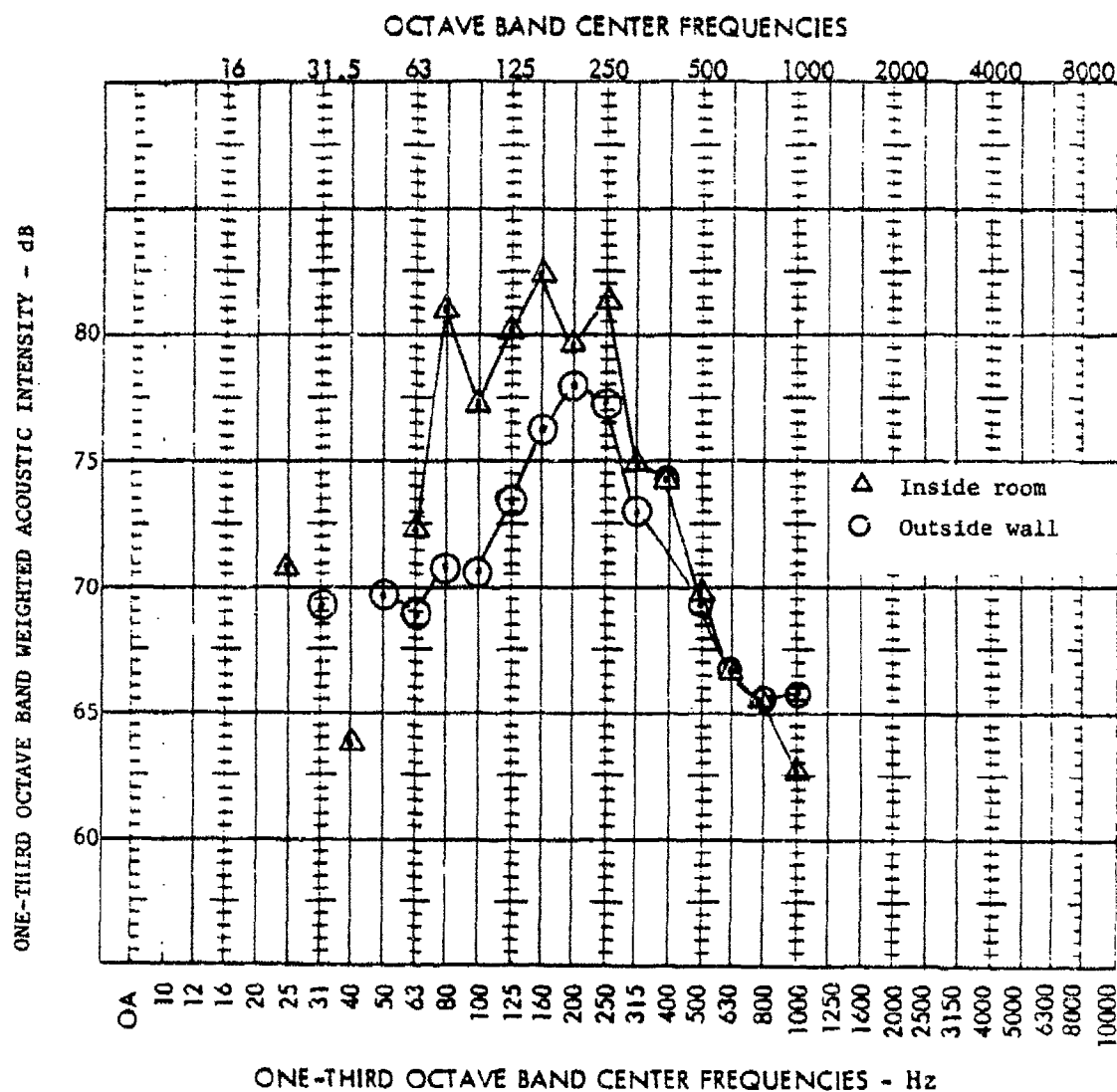


Figure 39. Comparison of acoustic intensity radiated into room by walls and windows with intensity measured outside room and flowing into wall.

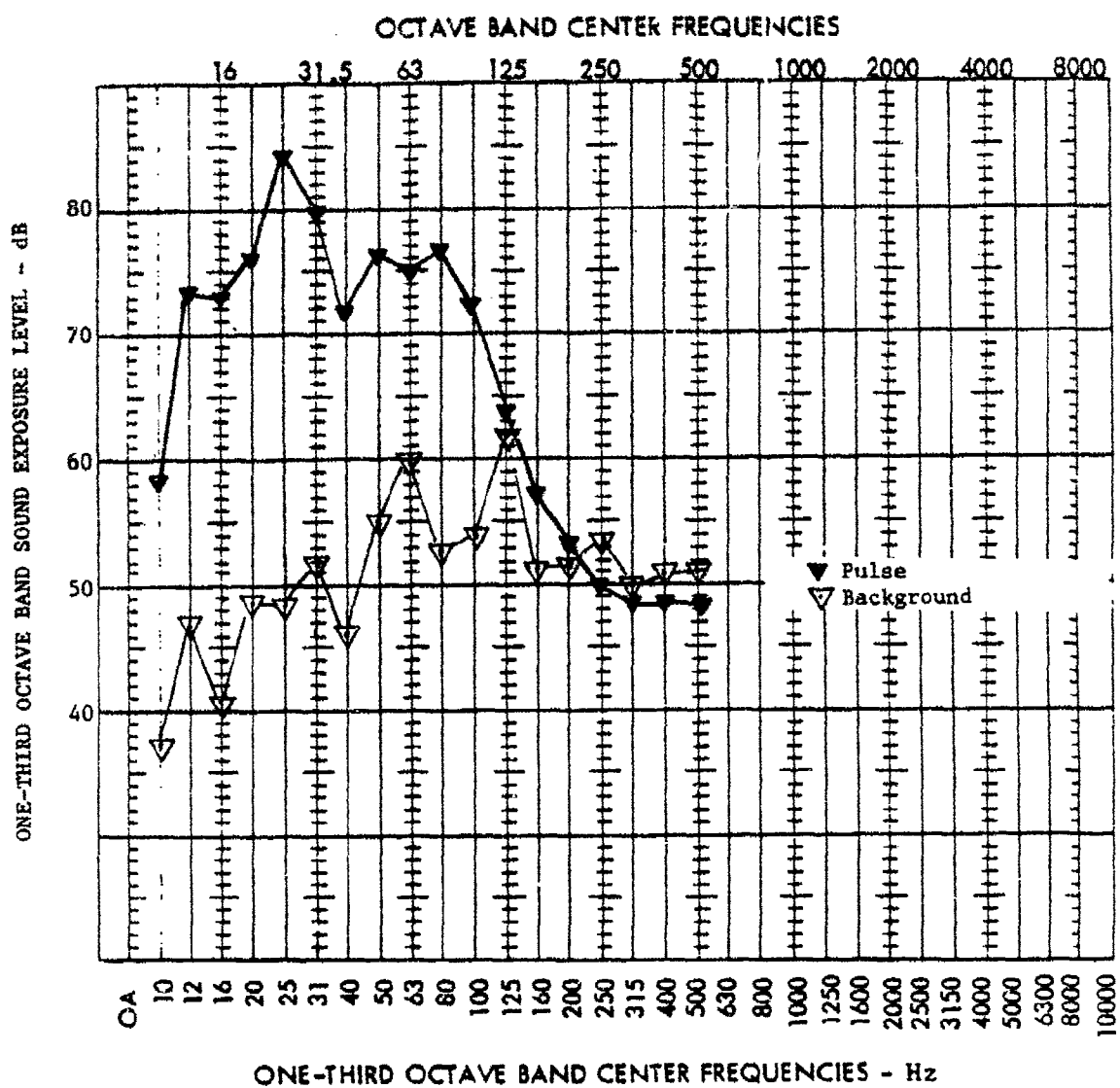


Figure 40. Comparison of 1/2-sec average 1/3-octave band levels in test house at the interior reference microphone position during and subsequent to a test impulse sound from reel 24, test 2.

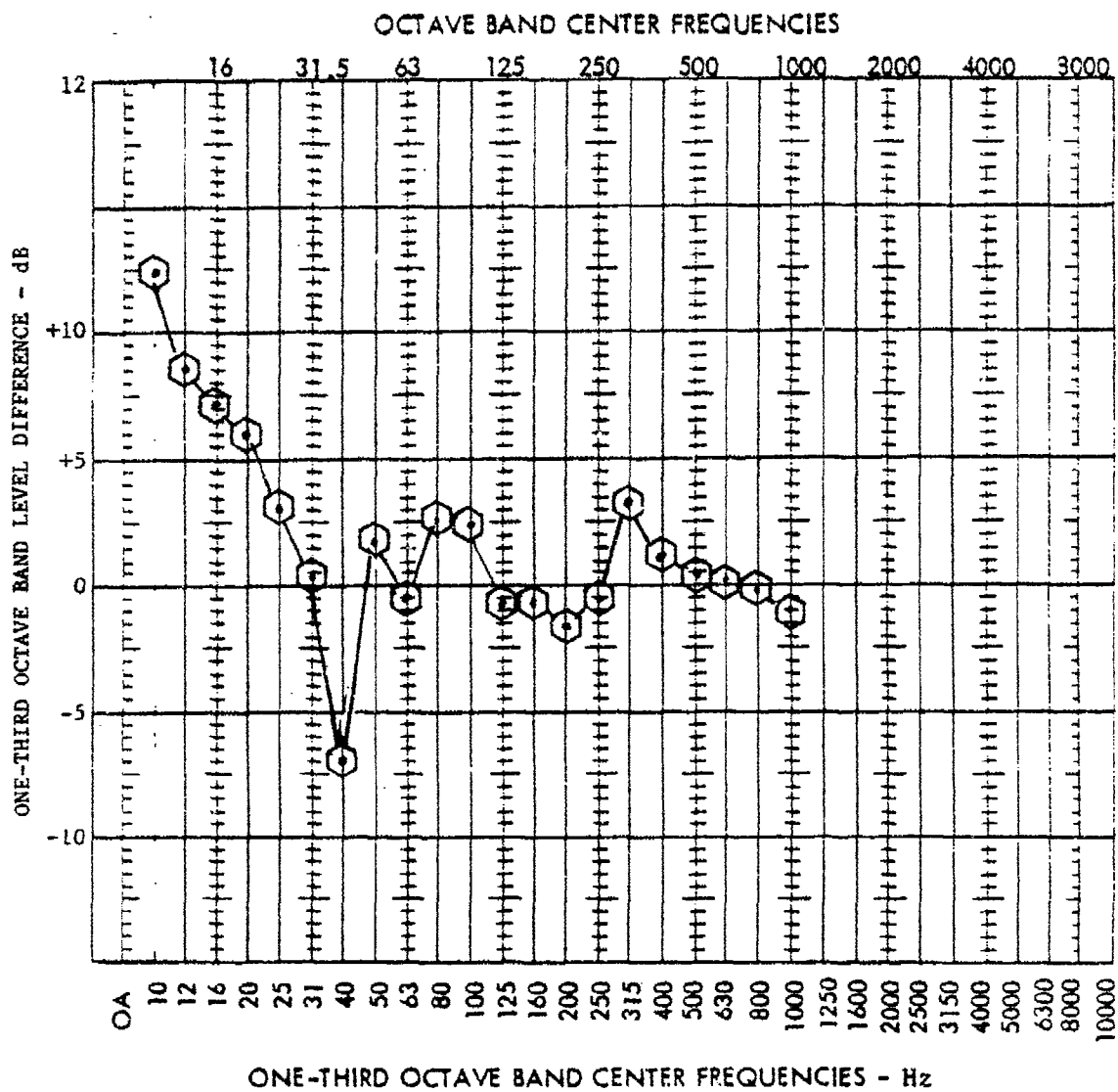


Figure 41. Difference between energy average of five microphones spaced at 1/6 intervals along the main diagonal (Figure 19) and direct electrical average.

REFERENCES

- Army Regulation (AR) 200-1, *Environmental Quality: Environmental Protection and Enhancement* (Headquarters, Department of the Army [HQDA], 15 June 1982).
- Beranek, L. L., *Acoustics* (McGraw-Hill, 1954).
- Borsky, P. N., *Community Reactions to Sonic Booms in the Oklahoma City Area, Vol II, Data on Community Reactions and Interpretations*, AMRL-TR-65-37 (U. S. Air Force, 1965).
- Buffa, J., and M. Crocker, "Background Noise Effects on the Measurement of Sound Power of Small Machines Using Intensity Techniques," *Noise Control Engineering Journal*, Vol 25, No. 1 (July-August 1985).
- Eldred, K. E., et al., *Home Soundproofing Pilot Project for the Los Angeles Department of Airports*, Wyle Research Report WCR 70-1 (Wyle Laboratories, March 1970).
- Hubbard, H. H., "Noise Induced House Vibrations and Human Perception," *Noise Control Engineering Journal*, Vol 19, No. 2 (September-October 1982).
- Kryster, K. D., P. J. Johnson, and J. P. Young, *Psychological Experiments on Sonic Booms Conducted at Edwards Air Force Base, Final Report*, Contract No. AF49(638)-1758 (National Sonic Boom Evaluation Office, Arlington, VA, 1968).
- Schomer, P. D., *Predicting Community Response to Blast Noise*, Technical Report E-17/ADA773690 (U.S. Army Construction Engineering Research Laboratory [USA-CERL], December 1973).
- Schomer, P. D., and R. D. Neathammer, *Community Reaction to Impulsive Noise: A 10-Year Research Summary*, Technical Report N-167/ADA159455 (Revised) (USA-CERL, 1985).
- Schomer, P. D., and R. D. Neathammer, *The Role of Vibration and Rattle in Human Response to Helicopter Noise*, Technical Report N-85/14/ADA162486 (USA-CERL, July 1985).
- Schomer, P. D., et al., *Blast Noise Prediction, Vol I: Data Bases and Computational Procedures*, and *Vol II: BNOISE 3.2 Computer Program Description and Listing*, Technical Report N-98/ADA099440 and ADA099335 (USA-CERL, March 1981).
- Schomer, P. D., et al. *The Statistics of Amplitude and Spectrum of Blasts Propagated in the Atmosphere, Vols I and II*, Technical Report N-13/ADA033361 (USA-CERL, November 1976).
- Siskind, D. E., et al., *Structure Response and Damage Produced by Airblast From Surface Mining*, Bureau of Mines Report of Investigation RI 8485, (U. S. Bureau of Mines, 1980).
- Sutherland, L. C., *Low Frequency Response of Structures*, Wyle Research Report WR 82-18 (Wyle Laboratories, May 1982).
- Sutherland, L. C., B. H. Sharp, and R. A. Mantey, *Preliminary Evaluation of Low Frequency Noise and Vibration Reduction Retrofit Concepts for Wood Frame Structures*, Wyle Research Report WR 83-26 (Wyle Laboratories, June 1983).

APPENDIX:

CHRONOLOGICAL LIST OF EXPERIMENTS BY REEL NUMBER

- Reel #1: Preliminary trial of test configuration.
- Reel #2: 2-microphone baseline--furniture in, doors and windows all closed, all storm sashes closed (winter conditions).
- Reel #3: 2 microphones, windows open, furniture in; 2nd baseline at end of tape.
- Reel #4: 3/4-in. plywood over N. windows, furniture in; pads under bric-a-brac, windows covered, furniture in (2 microphones).
- Reel #5: Front door/storm door variations, plywood over N. windows (2 microphones).
- Reel #6: 2 microphones, N. windows covered, with and without furniture; Channel #5 microphone position variations without furniture.
- Reel #7: 4 microphone position variations, plywood not on windows, furniture in, winter conditions.
- Reel #8: 4 microphones, pads under bric-a-brac, winter conditions.
- Reel #9: 4-microphone baseline--furniture in, winter conditions.
- Reel #10: Communications shelter vibration tests on Shake Table, sweep of 5 Hz to 200 Hz, 1 octave/min; many resonances of test article.
- Reel #11: Baseline, 4 microphones; baseline 2 microphones and geophones; storm sashes up (spring conditions).
- Reel #12: Summer conditions--all windows open, door open, all storm sashes up.
- Reel #13: 5- to 200-Hz Shake Table sweep on another test article--winter and summer conditions.
- Reel #14: All windows removed, door, storm door closed, storm door glass down.
- Reel #15: Windows replaced, no storm windows, doors closed, storm door glass down; different Shake Table settings.
- Reel #16: Summer conditions; fall conditions (windows, doors closed, storm windows open); pure tones from speakers, looking for resonances.
- Reel #17: Various conditions, 25-msec pulses, trying to record rattles.
- Reel #18: Tests of new Shake Table settings.
- Reel #19: Channel #12 to flat weight, 1 to 2 cm from sash window spring, attempting to record spring rattle (winter conditions).
- Reel #20: Channel #12 as in reel 19 but used 100-Hz high-pass filter before recording; then channel 12 near traverse rod pulley; then channel 12 near glass cruet.
- Reel #21: Shake Table settings/pulse refinement.
- Reel #22: Pulse refinement; baseline.
- Reel #23: Baseline; furniture out, winter conditions; then NW sash window and storm window open.
- Reel #24: Attic vents sealed, furniture in and out, winter conditions.

USA-CERL DISTRIBUTION

Chief of Engineers
ATTN: Tech Monitor
ATTN: CEEC-CE
ATTN: CEEC-EA
ATTN: CEEC-EI (2)
ATTN: DAEN-ZCF-B
ATTN: CEEC-ZA
ATTN: CEEC-M (2)
ATTN: CEIM-SL (2)

HQ USAF/LEEEU 20332

AMC 22333
ATTN: AMCEN-A

Naval Air Systems Command 20360
ATTN: Library

Little Rock AFB 72099
ATTN: 314/DEEE

Aberdeen PG, MD 21010
ATTN: Safety Office Range Safety Div.
ATTN: U.S. Army Ballistic Research Lab (2)
ATTN: ARNG Operating Activity Ctr.

Edgewood Arsenal, MD 21010
ATTN: HSHB-MO-B

Ft. Belvoir, VA 22060
ATTN: NACEC-FB

NAVFAC 22332
ATTN: Code 2003

Naval Surface Weapons Center 22448
ATTN: N-43

Ft. McPherson, GA 30330
ATTN: AFEN-FEB

US Army Aeromedical Res Lab. 36362
ATTN: SGRD-UAS-AS

FESA, ATTN: Library 03755
ATTN: DET III 79906

USA-WES 39180
ATTN: WESSE
ATTN: Soils & Pavements Lab
ATTN: C/Structures

Wright-Patterson AFB, OH 45433
ATTN: AAMRL/BB
ATTN: AAMRL/BBE

Department of Transportation
ATTN: Library 20590

Defense Technical Info. Center 22314
ATTN: DDA (2)

US Govt Print Office 22304
Receiving Sect/Depository (2)

NCEL
ATTN: Library, Code L08A 93043

WES, ATTN: Library 39180

CRREL, ATTN: Library 03755

Human Engr. Laboratory 21010

Naval Undersea Center, Code 401 92132

Bureau of National Affairs 20037

Building Research Board 20418

Transportation Research Board 20418

Federal Aviation Administration 20591

National Bureau of Standards 20899

47
+37
12/87